

UC Irvine

UC Irvine Electronic Theses and Dissertations

Title

The discovery of Sanguinarine as a dual-inhibitor of Androgen receptor and lysine-specific demethylase 1A for preventing or delaying lethal prostate cancer progression

Permalink

<https://escholarship.org/uc/item/673229zm>

Author

Pham, Victor

Publication Date

2020

Peer reviewed|Thesis/dissertation

UNIVERSITY OF CALIFORNIA,
IRVINE

The discovery of Sanguinarine as a dual-inhibitor of Androgen receptor and lysine-specific demethylase 1A for preventing or delaying lethal prostate cancer progression

DISSERTATION

submitted in partial satisfaction of the requirements
for the degree of

DOCTOR OF PHILOSOPHY

in Pharmaceutical Sciences

by

Victor Pham

Dissertation Committee:
Professor Xiaolin Zi
Professor Edward Uchio
Assistant Professor Claudia A Benavente

2020

TABLE OF CONTENTS

	Page
LIST OF FIGURES	iii
LIST OF TABLES	iv
ACKNOWLEDGEMENTS	v
VITA	vi
ABSTRACT OF THE DISSERTATION	vii
CHAPTER 1: Chapter 1 - Introduction to prostate cancer and androgen receptor	1
Normal Prostate structure and function	1
Chronic Inflammation in the prostate	2
Prostate Cancer Diagnosis	3
Prostate Cancer Treatment	3
Androgen Receptor	5
Androgen Deprivation Therapy	9
Androgen Receptor Splice Variant V7	10
CHAPTER 2: Introduction to Lysine-specific demethylase 1A	15
Eukaryotic Gene Regulation	15
Histone Lysine Methylation and Demethylation	17
Lysine demethylase 1A	18
LSD1 regulation of neuronal differentiation and development	19
CHAPTER 3: Introduction to Sanguinarine and its antitumor effects	21
CHAPTER 4: Sanguinarine is a novel dual-inhibitor of LSD1 and AR	26
CHAPTER 5: Nitidine degrades AR/AR-V7 mediated by Hsp70/STUB1 pathway	60
CHAPTER 6: Sanguinarine hinders Dovitinib-induced Neuronal-like differentiation	75
CHAPTER 7: Sanguinarine hinders cancer stem cell derived Prostate cancer	91
CHAPTER 8: Conclusion and remarks	107

LIST OF FIGURES

		Page
Figure 1.1	The anatomy of the male human.	1
Figure 1.2	The zone of the prostate.	2
Figure 4.1	The inhibitory effect of Sanguinarine against LSD1 activities	36
Figure 4.2	The inhibitory effect of Sanguinarine against AR activities.	37
Suppl. 4.1	Sanguinarine downregulates AR and AR-V7 activities	38
Figure 4.3	Sanguinarine targets LSD1 and AR/ARV7 to induce cytotoxicity	39
Suppl. 4.2	LSD1 Transduction and Transfection verification.	40
Figure 4.4	Sanguinarine and its naturally related structures.	41
Suppl. 4.3	Dual-inhibitors structures specificity against LSD1	42
Suppl. 4.4	LSD1 expression required dual inhibitors	43
Suppl. 4.5	Dual inhibitors inhibiting LSD1 and AR activities.	45
Figure 4.5	Sanguinarine downregulates AR and ARV7 through LSD1	51
Suppl. 4.6	Dual inhibitors inhibit AR and ARV7 through LSD1	52
Figure 4.6	Sanguinarine directly interacts with LSD1 and AR proteins.	54
Suppl. 4.7	Dual inhibitors engage in LSD1 and AR complexes.	55
Figure 5.1	Structure-related analogs and their influences on AR activities.	62
Figure 5.2	Nitidine induces cytotoxicity and apoptosis in CRPC cells.	64
Figure 5.3	Nitidine inhibits AR and AR-V7 expressions and activities	65
Figure 5.4	Nitidine induces AR and AR-V7 degradation in UPP manner.	67
Suppl. 5.1	Sanguinarine induces AR and AR-V7 degradation.	67
Figure 5.5	Nitidine induces AR degradation through Hsp70.	74
Figure 5.6	Nitidine induces STUB1-HSP70 interaction	74
Figure 6.1	Transfection with LSD1-8a results in sensitization to SNG.	78
Figure 6.2	DOV-induced neuroendocrine differentiation is inhibited by SNG.	80
Figure 6.3	DOV-induced NE differentiation reduced by LSD1 inhibitor, sp2509.	81
Figure 6.4	End result of the three-week study and western blot and qPCR results	81
Figure 6.5	Combination treatment resulted in a reduction in tumor growth.	83
Figure 6.6	SNG inhibits DOV-induced neuroendocrine differentiation in vivo.	84
Suppl. 6.1	Histology Part 1	85
Suppl. 6.2	Histology Part 2	86
Figure 7.1	FACS sorting assay of homogeneous CSC and Bulk-tumor cells	96
Figure 7.2	Sanguinarine inhibits LSD1 and AR gene expression in CSC.	97
Figure 7.3	Sanguinarine hinders cancer stem cell prostasphere formation	98
Figure 7.4	Sanguinarine hinders 22RV1 CSC prostasphere formation.	100
Suppl. 7.2	Sanguinarine hinders cancer stem cell prostasphere formation	101
Figure 7.5	Sanguinarine attenuates cancer stem cell progression in vivo.	102
Figure 7.6	Sanguinarine inhibits LSD1 and AR in xenograph cancer stem cells.	104
Suppl. 7.1	Sanguinarine attenuates H&E and Ki67 tumor staining	105

LIST OF TABLES

		Page
Suppl. Table 4.1	Classes of novel FAD analogs	28
Suppl. Table 4.2	Sanguinarine vs. dual inhibitors	44
Suppl. Table 4.3	Sanguinarine vs. A motif changes	46
Suppl. Table 4.4	Sanguinarine vs. A/B motif changes Part 1	48
Suppl. Table 4.5	Sanguinarine vs. A/B motif changes Part 2	49
Suppl. Table 4.6	Sanguinarine vs. A/B/C motif changes Part 1	50
Suppl. Table 4.7	Sanguinarine vs. A/B/C motif changes Part 2	50

ACKNOWLEDGEMENTS

Thank you so much Dr. Zi for giving me the opportunity to be part of your team and part of your lab. It has been quite an amazing journey working with you. As many of you already know, I grew up in a low-income family. I was a very quiet and shy person. I did not have great social skills or a strong educational background. However, what I did have was an open-mind and a willingness to learn.

I began my journey at Santa Ana College hoping to pursue a career in Art. Back then I feared science because it was difficult to understand. However, that all changed when I took my biology classes under the college's great professors. Their lasting influences led me to pursue science, teaching, and research. I would like to recognize Prof. Dan Goldman, Prof. Anson Lui, and Dr. Kimo Morris. I am honored to have had the privilege of being one of their students.

With their recommendation, I transferred to CSUF and participated in the HHMI research program working under Dr. Madeline Rasche. Afterwards, I did my undergraduate research under Dr. Nikolas Nikolaidis. It was later with their recommendation that I was further accepted into the CIRM BSCR program run by Dr. Niley Patel and Dr. Alison Miyamoto. This program gave me the opportunity to do research at UCI under Dr. Weian Zhao. It was in this lab that I co-authored TWO scientific papers as an undergraduate student.

With their extensive training and all their recommendations, I got into UCI's PhD program, funded by the prestigious NSF fellowship, and had the privilege of working with Dr. Xiaolin Zi. I ended up co-authoring 6 papers during the time I was completing my PhD, and we are expecting to see more papers published soon (see chapter 4, 5, 6, and 7).

These opportunities and achievements would not be possible without the great mentors who supported me. Thus, I want to personally thank and show my full gratitude to all my PI's, supervisors, and mentors. Still, I would not be able to get this far without the help from my students, friends, and family. I want to thank each of my students, friends, and family for giving me their time, hard-work, blood, and sweat for our projects.

My story would have never been possible alone. The story of who I am and who I will be is built and shaped by the mentors, teachers, friends and families, and students that were with me throughout my journey from the beginning of college to the beginning of my career. I will always owe my sincerest appreciation and gratitude to all of those who were with me and supported me.

Our success begins not just with you alone, but also with the people all around you, supporting you throughout your journey. Like the professors, colleagues, and students who supported me, I aim to be a strong role model for other students, and I hope to give them the experiences and opportunities to start a new chapter in their lives.

With all my heart, thank you,

VITA

Victor Pham

2011-19 Instructional Assistance, Santa Ana College
2012-18 Supplementary Instructor, Santa Ana College
2012-14 HHMI research Fellow, California State University, Fullerton
2013-14 Undergraduate Researcher, California State University, Fullerton
2014-16 CIRM BSCR research fellow, University of California, Irvine
2016 B.S. in Molecular and Biotechnology, California State University, Fullerton
2016-20 PhD research student, University of California, Irvine
2017 Lab Instructor, University of California, Irvine
2019-Cur Biology Professor, Fullerton College and Santiago Canyon College
2020 PhD in Pharmaceutical Science, University of California, Irvine
2020-Cur Director of Genomic Science, Hodigen Startup company, Westminster

AWARDS

HHMI Summer Research Fellowship Program
Stem Cell Research Trainee Certification Program
BSCR Fellowship Program
NSF Graduate Research Fellowship Program
Course Design Certification Program
CIRTL Associate Certification Program
OCBiotech Education Outstanding Support and Partnership
SBUR Annual Meeting – Travel Award Winner

PUBLICATIONS

Mesenchymal Stem Cells Engineered to Express Selectin Ligands and IL-10 Exert Enhanced Therapeutic efficacy in Murine EAE. Wenbin Liao, Victor Pham, Linan Liu, Milad Riazifar, Shirley Xian Zhang, Fengxia Ma, Mengrou Lu, Egest Pone, Craig Walsh, and Weian Zhao (2016). *Biomaterials*. 2015 Nov 10. 77: 87-97

Elucidation of Exosome Migration across the Blood-Brain Barrier Model In Vitro. Claire C. Chen, Linan Liu, Fengxia Ma, Chi W. Wong, Xuning E. Guo, Jenu V. Chacko, Henry P. Farhoodi, Shirley X. Zhang, Jan Zimak, Aude Ségaly, Milad Riazifar, Victor Pham, Michelle A Digman, Egest J Pone, and Weian Zhao (2016). *Cellular and Molecular Bioengineering*. 2016 Jul 7.

Rhodiola rosea L.: an herb with anti-stress, anti-aging and immunostimulating properties for cancer chemoprevention. Yonghong Li, Victor Pham, Michelle Bui, Liankun Song, Chunli Wu, Arman Walia, Edward Uchio, Feng Smith-Liu, Xiaolin Zi (September 17, 2017). *Pharmacology Reports*.

Dong-Jun Fu, Jia-Jia Yang; Ping Li; Yu-Hui Hou; Sheng-Nan Nan; Matthew Alexander Tippin; Victor Pham; Liankun Song; Xiaolin Zi; Wei-Li Xue; Li-Rong Zhang; Sai-Yang Zhang. Bioactive heterocycles containing a 3,4,5-trimethoxyphenyl fragment exerting potent antiproliferative activity through microtubule destabilization. (September 2018). *European Journal of Medicinal Chemistry* 2018 Jul 29.

Dongjun Fu, Victor Pham, Matthew Tippin, Liankun Song, Xiaolin Zi, and Hong-Min Liu. (1R,5S)-6-(4-methyl-2-oxo-2,5-dihydrofuran-3-yl)-3-phenyl-4-oxa-2,6-diazabicyclo [3.2.0] hept-2-en-7-one. (August 2018) *Journal of Molbank-short note*. 28 August 2018

Xuesen Li, Victor Pham, Matthew Tippin, Dongjun Fu, Raymond Rendon, Liankun Song, Edward Uchio, Bang H Hoang, and Xiaolin Zi. Flavokawain B targets protein neddylation for enhancing the anti-prostate cancer effect of Bortezomib via Skp2 degradation (2019). *Journal of Molecular Cancer*. 18 March 2019

Milad Riazifar, M. Rezaa Mohammadi, Egest J. Pone, Ashish Yeri, Cecilia Lasser, Aude Segaliny, Ganesh Shelke, Elizabeth Hutchins, Ashley Hamamoto, Erika Calle, Rossella Crescitelli, Wenbin Liao, Victor Pham, Yanan Yin, Craig Walsh, Kendall Van Keuren-Jensen, Jan Lötval, Weian Zhao. Stem Cell-derived Exosomes as Nanotherapeutics for Autoimmune and Neurodegenerative Disorders. (2019) *ACS Nano* 2019 May 29.

Victor Pham, Raymond Rendon, Vinh X Le, Matthew A Tippin, Dongjun Fu, Thanh NH Le, Marvin Miller, Ericka Agredano, Jose Cedano Gartanin is a novel NEDDylation inhibitor for induction of Skp2 degradation, FBXW2 expression and autophagy. (November 29, 2019) *Molecular Carcinogenesis*.

ABSTRACT OF THE THESIS

The discovery of Sanguinarine as a dual-inhibitor of Androgen receptor and lysine-specific demethylase 1A for preventing or delaying lethal prostate cancer progression

by

Victor Pham

Ph.D. in Pharmaceutical Sciences

University of California, Irvine, 2020

Professor Xiaolin Zi

Castration-resistant prostate cancer (CRPC) is a lethal disease and its progression is primarily driven by reactivation of androgen receptor (AR) signaling even after treatments with castration and multiple AR pathway inhibitors [CHAPTER 1]. In addition, epigenetic mechanisms, including lysine-specific demethylase 1A (LSD1) overexpression, have recently been appreciated as cell-fate determining drivers of the heterogeneity of CRPC and the associated treatment resistances [CHAPTER 2]. Therefore, we hypothesized that dual targeting of AR and LSD1 might be a more effective therapeutic approach in preventing or delaying the progression of CRPC. Through a series of structural similarity search of flavin adenine dinucleotide (FAD, a co-factor of LSD1) analogs, molecular docking studies and experimental screenings of inhibitors for LSD1 enzymatic activity and AR transcriptional activity, we have discovered for the first time that Sanguinarine, a naturally occurring compound from the root of *Sanguinaria canadensis* as well as other *Fumaria* species, is a potent dual inhibitor of both LSD1 and AR [CHAPTER 4]. In vitro Surface Plasmon Resonance (SPR) and in vivo Cellular thermal shift assay (CETSA) assays confirmed that Sanguinarine directly binds to both LSD1 and AR with equal or very close binding affinities. In addition, the growth inhibitory and anti-AR signaling effects of Sanguinarine are partially dependent on the expression levels of LSD1 as shown in LSD1 knockdown and overexpression experiments. To assess the effect of Sanguinarine on CRPC progression, we found that Sanguinarine

inhibited the neuroendocrine trans-differentiation of prostate cancer cell lines induced by Dovitinib, a pan—tyrosine kinase inhibitor in prostate cancer clinical trials, both in vitro and in vivo in xenograft models and significantly enhanced the anti-tumor efficacy of Dovitinib [CHAPTER 6]. Furthermore, Sanguinarine more effectively reduce the growth and regeneration of spheroids from stem cell-like prostate cancer cells or cancer initiation cells than bulk prostate cancer cells both in vitro and in an vivo xenograft model and down-regulates the expression of cancer stem cell markers (i.e. .Nanog, Sox2 and Oct4) [CHAPTER 7]. Overall, the results we have gathered demonstrate that Sanguinarine is a structural model as a dual inhibitor of LSD1 and AR for preventing or delay CRPC progression through mechanisms of down-regulation of AR signaling and inhibition of neuroendocrine differentiation and cancer stem cells. Our studies have provided a new strategy for treatment of CRPC.

CHAPTER 1

INTRODUCTION TO PROSTATE CANCER AND ANDROGEN RECEPTOR

Prostate cancer (PCa) is the second most lethal cancer in men in the United States [1]. In 2019, 174,650 new cases of PCa arose and 31,620 PCa-specific deaths occurred in the United States, accounting for more than 13% of all new cancer cases and 5% of all cancer deaths. PCa is also the fourth most diagnosed cancer worldwide, although the incidence for PCa varies by geographical region. The risk for PCa in African American men is the highest among other ethnicity groups. Early diagnosis is the best method to increase long-term survival for PCa patients since the 1990s and increased the 5-year survival rate to nearly 98%. However, for patients who were diagnosed with metastatic PCa, their 5-year survival rate dropped significantly to less than 28% [2]. In Chapter 1 of this dissertation, we provide an overview and discussion of the anatomy, pathophysiology, and current treatment strategies against PCa.

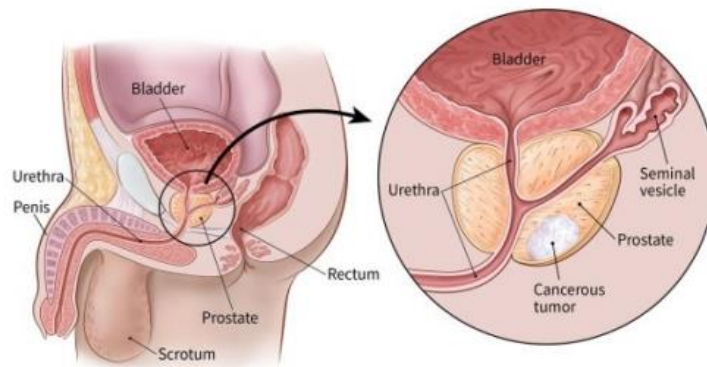


Figure 1: The anatomy of the male human. Prostate can be found under the bladder.

NORMAL PROSTATE STRUCTURE AND FUNCTION

The prostate is a walnut-size glandular organ that can be found surrounding the urethra and below the bladder (Figure 1). The prostate consists of (1) the inner transitional zone, (2) the central zone, and (3) the outer peripheral zones, all surrounding the urethra in that order (Figure 2). The transitional zone assists in maintaining the constriction of the natural passage or orifice of the urethra, whereas the central zone and the peripheral zones are for the secretion of semen. If any functional problems with the transitional zone exist, the benign prostatic hyperplasia (BPH) may develop and can cause urinary tract disease that is commonly developed in older males. PCa is commonly developed from the peripheral zone and the risk for PCa increases as age increases.

Zones of the Prostate

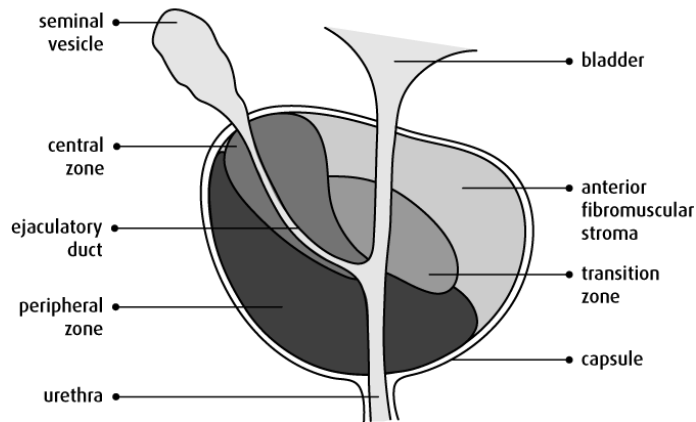


Figure 2: Different zones of the prostate.

The prostate produces fluid for semen, which is a mixture of prostatic fluid, seminal vesicle fluid, bulbourethral gland fluid, and sperms. Within the prostate gland, smooth muscle cells located at the basement membrane help contract to expel semen during ejaculation. The prostate gland also contains prostate-specific antigen (PSA), which is a serine protease that helps sperm move smoothly by liquidizing the semen [3]. PSA is a common biomarker used to detect the presence of PCa activity. In addition to its secretory function, the prostate can also aid in the transport of substances from the basal to the lumen side of the prostate.

CHRONIC INFLAMMATION IN THE PROSTATE

There has been extensive research delving into the origin of PCa, each of which came to the same consensus conclusion: that the manifestation of PCa is the result of the accumulation of both genetic and environmental influences, primarily as men get older. Inflammation in the prostate may also result from various other reasons, ranging from sexually and non-sexually transmitted infections to physical or dietary factors. Some chronic inflammation conditions of the prostate can exhibit molecular alteration similar to PCa, such as proliferative inflammatory atrophy, where cells proliferate at an increased rate within the atrophic region of the prostatic intraepithelial neoplasia, peripheral zone, or transitional zone. Due to its highly replicative nature, researchers believe this condition could possibly be the precursor to PCa development [4].

It is difficult to predetermine the molecular or genetic predisposition that causes men to develop PCa. There have been several genetic abnormalities identified to suggest an increased risk in carcinogenesis development, including the loss of GSTP1, PTEN, and tumor suppressor p53 [5]. In

addition, the increase in AR activities, androgen-responsive TMPRESS2 activities, or the expression of genes encoding 5 α -reductase, such as SRD52A, that converts testosterone into dihydrotestosterone may all be indicators for a higher risk in developing PCa [6]. Other PCa abnormal indications include unusual activity levels for genes involved in survival, proliferation, xenobiotic detoxification, and androgen receptor (AR) activity.

PROSTATE CANCER DIAGNOSIS

Patients screened and diagnosed with PCa at an earlier stage have a higher likelihood for long-term survival since early stage is still considered a curable stage. The most common PCa screening method involves measuring the PSA levels collected in serum [7]. PSA is usually overexpressed in PCa because of its excessive expression activities for androgen-responsive genes. Thus, PSA can be used to track PCa progression and can be used to correlate with patients' survival outcome. However, the correlation between PSA and PCa is controversial. There may be risks of misdiagnosis that can lead to the treatment of PCa for patients that have an inflamed prostate as a result of other factors. Moreover, there are several factors that show PSA may not be an optimal indicator of PCa. First, an increase of PSA in the serum can result from noncancerous conditions, such as BPH, trauma, or inflammation. Second, early stage PCa are slow-growing cancers, so the level of PSA is not significant to indicate PCa. Therefore, it is very important to search for other alternative biomarkers when monitoring PCa in conjunction with PSA [8]. Some biomarkers may include PTEN loss, gene fusion, and increased in long non-coding RNAs, to name a few [9].

Doctors may also diagnose PCa based on the histology features of the tissues after biopsy. There are a few histology aspects that are seen as an indication of cancerous tissue: the breakdown of organ structure that lead to gland infiltration, the increase in cell number, largened nuclei, mitotic figures, absence of basal cells, and the upregulation of α -methylacyl-CaA racemase. Doctors will usually measure the histology tissue biopsy using Gleason scoring, a method that determines a cancer's malignancy levels through correlation of prognosis and guides treatment decisions. The scoring system is based from 1-5, allowing for a grade to be submitted to the most prevalent and undifferentiated cells [10].

PROSTATE CANCER TREATMENT [12]

There are various treatment routine options for PCa, depending on the disease stage, age, and overall health of the patients. A treatment center's location may also play a significant role because one medical center may have historically different treatment methods.

For any PCa patient, it is important to watch and actively survey signs of health degradation. The term active surveillance means the treatment and the delay of localized cancer until it begins to show

evidence of local progression and higher Gleason grade migration. The reason for not outright treating the cancer disease is to spare the patients from treatment side effects. This is especially important for patients who have two or more other chronic diseases or for elderly patients with low grade and low volume cancer that may not show significant signs. In addition, treating these patients may be daunting as the potential benefit may not outweigh the risk of treatment-associated side effects. Thus, treatment is not given immediately after diagnosing these patients, but given only to alleviate and delay the progression of cancer.

Nonetheless, some PCa patients may even take an extra step to avoid the risks of developing progressive cancer entirely by going through surgery or radiation therapy. However, there are a few drawbacks to this decision; their quality of life will be lowered, which may lead to unforeseen and unnecessary suffering.

Radical prostatectomy

Radical prostatectomy occurs when a patient gets their prostate removed. Prostatectomies are usually performed on men with good health that can bear the trauma and after effect of the surgery and have an organ-confined disease. Patients who undergo radical prostatectomy may have trouble with erections for sexual activities and lose their ability to control their urine bowel motion.

Radiation therapy

Radiation therapy is the use of an external-radiation beam that focuses directly at the prostate and surrounding tissues. Brachytherapy is often applied to seal the radiation to focus inside or next to the affected area. Radiopharmaceutical therapy, which utilizes compounds with radioactive purposes, is typically used for the treatment of bone metastasis.

Hormonal therapy

One of the most common therapeutic treatments for patients with PCa is hormonal therapy, or androgen-deprivation therapy (ADT), which is administered to disrupt the androgen pathways that promote the growth and progression of PCa. Hormone therapy helps reduce the level of androgen available in the body that activates PCa growth and progression. The androgen receptor (AR) pathway is the primary target for PCa patients, in which the goal of the initial hormone therapy is to reduce the plasma testosterone levels. Certainly, castrations, which include surgical prostatectomy (bilateral orchiectomy) or pharmacological castration (luteinizing hormone-releasing hormone, LHRH, agonists/antagonists) can also achieve similar results. However, the side effects from these treatment methods will lead to decreased libido, inability to erect, weight gain, brittle or weakened bones, and

fatigue. In addition to undergoing castration, patients may also be treated with AR antagonists or inhibitors that directly block the AR enzymes, preventing the synthesis of adrenal or intratumoral androgens.

ANDROGEN RECEPTOR

Structure and function

AR is a nuclear receptor and a member of the nuclear hormone receptor (NHR) family of transcription factors. It is also a multidomain protein that contains three unique domains: (1) an N-terminus domain (NTD) that plays a role in transactivation of AR downstream genes, (2) DNA-binding domain (DBD) that is next to the NTD, (3) the hinge region, and (4) at the C-terminus domain (CTD) contains the ligand-binding domain (LBD), which is encoded by 8 exons located on Xq11-12 [12]. In order for AR to begin its activity, an agonist must bind onto the LBD. Hence, targeting and blocking the LBD will deactivate the AR activities.

Typically, in the prostate, testosterone is converted by the prostate cells into a more potent form of androgen, dihydrotestosterone (DHT), using a 5α -reductase enzyme. DHT is about 50 times more potent than testosterone. When AR is in its inactive state, it resides in the cell cytoplasm bound to heat shock protein-90 (HSP90) and heat shock protein-70 (HSP70). Once androgens bind to the LBD, AR dissociates from the HSP90 and HSP70 and enters the nucleus where it dimerizes with another activated AR [13]. Once in the nucleus, the dimerized AR can then interact with other cofactors or transcription factors, such as lysine specific demethylase 1A (LSD1, which will be discussed later in this dissertation paper) in order to regulate the expression of AR-specific genes, such as PSA and other metabolic, survival, and proliferation pathways.

The DBD and the hinge region play an important role in the nuclear translocation function of AR. These two regions of the AR contain two separate nuclear localization signals (NLS) that interact with the α/β nuclear import complex. In addition, upon androgen binding to AR, several intermolecular and intramolecular interactions induce conformational changes. These conformational changes allow the LBD and the FxxFL-like motifs of the NTD to tightly bind to the androgen. The FxxLF or LxxLL on the LBD in other nuclear hormone receptors mainly serves as a docking site for coactivator and corepressor proteins. The AR contains the NTD that competes with potential coregulators at the FxxLF or LxxLL regions for the binding to the LBD. This NTD-LBD binding stabilizes the ligand bound to the AR and protects the AR from degradation or denaturation through destabilization [14]. The interactions between AR to homodimerize with another AR are mediated by the DBD. In addition, the DBD also allows the AR to interact with the androgen response elements (ARE), which are inverted hexameric repeats spaced

by three nucleotides, such as the sequence 5' - AGGTCANNNTGACCT - 3' [15]. This ultimately allows for downstream AR transcription to occur. The DBD contains two zinc-fingers, with one binding to the ARE, and the other interacting with activated AR monomers. The way AR homodimerizes is the head-to-head fashion, whereas the LBD containing the androgen is faced towards each other and dimerized together [16].

When comparing AR to other members of the NHR family, such as glucocorticoid receptor (GR) and estrogen receptor (ER), AR is the only one that uses NTD for its transactivation activities compared to other NHR that use CTD instead. The NTD of the AR is composed of two transactivation units (TAUs), the TAU-1 and TAU-5 (amino acids 360-528) [17]. TAU-5 is responsible for the ligand-independent transactivation. TAUs are important as they bind to other coregulators, such as LSD1, that help to modify the chromatin structure to increase or decrease the access to the transcriptional machinery. There are over 170 AR coregulators identified, including LSD1 which can repress or activate transcription; histone acetyltransferases (HATs), such as p300/CBP and p160/SRC that can increase transcription of target genes by opening the chromatin structure; and histone deacetylases (HDACs) that can repress transcription [18]. AR interacting with some of these coregulators, including LSD1, can target its own gene to make more AR.

Growth and Development

During embryonic development, childhood development, and adulthood development, androgens play a critical role in puberty, fertility, and homeostasis. The downstream function and action of androgen is solely mediated through the AR. The development of being a male or a female can be determined by the presence of the sex-determining region Y protein on the Y sex chromosome. This factor plays an important role in testes development, which is responsible for the development for the prostate, seminal vesicle, and other male reproductive organs [19].

For young males, before hitting puberty, rather than being driven by synthesized testosterone from Leydig cells in the testes, their body is driven by adrenal androgens, such as DHEA and ACTH. During maturation and puberty, males undergo changes, such as experiencing increased pubic and underarm hair. In the process of puberty, males begin developing enlarged testes, penis, larynx, and bone and muscle mass, and height. They also develop a deeper voice, behavior changes, and begin spermatogenesis [20]. This is because during puberty, testosterone becomes the main mechanism of action creating androgenic and anabolic actions.

In both adult male and females, the testosterone can be aromatized into estrogen that subsequently activates the estrogen receptor, which plays an important role in bone mass during puberty

and the overall maintenance of bone health. Thus, testosterone can decrease bone resorption, increase bone formation, and help maintain bone mass due to its ability to increase the survival and proliferation level of cells that produce the bone matrix, such as osteoblasts [21].

Normal function of Androgen Receptor in the prostate

Although AR activity plays a role in the progression of PCa growth and survival, the AR in normal prostate epithelium inhibits proliferation and promotes differentiation. In prostate, only the luminal cells are AR-positive, highly differentiated, and androgen-dependent. These cells can go through proliferation and apoptosis under controlled stimulus, and express differentiation markers, such as PSA and prostatic acid phosphatase [22]. The prostate also has AR-negative cells, which are basal cells. Unlike luminal cells, basal cells are androgen-independent and are less differentiated. Basal cells experience high levels of proliferation and low levels of apoptosis. In addition, the prostate contains a small percentage of neuroendocrine cells (which will be discussed in more detail later in this dissertation paper). The prostate also contains prostate stem cells, which divide asymmetrically, with half of its division forming the transient self-renewal stem cell population, and the other half forming luminal cells or neuroendocrine cells [23].

Testosterone biosynthesis

To fully understand the mechanisms of action during ADT to prevent the activation of AR, or castration, it is important to understand testosterone biosynthesis, which creates the androgens in the male. Testosterone is derived and synthesized from cholesterol hormones. Testosterone biosynthesis initially begins in the hypothalamus, which secretes gonadotropin-releasing hormone (GnRH) that induces cells from the pituitary gland to produce gonadotropins luteinizing hormone (LH) and follicle stimulating hormone (FSH). Both FSH and LH affect the testes, while only the LH influence Leydig cells to begin testosterone production [24].

The initial step of testosterone biosynthesis begins when the GnRH binds onto the GnRH receptor on the gonadotrophs, which are dimeric hormones that contain a common α subunit and a unique β subunit. Upon binding, the 7-transmembrane G-protein coupled receptor, or the GnRH receptor activate phospholipase C, catalyzes the hydrolysis of phosphatidylinositol 4,5-bisphosphate at the inner leaflet of the plasma membrane into two second messengers, inositol 1,4,5-trisphosphate (IP3) and diacylglycerol. The IP3 then moves to the endoplasmic reticulum (ER) and binds to the ligand-gated Ca^{2+} channels in order to release Ca^{2+} into the cytoplasm and upregulate the cellular transcription as well as release FSH and LH into the circulating environment [25].

Once LH is released into the environment, it can stimulate the Leydig cells by binding onto their LH receptors, which are G protein-coupled receptors. The binding between the LH and its receptor stimulates the exchange of GDP for GTP on the α -subunit of the heterotrimeric G-protein, which can then activate the adenylate cyclase. The adenylate cyclase converts AMP to cAMP, which is important for the activation protein kinase A to phosphorylate the CREB transcription factor and stimulate the production of testosterone biosynthesis enzymes [26]. The cAMP production plays a critical role for the first step in testosterone synthesis as it helps cholesterol transport from the outer to the inner mitochondrial membrane [27].

LH stimulation may lead to either acute or chronic testosterone synthesis. Acute LH stimulation can be characterized by the rapid transport of cholesterol into the inner mitochondrial membrane. Chronic LH stimulation can be characterized by the upregulation of transcription of steroidogenic enzymes, one of which is the steroidogenic acute regulatory protein (StAR) that helps transport cholesterol from the outer to the inner mitochondrial membrane [28].

Now that the testosterone biosynthesis enzymes are created and cholesterol is in the inner membrane of the mitochondria, the next step in testosterone synthesis is to carry out a reduction-oxidation reaction. This is achieved by two classes of enzymes: the cytochrome p450s (CYP) and the hydroxysteroid dehydrogenases (HSD). Within the inner mitochondrial membrane, the CYP250 side chain cleavage (P450_{scc}), which requires oxygen and NADPH to function, can cleave the C22-C20 of the cholesterol to produce 21-carbon pregnenolone [29]. This reaction only takes place within the mitochondrial environment.

After the cleavage, the 21-carbon pregnenolone leaves the mitochondria and diffuses to the ER to begin the final step for testosterone biosynthesis. In the ER, β -HSD with NAD cofactor acting as an electron acceptor, can convert the Δ^5 - 3β hydroxysteroid of the 21-carbon pregnenolone into a Δ^4 -3 ketosteroid to create the pregnenolone hormone. Pregnenolone is further converted by CYP17 (17 α -hydroxylase), using hydroxylation catalysis and requiring one molecule of oxygen and NADPH to cleave pregnenolone at the C17-C20 bond, forming a 17 α -hydroxyprogesterone, or androstenedione. This newly formed 17 α -hydroxyprogesterone hormone is then further converted by 17 β -HSD that uses oxygen and an NADPH-dependent reaction to reduce the C17 and form testosterone. Within the cytoplasm, the 5 α -reductase uses NADH as an electron donor to metabolize testosterone into a more potent and naturally occurring androgen, dihydrotestosterone (DHT). 5 α -reductase can also function to aromatize testosterone into estrogen. Estrogen can then be metabolized even further by 3 α -hydroxysteroid dehydrogenase into 3 α -androstenediol, a weaker type of androgen [30].

Testosterone makes up about 90% of all circulating androgen, while the remaining 10% of circulation androgen comes from the release of adrenocorticotrophic hormone from the pituitary gland, which also stimulates further androgen release from the adrenal gland [31].

ANDROGEN DEPRIVATION THERAPY

In 1941, Dr. Charles Huggins discovered the correlation between the hormones given to PCa and their rate of activity, concluding that PCa is a hormonal-responsive disease. He observed that the activity of serum acid phosphatase activity was strongly correlated with metastatic PCa. When castration was done or estrogen was injected, he noticed that the activity of the acid phosphatase was decreased, whereas when testosterone was injected, acid phosphatase activity increased. This finding laid out the fundamental foundation for the widely used ADT [32]. The treatment methods of castration and estrogen injection for men with advanced stage PCa was proven to be very effective. Thus, in 1966, Dr. Charles Huggins was awarded the Nobel Prize in Physiology and Medicine for his findings and contribution in treating PCa [33].

ADT is typically used when patients have recurrence after castration and develop a more progressive castration-resistant prostate cancer (CRPC). There are a couple drugs approved as ADT against CRPC, with LHRH (or GnRH) agonists. Patients initially experience tumor flare, as their level of hormones goes up, resulting in the internalization of the LHRH receptor that eventually leads to testosterone downregulation. Abiraterone, a CYP17 inhibitor, can also be used to achieve the total androgen blockade by inhibiting the synthesis of adrenal and intratumoral androgens [34]. Other commonly used drugs are AR antagonists, including enzalutamide which directly binds and competes with androgen on the LBD of the AR [35].

Enzalutamide

There are many mechanisms that lead to AR signaling in CRPC, and more than 70% of these CRPC are AR dependent and require AR for survival and progression [36]. Thus, it is critical to seek out therapy that can target AR, and at the same time can overcome the CRPC resistance mechanism.

In 2009, Dr. Charles Sawyers discovered a novel compound, enzalutamide, which is an anti-androgen that inhibits AR signaling. His discovery was very significant because during the time, bicalutamide and flutamide were used as AR antagonists. However, AR overexpression or mutations in the LBD of the AR rendered these drugs useless, whereas enzalutamide continued to reduce AR signaling. In addition, unlike bicalutamide, enzalutamide did not contain any agonist activities on mutant AR, but instead enzalutamide continued to reduce AR nuclear translocation, DNA-binding, and the recruitment of coactivators [37].

During the clinical trial phase I and phase II, enzalutamide had shown promising effect in PCa patients in decreasing PSA levels indicated from the FDHT-PET scan. The effects of enzalutamide were very effective in both patient groups: one without prior chemotherapy experience and one with chemotherapy [38]. This led enzalutamide to hit phase III clinical trials where its effect was shown to reduce death rates by 29-37% and increased overall survival by 2-5 months for chemotherapy-naïve and chemotherapy-treated patients, respectively, compared to the control group. Eventually, enzalutamide was approved by FDA in 2012 to treat CRPC [39].

Resistance

It remains unclear how PCa developed resistance towards hormonal therapy, and there are numerous research teams currently studying this mechanism. The development of CRPC includes AR amplification, ligand-independent mutations, increased AR sensitivity to low levels of androgen, and the bypassment of AR signaling with other survival pathways under AR loss conditions and the aberrant splicing of the AR, resulting in truncated AR variants, such as ARV7 (or AR3), that have lost their ligand-binding domain (LBD) [40]. This ARV7 isoform was discovered to have strong ties with enzalutamide and abiraterone resistance. ARV7 is constitutively active, which allows for AR signaling to resume, leading to cancer survival and proliferation even in the absence of androgens.

ANDROGEN RECEPTOR SPLICE VARIANT V7

Androgen Receptor V7

ARV7 was first discovered from two independent groups: one from John Hopkins University and the other from the University of Maryland. The first group, Hu et al., discovered seven different AR splice variants, all of which were truncated and missing the LBD after exon 3. Of the seven expressed truncated forms of AR, only ARV7 predominantly showed correlation with increased PSA levels after post-surgical and biochemical procedures [41]. ARV7 is a truncated form of AR, but its exon 3 is modified and merged with part of intron 3 spliced to form the cryptic exon 3 (CE3). Since ARV7 is truncated after the exon 3, it is missing the hinge region, which plays an important role with NLS alongside with the DBD. Chan et al., demonstrated that the truncation of the ARV7 does not completely exclude ARV7 from entering the nucleus. This is because the amino acid K629 and R631 in the CE3 of the ARV7 align with the K629 and R631 of the hinge region of the AR full length (AR-FL). These two residues at that position are partly necessary for ARV7 nuclear localization [42]. In addition, LBD contains the nuclear export signal (NES) that helps export the proteins from the nucleus into the cytoplasm [43]. Since ARV7 lacks the LBD, it also lacks the NES; and thus, it is possible that once ARV7 is made, it remains in the nucleus.

Unlike AR-FL, ARV7 is a ligand-independent nuclear receptor, which means that it is constitutively active for nuclear localization and transcriptional activity even when there exists androgen or lack of androgen. ARV7 also regulates the expression normally expressed by AR, such as PSA. However, ARV7 can regulate proliferation gene subsets, whereas the AR-FL regulates its proliferative genes to be more associated with differentiation. For clarification, both AR-FL and ARV7 affect the same genes, but the way the genes are regulated by the AR or ARV7 is different as they may interact with different coregulators and push the cells towards differentiation versus proliferation. In either case, the expression of PSA increases; and hence, can be used as a cancer biomarker.

Interestingly, in several prostate cancer cell lines, the transcriptional expression level of ARV7 can be upregulated or downregulated by androgen or antiandrogen compounds, such as DHT or enzalutamide, respectively. Liu et al., demonstrated that ARV7 splicing was dependent on the transcriptional rate of AR. In other words, an increase in AR transcription rate led to an increase in alteration in the loading of splicing factors leading to an increased expression in ARV7. Lui et al., also showed that in enzalutamide treated VcaP cells, there was the same expression level of splicing factors, but the activities and recruitment of the splicing factors to the AR transcripts were increased. Under enzalutamide treated PCa, splicing factor was reported to be recruited at the exon-intron junction of exon 3, cryptic exon 3b, and exon 4. However, there was no observed recruitment of splicing factors at cryptic exon 3b, consistent with their low ARV7 expression in LNCaP cells. In addition, mutations identified at the intronic and exonic splicing enhancers around the cryptic exon 3b could lead to the decrease in ARV7 expression, not affecting the AR-FL. Although enzalutamide did not change the expression levels of splicing factors, studies have shown that siRNA knockdown of splicing factors, hnRNP1/U2AF65 that bound the intronic splicing enhancers, or ASF/SF2 that bound to the exonic splicing enhancers decreased the ARV7 expression levels [44].

There are several types of PCa cell line models that express ARV7, such as 22RV1. Interestingly, the expression of ARV7 in VcaP and LNCaP95 cell lines are regulated by androgens, while the expression of ARV7 in 22RV1 are not affected by hormonal changes but are more robust and are expressed at nearly similar level to its AR-FL. These unique characteristics of 22RV1 are mainly due to their repeated copies of their exon 3 region, which evolve from cancer relapsing. This duplication or repeat occurs between exon 2b and exon 3 and between cryptic exon 3c and exon 4, which are common sites where DNA is spliced [45]. This duplication phenomenon is mainly found in metastatic CRPC and not in primary tumors.

Clinical resistance

There existed a strong association between ARV7 expression and enzalutamide resistance in vitro and in clinical. The knockdown of ARV7 by siRNA in the 22RV1 cell line resensitized the cells to enzalutamide as well as to androgen depleted conditions. Also, the addition of androgens enhanced the ARV7-knockdown 22RV1 sensitivity to growth and progression [46]. To determine how clinically relevant ARV7 was, a study was done on 62 men with CRPC, receiving either enzalutamide or abiraterone in addition to ADT. Of these 62 men, 30% were ARV7 positive. Men that had previous treatment with enzalutamide were treated with abiraterone for this study, and vice versa. The mRNA level of ARV7 from each patient was measured prior to their treatment. At the conclusion of the study, ARV7-positive men had no responses to either enzalutamide or abiraterone treatment, while more than half of the men that were ARV7 negative responded to their treatment. In addition, ARV7-positive men also had lower progression-free survival. More than 50% of ARV7-negative men responded well to the treatment [47]. However, the other half of the ARV7-negative men might have other forms of resistance mechanisms that caused androgen therapy resistance. In addition, the nonresponsive phenomenon from both ARV7-positive and ARV7-negative men might be from their prior treatment with enzalutamide or abiraterone, which had no statistical differences in their response rate to their received treatment. However, there were significant differences in ARV7-positive versus ARV7-negative men who did not previously receive these treatments. Overall, this finding suggested that the treatment from these drugs could possibly stimulate other resistance mechanisms by the CRPC.

In another study, ARV7 expression was suggested to be the result of ADT. The authors wanted to determine if ARV7-negative men could have the transition to ARV7-positive through the use of ADT. A study was carried out with 42 ARV7-negative men, in which 6 patients developed ARV7. Although the result was not clear, it raised the question of whether ADT could cause ARV7 expression, and whether ARV7 expression could lead to resistance to enzalutamide and abiraterone.

Some studies hypothesized that ARV7 could also play a role in docetaxel resistance, which was a microtubule inhibitor that impaired the depolymerization required for nuclear trafficking, preventing AR nuclear translocation and AR transcription [48]. Since ARV7 was constitutively active and was primarily located in the nucleus, it could help resist the effect from docetaxel especially since ARV7 did not require microtubules to translocate to the nucleus. Although there were no direct and concrete studies on this hypothesis, there were a few studies that gave subtle evidence to these phenomena. For example, men that were previously treated with abiraterone or enzalutamide were less responsive to their current treatment with docetaxel.

REFERENCES

- 1) Xie SW, Wang YQ, Dong BJ, Xia JG, Li HL, Zhang SJ, Li FH, Xue W (2018) A Nomogram Based on a TRUS Five-Grade Scoring System for the Prediction of Prostate Cancer and High Grade Prostate Cancer at Initial TRUS-Guided Biopsy. *Journal of Cancer* 9 (23):4382-4390. doi:10.7150/jca.27344
- 2) Barry MJ, Simmons LH (2017) Prevention of Prostate Cancer Morbidity and Mortality: Primary Prevention and Early Detection. *Medical Clinics of North America* 101 (4):787-806. doi:https://doi.org/10.1016/j.mcna.2017.03.0091) Prostate cancer statistics 2020, American institute for cancer research.
- 3) Karen S Sfanos and Angelo M De Marzo. Prostate cancer and inflammation: the evidence (2014)., *Histopathology*.
- 4) Martignano et al., GSTP1 Methylation and Protein Expression in Prostate Cancer: Diagnostic Implications. (2016)., *Disease Marker*.
- 6) Seo et al., Regulation of Steroid 5-alpha reductase type 2 (Srd5a2) by Sterol Regulatory Element Binding Proteins and Statins., 2011. *Experimental Cell Research*.
- 7) The PSA Test., 2020. Prostate Cancer Foundation
- 8) Christopher M Rembold., 1998. Number needed to screen: development of a statistic for disease screening. *British Medical Journal*.
- 9) Indu Kohaar et al., 2019. A Rich Array of Prostate Cancer Molecular Biomarkers: Opportunities and Challenges. *International Journal of Molecular Sciences*.
- 10) Peter Lawson et al., 2019. Persistent Homology for the Quantitative Evaluation of Architectural Features in Prostate Cancer Histology. *Scientific Reports*.
- 11) NCI Staff. 2017. Alternate Driver of Treatment-Resistant Prostate Cancer Identified. National cancer institute.
- 12) Vanessa Duong. (2008) Regulation of hormone signaling by nuclear receptor interacting proteins. *Advance Experimental Medical Biology*.
- 13) Arun K Roy., 2006. Androgen Receptor: Structural Domains and Functional Dynamics after Ligand-Receptor Interaction. *Annals of the New York Academy of Sciences*
- 14) Folake A Orafidiya and Iain J McEwan, 2015., Trinucleotide repeats and protein folding and disease: the perspective from studies with the androgen receptor. *Future Science OA*.
- 15) Unnati Jariwala et al., (2007). Identification of novel androgen receptor target genes in prostate cancer., *Molecular Cancer*.
- 16) Marta Nadal et al., (2017). Structure of the homodimeric androgen receptor ligand-binding domain. *Nature communication*.
- 17) Raj Kumar et al., (2004). Induced α -Helix Structure in AF1 of the Androgen Receptor upon Binding Transcription Factor TFIIF. *Journal of Biochemistry*.
- 18) Yepeng Luan et al., (2015) Histone acetyltransferases (HATs) are enzymes that acetylate conserved lysine residuals on histone proteins by transferring an acetyl group from acetyl CoA to form ϵ -N-acetyl lysine. *Epigenetic in Human Disease*.
- 19) Matt Quin. 2019. The seminal Vesicles. *TeachMe Anatomy*.
- 20) Emily Crawling. 2020. Puberty. *TeachMe Physiology*.
- 21) Amjob Javed. 2016. Genetic and Transcriptional Control of Bone Formation. *Oral Moaxillofac Surgical Clinic North American*.
- 22) Emma E Oldridge et al., (2011). Prostate cancer stem cells: Are they androgen-responsive? *Molecular Cellular Endocrinology*.
- 23) Yin Sun et al., (2009) Neuroendocrine differentiation in prostate cancer. *American Journal of Translational Research*.
- 24) Richard Bowen (2018). Gonadotropins: Luteinizing and Follicle Stimulating Hormones. *VIVO pathophysiology*.
- 25) Seung H Yoo. 2000. Coupling of the IP3 receptor/Ca²⁺ channel with Ca²⁺ storage proteins chromogranins A and B in secretory granules. *Trends in NeuroScience*
- 26) (2005). CREB is a member of the bZIP transcription factor superfamily, which contains a subfamily of cAMP and calcium-responsive transcriptional activators. *Methods in Enzymology*.
- 27) Malena B Rone et al., (2010). Cholesterol transport in steroid biosynthesis: Role of protein-protein interactions and implications in disease states. *Biochimica et Biophysica Acta*.
- 28) Vicent Ribas et al., (2016). Mitochondria, cholesterol and cancer cell metabolism. *Clinical Translational Medicine*.
- 29) Hani Atamna et al., (2012). Mitochondrial pharmacology: Electron transport chain bypass as strategies to treat mitochondrial dysfunction. *Biofactors*.
- 30) Ethan D Grober (2014). Testosterone deficiency and replacement: Myths and realities. *Cancer Urology Association Journal*.
- 31) (2018). Testosterone. You and your hormone.
- 32) Kurtis Eisermann et al., (2013). Androgen receptor gene mutation, rearrangement, polymorphism. *Translational Andrology and Urology*.
- 33) Alicia Di Rado. (2005). USC surgeon receives urologic oncology society's top honor. *USC News*.
- 34) Prostate cancer hormone Therapy – Combined Androgen Blockade. *Prostate Cancer Treatment Guide*.
- 35) Kush Dalal et al., 2014. Selectively Targeting the DNA-binding Domain of the Androgen Receptor as a Prospective Therapy for Prostate Cancer. *Journal of Biological Chemistry*.
- 36) Zhuangzhuang Zhang et al., 2018. Inhibition of the Wnt/ β -catenin pathway overcomes resistance to enzalutamide in castration-resistant prostate cancer. *Cancer Research*.
- 37) Javier Guerrero et al., (2013). Enzalutamide, an androgen receptor signaling inhibitor, induces tumor regression in a mouse model of castration-resistant prostate cancer. *The Prostate*.
- 38) Ernest N Lo et al., (2015). Prospective Evaluation of Low-Dose Ketoconazole Plus Hydrocortisone (HC) in Docetaxel Pre-treated Castration-Resistant Prostate Cancer (CRPC) Patients. *Prostate Cancer Prostatic disease*.
- 39) Xtandi (enzalutamide). Xtandi.com
- 40) MH Eileen Tan et al., 2014. Androgen receptor: structure, role in prostate cancer and drug discovery. *Acta Pharmacologica Sinica*.
- 41) Laura Cato et al., 2019. ARV7 Represses Tumor-Suppressor Genes in Castration-Resistant Prostate Cancer. *Cancer Cell*.
- 42) Anthony Saprita et al., 2003. Identification and Characterization of a Ligand-regulated Nuclear Export Signal in Androgen Receptor. *Journal of Biological Chemistry*.
- 43) Kosugi et al., 2008. NES sequences are diverse and 11 patterns were defined by a peptide library-based study and structural analyses of exportin-1/CRM1-NES. *Encyclopedia of Bioinformatics and Computational Biology*.
- 44) Mary Nakazawa et al., 2015. Androgen Receptor Splice Variants in the Era of Enzalutamide and Abiraterone. *Hormone Cancer*.

- 45) ES Antonarakis et al., 2016. Androgen receptor variant-driven prostate cancer: clinical implications and therapeutic targeting. *Prostate Cancer Prostatic Disease*.
- 46) Bo Cao et al., 2014. Androgen receptor splice variants activating the full-length receptor in mediating resistance to androgen-directed therapy. *Oncotarget*.
- 47) Emanuel S Antonarakis et al., 2015 AR-V7 and Resistance to Enzalutamide and Abiraterone in Prostate Cancer. *New England Journal of Medicine*.
- 48) Emmanuel S Antonarakis et al., 2016. Androgen Receptor Splice Variant 7 and Efficacy of Taxane Chemotherapy in Patients With Metastatic Castration-Resistant Prostate Cancer. *JAMA Oncology*.

CHAPTER 2

INTRODUCTION TO LYSINE-SPECIFIC DEMETHYLASE 1A

Lysine-specific Demethylase 1A (LSD1) is one candidate that may play a critical role in the progression of CRPC by inducing androgen-independent transitions in PCa. LSD1, a flavin adenine dinucleotide (FAD)-dependent histone-modifying enzyme responsible for demethylation of histone H3 lysine 4 (H3K4) and histone H3 lysine 9 (H3K9), plays a key role in the progression of CRPC by interacting with AR and being involved in neural differentiation, in general. We suggest LSD1 may be a promising target for developing new treatments against CRPC with either low or high AR activity. In this chapter, we review pharmacological, biochemical, and the genetic evidence of LSD1 and how it may mediate PCa neuroendocrine differentiation and regulate AR and ARV7.

EUKARYOTIC GENE REGULATION

Regulation of gene expression requires many complex activities to involve specific operation of cells. Within prostate cancer and many other cancer types, the control over gene expression is disrupted where gain-of-function or loss-of-function activities may dysregulate the normal process of the cells. Here, we will review over some mechanisms for how such gene misregulation may arise within specific cellular components.

The nucleosome

Within the nucleus of a cell, DNA can be found wrapped around a protein called histone, which helps compact the DNA. The DNA-wrapped histones can also be called a nucleosome that have approximately 146 DNA base pairs wrapped around. The histones are pairs of H2A, H2B, H3, and H4 subunits where the pair of H2A and H2B histone subunits join with the pair of H3 and H4 histones to form an octamer core [1]. The histones contain some positively charged amino acids that interact with the negatively charged phosphate group of the DNA backbone. These interactions allow the DNA to wrap around the histones, and with multiple nucleosome interactions, they can appear like beads on a string [2].

The strength of the DNA and histone can greatly vary. For example, when the DNA is wrapped around the histone tightly, termed a heterochromatin, it prevents proteins and other regulatory proteins from accessing the DNA; and thus, repressing transcription or replication [3]. On the other hand, when the DNA is loosely wrapped around the histone, termed a euchromatin, it allows the opportunity for many proteins and regulatory proteins to interact with the DNA promoting transcription or replication. The

heterochromatin and euchromatin of the DNA can change throughout the cells if influenced by a series of chromatin remodeling complexes [4].

Post-translational modification of histones

The histones contain multiple freely extended tails that can be altered to affect gene transcription by interacting with proteins and transcription factors. The alteration induced by the tails can also be referred to as epigenetic modification, which is the turning on or off genes [5]. The type of histone tail alteration includes methylation, phosphorylation, acetylation, biotinylation, ubiquitination, and SUMOylation. Depending on the modification and the site of the modification, the histone tails can be induced to repress or activate gene expression. For example, once marked to become active, the histone tails can recruit activator and polymerase proteins for transcription [6]. Whereas, when the histone tails are negatively marked, they can recruit repressors that induce them into a heterochromatin state.

Histone acetylation is usually associated with active gene transcription, and so when there is excessive acetylation of the tail, or hyperacetylation, gene transcription is active [7]. On the other hand, when there is low level of acetylation of the tail, or hypoacetylation, gene transcripts are low or reduced. Acetyl is a negatively charged molecule that works by interacting with positively charged amino acid residues, such as lysine and arginine that enhance the binding interaction with the DNA phosphate backbone. Thus, once these positively charged amino acids are acetylated, they become neutralized and loosen their binding to DNA, allowing access and opportunity for transcription. Moreover, active gene transcription may also be induced through histone phosphorylation where phosphate interacts with threonine and serine to enhance its negative charge, which can repel against the negatively charged phosphate backbone of the DNA. On the other hand, the methylation of the histone tails can either turn on or turn off gene expression [8].

The study of epigenetics has been very complicated and has many contradictory observations [9]. For example, acetylation of histone 4 at lysine 12 (H4K12) is expected to lead to euchromatin and active transcription, however, heterochromatin is formed instead [10]. Furthermore, the methylation of H3K4 can go either direction where it can recruit chromatin remodeler CDH1 and acetyltransferase to induce gene transcription or recruit Sin3-HDAC1 deacetylase to repress gene transcription [11]. Due to these contradictions and complexities, the turning off or on of a gene depends on the number and variety of histone modifications [12].

Determining the role of proteins in post-translational modification can help us understand the control processes of cellular proliferation and differentiation. Histone acetyltransferase (HAT) and histone deacetylase (HDAC) are enzymes that counteract with one another in the control of histone acetylation to

keep balance of our gene expression. Moreover, histone methylase transferase (HMT) and histone demethylase (HDM) control the histone methylation balance for gene expression [13]. The function of these enzymes typically depends on their complex with other proteins, such as binding to Androgen Receptors (AR) to carry out gene transcription. HDM, such as Lysine-demethylase 1A (LSD1), has function in cell-cycle regulation, cellular differentiation, and proliferation. Studies have shown that inhibiting LSD1 as tumor treatment can suppress growth and induce apoptosis [14]. Thus, for the remainder of this chapter, we focus on the types of HDM, including LSD1, which remove methyl groups from amino acids.

HISTONE LYSINE METHYLATION AND DEMETHYLATION

The amino acids Arginine and Lysine on the histone tail can be epigenetically modified with the addition of attached methyl groups, allowing them to be mono-, di-, or tri-methylated. Due to its small chemical size and lack of charges, the methyl group does not directly affect the turning on and off of the chromatin complex, but rather becomes a site for regulatory protein binding [15]. Having multiple methyl groups at numerous sites on the histone tail gives out numerous functional possibilities.

Not all proteins can recognize the methylated tails, so there are limited regulatory proteins that can bind to the methyl histone tails. For example, heterochromatin protein 1 (HP1) or chromodomain helicase DNA-binding protein (CDH1) can bind to methylated H3K9 [16] while checkpoint protein p53-binding protein 1 (P53BP1) and vertebrate transcriptional activator WDR5 can bind to methylated H3K79 to either assist in the activation or repression of the gene [17].

It was once thought that the methylation of the histone tail was irreversible, but it was not until the 2000s that the discovery of KDMs, such as LSD1, caused a paradigm shift in the study of epigenetics [18]. The first class of KDMs discovered were LSD1 and LSD2, which used FAD as a cofactor to demethylate specific sites on the histone tails or proteins. However, these amine oxidase enzymes could only remove mono- and di-methylated proteins, and so they required additional enzymes involvement to assist with the initial removal of tri-methylated proteins. On the other hand, the second class of KDM were JmjC-domain containing proteins, including KDM2A, KDM4C, and KDM5A, which were metalloenzymes that used iron and α -ketoglutarate as cofactors and could demethylate mono-, di-, and tri-methylated sites on the histone tails.

The level of methylated lysine on the histone tail had a corresponding relationship with the progression of various cancers, including prostate cancer. There was considerable evidence that indicated HDMs, such as LSD1, play a direct interactive role with nuclear receptors, such as Androgen receptor (AR) [19]. After AR was activated by binding with an agonist, the AR translocated into the nucleus. Once

in a nucleus, HDMs, such as LSD1 and KDM4C bound onto the AR and acted as coactivators, guiding AR to find a specific AR at the promoter region to induce the demethylation of H3K9 [20].

LYSINE DEMETHYLASE 1A

LSD1 mechanism and function

LSD1 is grouped into the class of KDMs that are FAD-dependent amine oxidase. LSD1 requires FAD as its cofactor for it to function in lysine demethylation and can only demethylate the mono- and di-methylated lysine. It is because LSD1 can only oxidize the carbon-nitrogen bond between the methyl groups and the epsilon amine of the lysine residues to form an imine intermediate, which later gets hydrolyzed through a non-enzymic hydrolysis reaction into formaldehyde with the removal of this methyl group. Due to this mechanism, tri-methylated lysine residues cannot be oxidized and require a recruitment with additional enzymes or factors to help if demethylation of tri-methylated lysine is to be achieved.

LSD1 can function as a gene repressor by demethylating H3K4, or it can function as a gene activator demethylating H3K9, such as when it interacts with AR to upregulate AR-target genes [21-22]. Interestingly, it has been shown that LSD1 may occupy approximately 80% of the promoter regions to recruit RNA polymerase II for transcription, and so LSD1 may function more as an activator [23]. Some cellular functions that LSD1 helps induce include cellular differentiation and proliferation, repression of hTERT genes from making telomerases, and repression of metastasis genes by complexing with Snail1[24,25]. LSD1 can also demethylate lysines from other enzymes or proteins besides the histone tails. For example, LSD1 can remove the methyl group at K370 of the tumor suppressor p53, disrupting its interaction with a DNA damage checkpoint 53BP1[26]. LSD1 expression is also shown to correlate with the development of neuroblastoma and prostate cancer [27].

LSD1 structure

LSD1 contains three domains[28]; (1) The amine oxidase domain containing the FAD-binding domain; (2) the tower domain that can interact with compressors proteins [29]; and (3) the SWIRM domain that can bind to DNA or other factors such as AR.

LSD1 inhibitors

LSD1 is an important target as it has shown strong correlation with various disease progression. For example, studies that used tranylcyproline and phenelzine, an inhibitor of MAO, were shown to inhibit the demethylation of H3K4 leading to the differentiation induction of promyelocytic leukemia and slowed prostate cancer progression [30-32]. Another inhibitor, pargyline, a MAO B inhibitor was reported to inhibit the H3K9 demethylation activity of LSD1, which leads to decreased AR

gene expression in prostate cancer. Aziridine and propargylamine peptides are competitive inhibitors that can also be used to inhibit LSD1, while bisguinidine and biguanide are noncompetitive inhibitors of LSD1 that can lead to the reactivation of tumor suppressor genes in cancer cells [33].

LSD1 REGULATION OF NEURONAL DIFFERENTIATION AND DEVELOPMENT

LSD1 regulates neuronal gene expression programs

LSD1 was shown to play an important role in neuronal differentiation. RE1-silencing transcription factor (REST) is an important factor that can recruit LSD1 to the neuronal gene promoter site, which would repress neuron-specific genes, such as ion channels, synaptic vesicle proteins, and neurotransmitter receptors as well as chromogranin A, synaptophysin, and γ -enolase. In addition, other factors, such as orphan nuclear hormone receptors (TLX) can recruit LSD1 to maintain neuronal stem cell self-renewal, proliferative, and neurogenesis [34]. Moreover, knockdown of LSD1 via RNAi leads to a delay in neuronal differentiation. This evidence suggests that LSD1 has a positive role in neurogenesis regulation and stem cell maintenance, hinting that LSD1 may play an important role in neuroendocrine differentiation in cancer and in cellular proliferation and self-renewal in cancer stem cells; and thus, LSD1 may be a novel therapeutic target for both neuroendocrine prostate cancer and cancer stem cell derived prostate cancer [35].

REFERENCES

1. McClung CA et al., (2008). Neuroplasticity mediated by altered gene expression. *Neuropsychopharmacology*
2. Ronan JL et al., (2013). From neural development to cognition: unexpected roles for chromatin. *Nature Reviews Genetics*.
3. Millan MJ (2013). An epigenetic framework for neurodevelopmental disorders: from pathogenesis to potential therapy. *Neuropharmacology*.
4. Maze I et al., (2013). Histone regulation in the CNS: basic principles of epigenetic plasticity. *Neuropsychopharmacology*.
5. Nestler EJ et al., (2013). Epigenetic Basis of Mental Illness. *The Neuroscientist*.
6. Szyf M et al., (2015). Prospects for the development of epigenetic drugs for CNS conditions. *Nature Reviews Drug Discovery*.
7. Jenuwein T et al., (2001). Translating the histone code. *Science*.
8. Black JC et al., (2012) Histone lysine methylation dynamics: establishment, regulation, and biological impact. *Molecular cell*.
9. Akbarian S et al., (2009). Epigenetic regulation in human brain—focus on histone lysine methylation. *Biological psychiatry*.
10. Gupta S et al., (2010). Histone methylation regulates memory formation. *The Journal of neuroscience*.
11. Network T et al., (2015). Psychiatric genome-wide association study analyses implicate neuronal, immune and histone pathways. *Nature neuroscience*
12. Hawrylycz et al., (2012). An anatomically comprehensive atlas of the adult human brain transcriptome. *Nature*
13. Sáez JE et al., (2015) Decreased expression of CoREST1 and CoREST2 together with LSD1 and HDAC1/2 during neuronal differentiation. *PLoS one*
14. Burg et al., (2015). KDM1 class flavin-dependent protein lysine demethylases. *Peptide Science*.
15. López-Muñoz F et al., (2009). Monoaminergic neurotransmission: the history of the discovery of antidepressants from 1950s until today. *Current pharmaceutical design*
16. Khan MN et al., (2013). An overview of phenylcyclopropylamine derivatives: biochemical and biological significance and recent developments. *Medicinal research reviews*
17. Frieling H et al., (2006). Tranylcypromine. *European archives of psychiatry and clinical neuroscience*
18. Sandler M et al., (1990). Monoamine oxidase inhibitors in depression: history and mythology. *Journal of Psychopharmacology*
19. Shen et al., (1999). A history of antipsychotic drug development. *Comprehensive psychiatry*
20. Chen JJ et al., (2007). Comprehensive review of rasagiline, a second-generation monoamine oxidase inhibitor, for the treatment of Parkinson's disease. *Clinical therapeutics*.
21. Metzger E et al., (2005). LSD1 demethylates repressive histone marks to promote androgen-receptor-dependent transcription. *Nature*
22. Gaweska H et al., (2009). Use of pH and kinetic isotope effects to establish chemistry as rate-limiting in oxidation of a peptide substrate by LSD1. *Biochemistry*.
23. Shi Y et al., (2004). Histone demethylation mediated by the nuclear amine oxidase homolog LSD1. *Cell*
24. Huang J et al., (2007). p53 is regulated by the lysine demethylase LSD1. *Nature*.
25. Sakane N et al., (2011). Activation of HIV transcription by the viral Tat protein requires a demethylation step mediated by lysine-specific demethylase 1 (LSD1/KDM1). *PLoS Pathog*
26. Wang J et al., (2009). The lysine demethylase LSD1 (KDM1) is required for maintenance of global DNA methylation. *Nature genetics*.
27. Essen VD et al., (2010). A feed-forward circuit controlling inducible NF- κ B target gene activation by promoter histone demethylation. *Molecular cell*.
28. Schmidt DM et al., (2007). trans-2-Phenylcyclopropylamine is a mechanism-based inactivator of the histone demethylase LSD1. *Biochemistry*
29. Fang R et al., (2013). LSD2/KDM1B and its cofactor NPAC/GLYR1 endow a structural and molecular model for regulation of H3K4 demethylation. *Molecular cell*.
30. Colibus DL et al., (2005). Threedimensional structure of human monoamine oxidase A (MAO A): relation to the structures of rat MAO A and human MAO B. *Proceedings of the National Academy of Sciences of the United States of America*.
31. Binda C et al., (2003). Insights into the mode of inhibition of human mitochondrial monoamine oxidase B from high-resolution crystal structures. *Proceedings of the National Academy of Sciences*.
32. Edmondson D et al., (2003). Structure and mechanism of monoamine oxidase. *Burger's Medicinal Chemistry and Drug Discovery*
33. Yang M et al., (2007). Structural basis of histone demethylation by LSD1 revealed by suicide inactivation. *Nature structural & molecular biology* 58.
34. Islam MM et al., (2015). LX: A master regulator for neural stem cell maintenance and neurogenesis. *Biochimica et Biophysica Acta (BBA)-Gene Regulatory Mechanisms*
35. Fuentes P et al., (2011). CoREST/LSD1 control the development of pyramidal cortical neurons. *Cerebral cortex*.

CHAPTER 3

INTRODUCTION TO SANGUINARINE AND ITS ANTITUMOR EFFECTS

Sanguinarine (SNG) is a natural compound and a benzophenanthridine alkaloid that can be found from the root of *Sanguinaria canadensis* as well as other *Fumaria* species. These plants are from the poppy plant family. Throughout history, many anticancer agents have been found derived from plants, and so SNG may be a potential natural molecule with anticancer activities. Evidence has shown that SNG has anticancer and antiproliferative effects against tumor cells. The attenuation of tumors was shown to be due to SNG's pro-apoptotic and growth inhibitory effects. Other evidence has shown that SNG also has antiangiogenic and anti-invasive properties. In our studies, we will look at some of the recent evidence about the antitumor pathway by SNG, and then discuss its potential therapeutic applications.

Introduction

There are many different mechanisms that can result in tumor development, including uncontrollable cellular proliferation, avoiding cellular apoptosis, and the induction of metastasis and angiogenesis. Current treatment for these tumor phenomena includes surgery, radiation therapy, immunotherapy, cryogenic therapy, and hormone therapy. However, many tumors typically relapse, and these types of treatment have reduced efficacy, making it important to find more effective therapies. SNG may be an alternative anticancer therapeutic approach due to its low toxicity, antitumor, anti-inflammatory, and anti-angiogenesis activities [1].

Sanguinarine and its apoptotic activities

Typically, our body can induce cellular apoptosis to eliminate any damaged or mutant cells. However, some cells may develop mechanisms to avoid apoptosis and experience unregulated proliferation [2,3]. In cancer, pro-apoptotic factors, such as protease activating factor-1, Bax, caspases can be downregulated or dysfunctional, while anti-apoptotic factors, such as B cell lymphoma-2 (Bcl2) and cytochrome c may be upregulated. SNG has been shown to be able to inhibit the growth of several cancer cells, including prostate, breast, neuroendocrine, neuroblastoma, osteosarcoma, and many more through the induction of apoptosis at a micromolar concentration. However, there are not many studies that display the efficacy of SNG in vivo animal models.

Studies have demonstrated that SNG can inhibit tumor growth of B16 melanoma 4AS in C57L mice and of A375 human melanoma in athymic nude mice in vivo study [4]. In addition, we have shown that SNG can also inhibit tumor xenograft growth of 22Rv1, C42B-MDVR, and Cancer stem cells derived from 22Rv1 in nod scid balb/c mice. Although our studies did not focus on apoptotic

mechanisms, there are many other studies that did focus on apoptosis. For example, studies showed that SNG induced apoptosis through the activation of nuclear factor-kB (NF-kB), mitochondrial damage, and cell cycle arrest [5]. SNG can induce apoptosis through the induction of caspase-9 or through caspase-8 via DR pathway [6]. In addition, SNG can also induce apoptosis in several cancer cell lines through the cleavage of caspase-3 and PARP, which overall may downregulate pro-apoptotic genes such as Bcl2, cFLIP, cLAP2, XIAP, NOL3, and HRK[7,8]. Further, SNG can also act as an intercalating agent to induce DNA damage that can also induce apoptosis as shown in colon cancer and melanoma cells [9].

In normal cells, proliferation is very specific and requires the signaled activation of mitosis growth factors like cyclins and cyclin-dependent kinases (CDK) as well as the deactivation of CDK-inhibitor anti-growth signals like p21 and p27 [10]. SNG was shown to downregulate cyclin D1, D2, E, and CDK2, 4, and 6 in prostate cancers. SNG was also shown to inhibit cell cycle and proliferation progression at the G0/G1 phase through cyclin D1 and topoisomerase II in MCF-2 breast cancer [11].

Interestingly, the induction of apoptosis by SNG also leads to the byproduct of reactive oxygen species (ROS), which includes hydrogen peroxide, singlet oxygen, and superoxide anion radicals [12]. At a high level, these ROS can cause DNA and protein damage and so they would cause apoptosis in cells. A study was performed using antioxidants N-acetylcysteine or glutathione, which hindered cellular apoptosis induced by SNG. In addition, when cyclooxygenase-2 (COX2) is upregulated in cells, it also hinders cellular apoptosis induced by SNG. Thus, COX-2 inhibitors and SNG may have potential synergistic effects to induce further apoptosis [13].

Inflammatory factors, such as NF-kB, play an important role to control tumor developments [14]. When activated, NF-kB interacts with p50, p65, and IκBα, which later gets phosphorylated and ubiquitinated for degradation [15]. This would allow p50 and p65 to enter the nucleus to promote their gene transcription to promote cancer growth. SNG was shown to block the phosphorylation and the ubiquitination of IκBα leading to the induction of tumor necrosis as shown in human myeloid ML-1a cells [16].

The progression and growth of many solid tumors requires active angiogenesis, and SNG was shown to be able to inhibit tumor growth and proliferation by blocking de novo blood vessel formation *in vivo*, and repressing angiogenesis through the inhibition of VEGF, a known angiogenic growth factor [17]. Other angiogenesis factors that are suppressed by SNG are Akt, p38, and VE-cadherin [18]. There exists a potential for a combination therapy using SNG and VEGF promoting chemotherapeutics, such as dacarbazine [19].

Cellular metastasis is the leading cause of many cancer-related deaths. Metastasis can result from inflammation caused by the cancer to its environment where it induces proteases, such as matrix metalloproteinases (MMPs) to degrade the extracellular matrix of the basement membrane, which then allows the cancer to initiate cellular invasion [20]. SNG was shown to inhibit the expression of MMP-9, NF- κ B, and AP-1 pathways hindering cancer migration and invasion in breast cancer [21]. In addition, SNG can also inhibit STAT3, which is important for prostate cancer metastasis, migration, and invasion [22]. Thus, SNG can promote cancer apoptosis and prevent cancer invasion.

Sanguinarine and Cancer stem cell and Neuroendocrine

SNG was found to significantly inhibit lung CSC growth and invasion [23]. This was possibly achieved via downregulation of the Wnt/B-catenin signaling pathway. Stem cell recognized and regulatory genes OCT4, Nanog, SOX2, and Klf4 were recognized during this process. Lung CSCs were inhibited by more than 60%, showcasing its strong anti-cancer effects. Another study in which SNG is shown to regulate CSC development, in this example pancreatic CSCs. Cell proliferation and colony development capabilities decreased through apoptosis caused by oxidative stress, and a reduction of CSC cell renewal properties from human and mouse isolated pancreatic CSC samples was also observed. The Shh-Gli pathway was shown to be inhibited in this case. Cells with the CD133+CD44+CD24+ESA phenotype represented the CSC population in this study. First, second, and third generation spheroids were shown to decrease in viability as dosage was increased [24].

Sanguinarine has been found to induce apoptosis of neuroendocrine tumors through activation of the extrinsic apoptosis pathway. Treatment with sanguinarine caused an increase in caspase-3 levels in as little as 48 hours of incubation. This treatment also caused nuclear morphology changes to caspase 3. This study also showed that induction of apoptosis was a result of caspase induction [25]. Neuroblastoma has been found to exhibit properties that are like neuroendocrine tumors. CgA and NSE, which are found at higher concentration in neuroendocrine tumors, were also found in neuroblastoma [26]. A separate study also found that neuroblastoma tumors treated with sanguinarine showed similar results. The authors suggested that sanguinarine induced apoptosis could be mediated by the caspase-9-dependent mitochondrial pathways or the activation of caspase-3 and cleavage of PARP and the downregulation of Bcl-2 and c-FLIP or through a combination of all of them [27]. Sanguinarine causes upregulation in inhibition genes while also downregulating inhibition of apoptosis genes. Survivin is a gene involved in the control of cell division as well as inhibition of apoptosis. Sanguinarine has been shown to downregulate survivin and as a result can induce apoptosis and inhibit growth of human prostate cancer cells [28].

Synergistic therapies with Sanguinarine

Several naturally occurring products have been shown to resensitize multidrug resistance tumor, and studies have shown that combining these natural products with chemotherapeutics may be an effective means of treatment against various human diseases. A study has shown using SNG and digitonin with doxorubicin synergistically reduce colorectal cancer, Caco-2, and leukemia cells [29]. The main advantage of exploring the synergism of SNG with other chemotherapeutic agents is to reduce the dosage and maintain its effectiveness. In our study, we studied SNG and its synergism with dovitinib, another chemotherapeutic that is effective against cancer. Dovitinib was shown to induce neuroendocrine differentiation, a deadlier outcome of cancer. We have provided evidence that SNG can prevent neuroendocrine differentiation through the inhibition of LSD1, and that SNG and dovitinib may work synergistically by downregulating cellular growth and progression without the induction of neuroendocrine differentiation.

REFERENCES

1. Reddy L et al., (2003). Natural products for cancer prevention: a global perspective. *Pharmacol Ther.*
2. Steller H et al., (1995). Mechanisms and genes of cellular suicide. *Science.*
3. Meier P et al., (2000). Apoptosis in development. *Nature*
4. Stefano DI et al., (2009). Antiproliferative and antiangiogenic effects of the benzophenanthridine alkaloid sanguinarine in melanoma. *Biochem Pharmacol.*
5. Chaturvedi MM et al., (1997). Sanguinarine (pseudocheletrythrine) is a potent inhibitor of NF-kappaB activation, IkappaBalpha phosphorylation, and degradation. *J Biol Chem.*
6. Malíková J et al., (2006). The effect of cheletrythrine on cell growth, apoptosis, and cell cycle in human normal and cancer cells in comparison with sanguinarine. *Cell Biol Toxicol.*
7. Choi WY et al., (2008). Sanguinarine, a benzophenanthridine alkaloid, induces apoptosis in MDA-MB-231 human breast carcinoma cells through a reactive oxygen species-mediated mitochondrial pathway. *Chemotherapy.*
8. Kim S et al., (2008). Sanguinarine-induced apoptosis: generation of ROS, down-regulation of Bcl-2, c-FLIP, and synergy with TRAIL. *J Cell Biochem.*
9. Hammerová J et al., (2011). Benzo[c] phenanthridine alkaloids exhibit strong anti-proliferative activity in malignant melanoma cells regardless of their p53 status. *J Dermatol Sci.*
10. Adhami VM et al., (2004). Sanguinarine causes cell cycle blockade and apoptosis of human prostate carcinoma cells via modulation of cyclin kinase inhibitor-cyclin-cyclin-dependent kinase machinery. *Mol Cancer Ther.*
11. Kalogris C et al., (2014). Sanguinarine suppresses basal-like breast cancer growth through dihydrofolate reductase inhibition. *Biochem Pharmacol.*
12. Hussain AR et al., (2007). Sanguinarine-dependent induction of apoptosis in primary effusion lymphoma cells. *Cancer Res*
13. Huh J et al., (2006). Cyclooxygenase 2 rescues LNCaP prostate cancer cells from sanguinarine-induced apoptosis by a mechanism involving inhibition of nitric oxide synthase activity. *Cancer Res*
14. Karin M., (2009). NF-kappaB as a critical link between inflammation and cancer. *Cold Spring Harb Perspect Biol*
15. Ghosh S et al., (2002). Missing pieces in the NF-kappaB puzzle. *Cell.*
16. Chaturvedi MM et al., (1997) Sanguinarine (pseudocheletrythrine) is a potent inhibitor of NF-kappaB activation, IkappaBalpha phosphorylation, and degradation. *J Biol Chem.*
17. Dong XZ et al., (2013). Sanguinarine inhibits vascular endothelial growth factor release by generation of reactive oxygen species in MCF-7 human mammary adenocarcinoma cells. *Biomed Res Int*
18. Basini G et al., (2007). Sanguinarine inhibits VEGF-induced angiogenesis in a fibrin gel matrix. *Biofactors.*
19. Lev DC et al., (2003). Dacarbazine causes transcriptional up-regulation of interleukin 8 and vascular endothelial growth factor in melanoma cells: a possible escape mechanism from chemotherapy. *Mol Cancer Ther*
20. Sternlicht MD et al., (2001). How matrix metalloproteinases regulate cell behavior. *Annu Rev Cell Dev Biol.*
21. Park SY et al., (2014). Sanguinarine inhibits invasiveness and the MMP-9 and COX-2 expression in TPA-induced breast cancer cells by inducing HO-1 expression. *Oncol Rep.*
22. Abdulghani J et al., (2008). Stat3 promotes metastatic progression of prostate cancer. *Am J Pathol*
23. Yang J et al., (2016). Construction and application of a lung cancer stem cell model: antitumor drug screening and molecular mechanism of the inhibitory effects of sanguinarine. *Tumor Biol*
24. Yiming M et al. (2017). Sanguinarine Inhibits Pancreatic Cancer Stem Cell Characteristics by Inducing Oxidative Stress and Suppressing Sonic Hedgehog-Gli-Nanog Pathway. *Carcinogenesis*
25. Larsson DE et al., (2010). The Cytotoxic Agents NSC-95397, Brefeldin A, Bortezomib and Sanguinarine Induce Apoptosis in Neuroendocrine Tumors In Vitro. *Journal of Cancer Research and Treatment.*
26. Georgantzi K et al., (2018) Chromogranin A and neuron-specific enolase in neuroblastoma: Correlation to stage and prognostic factors. *Pediatr Hematol Oncology*
27. Cacen E et al., (2014). Promoting Effects of Sanguinarine on Apoptotic Gene Expression in Human Neuroblastoma Cells. *Journal of Cancer Prevention.*
28. Sun Meng et al., (2010). Sanguinarine Suppresses Prostate Tumor Growth and Inhibits Survivin Expression. *Genes Cancer.*
29. Eid SY et al., (2012). Synergism of three-drug combinations of sanguinarine and other plant secondary metabolites with digitonin and doxorubicin in multi-drug resistant cancer cells. *Phytomedicine*

CHAPTER 4

Sanguinarine (SNG) is a novel dual-inhibitor of Lysine-specific demethylase 1A (LSD1) and androgen receptor (AR) against castration-resistant prostate cancer

Victor Pham, Vinh X. Le, Thanh NH Le, Dongjun Fu, Matthew Tippin, Marvin Miller, Erik D. Tran, Raymond Rendon, Liankun Song, and Xiaolin Zi

ABSTRACT

Background: Lysine-specific demethylase 1A (LSD1) is considered as a promising target for treatments of castration-resistant prostate cancer ascribed to its interaction with androgen receptor (AR) and critical involvement in neuroendocrine differentiation. However, LSD1 inhibitors currently on clinical trials (i.e. GSK2879552 and ORY-1001) are not highly potent and specific to prostate cancer. Subsequently, we are seeking novel LSD1 inhibitors which can target specific molecular mechanisms that accelerate the progression to castration-resistant prostate cancer and the resistance to anti-androgen therapies, such as Enzalutamide.

Methods: Structural similarity search was performed for a series of analogs of flavin adenine dinucleotide (FAD), which is a cofactor of LSD1, and analogs of dihydrotestosterone (DHT), which is a cofactor of AR. Molecular docking was used to predict the binding energy within the putative activity pocket of LSD1 and AR. LSD1 enzyme activity was tested using H3K4Me and H3K9Me peptides as substrates. AR transcriptional activity luciferase reporter assay was carried out for screening AR inhibitors. Cellular thermal shift assay (CETSA) was performed to evaluate the target engagement in prostate cancer cell lines. The *in vitro* Surface Plasmon Resonance (SPR) assay was set up for direct binding affinity of inhibitors to LSD1. Western blotting analysis and quantitative PCR methods were used to detect the substrate modification of LSD1 and the expression of AR target genes. Cell growth inhibition was tested against androgen-sensitive, castration-resistant, and neuroendocrine/small cell carcinoma cell lines. Stable LSD1 suppression by short-hairpin RNA (shRNA) and LSD1 overexpression in prostate cancer cell lines were established to determine whether LSD1 is partially a required target for the growth-inhibitory activity of SNG. Patient-derived organoids were used to test the activity of SNG against the heterogeneity of prostate cancer.

Results: A series of naturally occurring polycyclic ammonium ions were identified to inhibit LSD1 enzyme, AR transcription, or both activities. Among the screened compounds, SNG is the most potent compound that equally inhibits both LSD1 and AR activities with an IC_{50} of about $2.13 \pm 0.18 \mu\text{M}$ and $2.07 \pm 0.45 \mu\text{M}$, respectively. SNG directly engages both LSD1 and AR protein complex, resulting in downregulation of the expression of AR, AR variant 7 (ARV7), and AR target genes. The binding affinities of SNG to LSD1 and AR are $1.10 \pm 0.42 \mu\text{M}$ and $2.54 \pm 0.89 \mu\text{M}$, respectively based on our SPR results. These effects of SNG are partially dependent on the expression levels of LSD1 as shown in LSD1 knockdown (shRNA) and overexpression experiments.

Conclusion: We provide strong evidence that SNG can be a structural model as a dual inhibitor to both LSD1 and AR in prostate cancer. SNG or its derivatives are the newly potential generation of LSD1 inhibitors particularly deserving further investigation for treatment of castration-resistant prostate cancer, including its neuroendocrine subtype and cancer stem cell subtype.

BACKGROUND

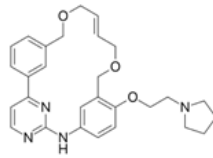
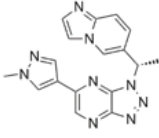
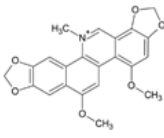
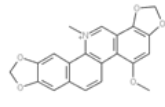
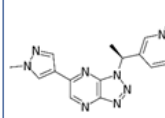
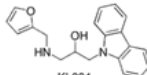
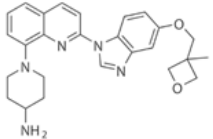
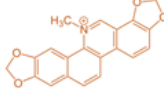
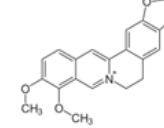
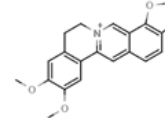
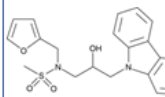
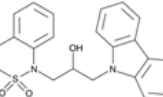
Prostate cancer (PCa) is the second most lethal cancer in men in the United States [1,2]. In 2019, 174,650 new cases of PCa arose and 31,620 PCa-specific deaths occurred. Androgen-Deprivation Therapy (ADT), including the new generation of anti-androgen agents (i.e. Abiraterone Acetate, Enzalutamide, and Apalutamide) known as the castration that deactivates the function of the AR, is the principal treatment for metastatic PCa [3-5]. This therapy could temporarily suppress the level of androgens at the early stage of treatments, but there are various factors and mechanisms involved in the development into treatment-resistance in cancerous cells, named castration-resistant PCa (CRPC) [6]. The mechanisms of the resistance are associated with an adaptive feedback enhancement of androgen receptor (AR) signaling, appearance of PCa neuroendocrine (NE) phenotype, an increasingly prevalent histologic subtype in CRPC with low AR activity in PCa tumors, and aberrant splicing of the AR which results in truncated AR variants such as ARV7 which has lost the ligand-binding domain (LBD). ARV7 is constitutively active, allowing AR signaling to be retrieved. Consequently, it leads to cancer survival and proliferation even in the absence of androgens [7-9]. In general, there are at least two molecular subsets of CRPC: AR gain, which exists in 50 to 75% of CRPC; and low AR activities in about 20% of CRPC, which is commonly associated with the development of small cells/neuroendocrine-like differentiation [20]. Thus, treatments that target only AR are not adequate; therefore, identifying a new target that is involved in both molecular subtypes (i.e. AR gain and loss) of CRPC is a highly demanding therapeutic approach.

Lysine-specific Demethylase 1A (LSD1) is one candidate that may play a critical role in the progression of CRPC by inducing androgen-independent transitions in PCa [10-12]. LSD1, a flavin adenine dinucleotide (FAD)-dependent histone-modifying enzyme responsible for demethylation of histone H3 lysine 4 (H3K4) and histone H3 lysine 9 (H3K9), plays a key role in the progression of CRPC by interacting with AR [21] and being involved in neural differentiation, in general [19]. Suggesting LSD1 may be a promising target for developing new treatments against CRPC with either low or high AR activity, we have screened a series of FAD (a co-factor for LSD1) analogs, including naturally occurring polycyclic ammonium ions, for their inhibitory activities against both LSD1 and AR.

Sanguinarine (SNG) has been determined to be the best candidate that can reasonably inhibit LSD1 enzymatic activity with an IC_{50} of approximately $2.13 \pm 0.18 \mu M$ concentrations (Supplemental Table 1). SNG is an isoquinoline alkaloid with ammonium ions derived from the root of *Sanguinaria canadensis* and other poppy *fumaria* species [14]. It exerts a broad spectrum of properties such as antioxidant, anticancer, antiviral and anti-inflammatory activities [15,16]. Furthermore, it induces apoptosis by inducing oxidative stress, damages mitochondria leading to activation of caspases and

synergistically enhances the sensitivity of several chemotherapeutic agents [17]. However, the molecular mechanisms by which it inhibits prostate cancer by targeting LSD1 and AR have never been reported.

In the present study, we have determined SNG to prevent CRPC progression through the dual-target inhibition of LSD1 and AR/ARV7 mediated genomic reprogramming of gene expression networks. Overall, our results demonstrate that SNG could be a structural model as a dual inhibitor of both LSD1 and AR in prostate cancer.

 <p>Binding Energy: -9.4 Predicted 133nM IC₅₀ ~5.45μM Pacritinib</p>	 <p>Binding Energy: -10.1 Predicted 39nM IC₅₀ >16μM Volitinib</p>	 <p>Binding Energy: -8.4 Predicted 746nM IC₅₀ >16μM Macarpine</p>	 <p>Binding Energy: -8.4 Predicted 647nM IC₅₀ >16μM Chelirubine</p>	 <p>Binding Energy: -8.8 Predicted 329nM IC₅₀ >16μM Savolitinib</p>	 <p>Binding Energy: -8.5 Predicted 616nM IC₅₀ >16μM KL004</p>
 <p>Binding Energy: -10.4 Predicted 22nM IC₅₀ >16μM Crenolanib</p>	 <p>Binding Energy: -9.2 Predicted 630nM IC₅₀ ~2.13 μM Sanguinarine</p>	 <p>Binding Energy: -8.2 Predicted 950nM IC₅₀ >16μM Berberine</p>	 <p>Binding Energy: -7.6 Predicted 2.3uM IC₅₀ >16μM Epiberberine</p>	 <p>Binding Energy: -9.1 Predicted 226nM IC₅₀ >16μM KL001</p>	 <p>Binding Energy: -10 Predicted 44nM IC₅₀ >16μM KL002</p>

Supplementary Table 1 - Classes of novel FAD analogs and their inhibitory activities against LSD1. Molecular docking via Pymol and Autodocktools program were used to screen these molecular compounds onto LSD1 (2DW4). Compounds that had promising predicted binding or potency, such as FAD overlay, or low predicted binding affinity were then screened for LSD1 activity using an LSD1 activity assay kit. Overall, Sanguinarine ended up being the only LSD1 inhibitor with a reasonable IC₅₀.

MATERIALS AND METHODS

Molecular docking

Visual demonstration of ligand-protein binding was illustrated using Pymol, while the binding affinity values, and the predicted binding location were computationally predicted within the Autodocktools program. Molecular docking is a computational method used to predict several protein-binding mechanisms. We searched for a list of LSD1 and AR proteins from <https://www.rcsb.org/>. We chose the pdb file 2DW4 with a resolution value of 2.3Å as the molecular docking model for LSD1, and 2PIV with a resolution value of 1.95Å as the molecular docking model for AR. We added Gasteiger charges from the PyMol program that adds partial charges to both our compound model and our protein

models. In addition, we also applied the Larmakian output application found in the program, so that the program does not randomly predict the ligand-binding, but rather predicts the binding through a unique algorithm that follows a similar Lamarckian-type evolution. We used the standard grid box size of 0.385 within the FAD-binding domain spacing site of the LSD1 protein or Ligand-binding domain of the AR protein.

LSD1 inhibition assay

LSD1 inhibitor screening kits can be purchased from Cayman Chemicals with the catalog number 700120. The LSD1 activity assay is a method that determines whether a compound can reduce the enzymatic activity using fluorescence measurements. Human recombinant LSD1 enzymes are incubated with a selected concentration of compounds or with DMSO for 10 minutes. Then a premix of reaction buffers solution that contains fluorescence substrate and Horseradish peroxidase (HRP) are added to the LSD1 solution. Finally, methylated peptides, which are first 21 amino acids of the N-terminal tail of histone H3 with lysine 4 methylated (H3K4) or with lysine 9 methylated (H3K9), are added to the LSD1-buffer solution to begin the enzymatic processing. This process takes place at 37°C for 60 minutes. In the process of demethylation, hydrogen peroxide (H₂O₂) is formed as a byproduct. HRP then can use H₂O₂ to convert the non-fluorescence substrate resazurin into the fluorescence substrate resorufin, which can be measured by a fluorescence spectrophotometer using the excitation value of 530nm and the emission value of 585nm.

FAD competitive binding assay

LSD1 inhibitor screening kit was used following the similar protocol as mentioned above. Human recombinant LSD1 enzymes are incubated with a selected concentration of compounds or with DMSO within a dialysis membrane submerged in 500mL of LSD1 assay buffer for 10 minutes (pre-dialysis) or 24 hours (post-dialysis). The LSD1 assay buffer in our experiments contains proprietary concentration of FAD with an additional 2uM FAD, additional 2uM SNG, or no additional substances. After dialysis, the samples within the dialysis membrane are transferred to a 96-well plate, and then a premixture of reaction buffers solution that contain fluorescence substrate and Horseradish peroxidase (HRP) are added to the dialyzed LSD1 samples. Finally, methylated peptides are added to the LSD1-buffer solution to begin the enzymatic processing following the exact protocol as mentioned above.

Western Blotting Analysis

Western Blotting analysis (WB) is a method that combines the use of electrophoresis and immunostaining techniques to separate and analyze or diagnose specific proteins for various processes. Proteins can be extracted from the PCa cells that are treated or untreated. Protein extraction method is then applied to collect all the proteins in the cell cytosol. This is done on ice with protease inhibitors within the RIPA lysis buffer to prevent protein denaturation. After protein extraction, protein

concentration is measured using a Lowry Assay method via spectrophotometer to ensure that the samples are being compared on an equivalent basis. After the appropriate volume of samples is determined, the proteins are diluted into a loading buffer, which will contain the Glycerol, Tracking dye (bromophenol blue), SDS, and beta-mercaptoethanol. A positive control would be a non-treated lysate, and the negative control would be staining for β -tubulin. The proteins are loaded onto an acrylamide gel and run using electrophoresis method at 100 voltage for 1:30 hours. After the separation, the protein samples are transferred into a PVDF membrane through electrophoretic transfer method at 100V for 45 minutes. After transferring, blocking with 5% nonfat dried milk diluted in 1X TBST buffer was applied to prevent antibodies from binding to nonspecific proteins in order to reduce background noise. Antibodies are diluted in the blocking buffer. After probing overnight at 4°C, excess antibodies are washed out by 1X TBST. The remaining bound antibodies can be detected using a horseradish peroxidase (HRP) labeled antibody. The signal is captured on a developing film from the dark room.

AR-Luciferase reporter assay

AR is an important protein in the development and progression of PCa. When activated by stimuli, such as DHT, the AR translocates from the cytoplasm into the nucleus to regulate any downstream target genes. In this assay, we purchased an established AR-luciferase reporter stable cell line, MDA-MB-453 (Signosis, SL-0008), which luciferase activity is associated with its AR activity. Thus, we will use this cell to monitor for AR activities. MDA-MB-453 AR reporter cell lines were grown in the DMEM medium containing 10% FBS, 1% Penicillin-streptomycin, and 75ug/mL G418 at 37°C with a 5% CO₂ incubator. These cells were split equally in a 24-well plate until they were approximately 70% confluent. Then the cells were treated with 1nM of DHT for 2 hours prior to 8 hours of drug treatment. No DHT was used as negative control and no drug treatment was used as positive control. After treatment, the cells were washed with PBS twice prior adding luciferase lysis buffer and shake at room temperature for 20 minutes. The lysed solutions were transferred into a 96-well plate with the additional luciferase substrate. The plate was read immediately with a luminometer.

RNA extraction

RNA extraction methods are powerful tools that use chaotropic salt solution to rapidly disrupt cells without destroying their nucleic acid. RNA can be extracted by RNA-Bee reagent, which contains phenol and guanidine thiocyanate to burst the cells. The reason RNA-Bee is used instead of other lysis buffers like RIPA is because RNA-Bee contains phenol, which is nonpolar. Since RNA is highly polar, it cannot dissolve in phenol, but in aqueous phase instead. The phenol will keep denatured proteins and other cellular components, such as cell membranes at the bottom layer, while the top aqueous layer contains nucleotides. The treated or 0.1% DMSO treated cells in a 10cm TC dish are washed twice in 1X PBS, and then lysed in 1mL of RNA-Bee for 5 minutes on ice. Afterwards, the lysates are transferred to a

2-mL centrifuge tube with an additional 600uL of chloroform and vigorously mixed by inverting. Chloroform is also nonpolar and denser than phenol, which can easily be mixed with phenol to create a denser solution. Thus, the separation of organic and aqueous layers will be more obvious to ensure that the RNA nucleotides are separated from the bottom layer. The chloroform-lysate solution is settled on ice for 5 minutes, and then centrifuge at 6000rpm for 20 minutes at 4oC. After the aqueous layer is transferred to a new tube, 600uL of isopropanol is mixed to that aqueous layer and incubated overnight at 4oC to precipitate the RNA and to wash out any contaminants and salts. The aqueous solution is then removed after it is spun down at 6000rpm for 20 minutes at 4oC. Absolute ethanol is then added to the RNA precipitants to further reduce the RNA solubility in the aqueous solution, and then centrifuge at 6000rpm for 10 minutes at 4oC. Ethanol is then removed, and the RNA precipitants are air-dried. RNA-free water is added, and the RNA can be quantified via nanodrop, and then stored or used for other experiments.

Reverse transcription Polymerase Chain Reaction

Reverse transcription PCR (RT-PCR) is a technique that reverse transcribes RNA into DNA (cDNA) and also amplifies specific cDNA sequence. The 1-5 ug of the extracted RNAs were mixed with 500ng/ug oligo dT primers and random primers with the volume topped off to 10uL with nuclease-free water. Afterwards, the RNA solutions were preheated at 70oC for 5 minutes to anneal the primers, and then cooled to 4oC for 10 minutes. During the cooling, a mastermix of 1X reaction buffer, MgCl₂, dNTP mix, RNasin inhibitor, and reverse transcriptase are prepared. After the cooling, the master mix is added to the RNA solution, and then reverse transcription PCR (RT-PCR) can be run. The condition was heated at 42oC for 1 hour, then 70oC for 15 minutes, and then cooled at 4oC. The newly synthesized cDNA can now be stored or used for other experiments.

Quantitative Polymerase Chain Reaction

Quantitative polymerase chain reaction (qPCR) is a method to characterize and quantify gene sequence. After cDNA is obtained, 50ng of cDNA is diluted in nuclease free water and aliquot in SYBR green containing 50uM forward and reverse primers. The cDNA mixtures are then ran using a qPCR machine that was preprogramed with the following setting: 95oC for 10 seconds, 55oC for 30 seconds, 72oC for 30 seconds, and read. After repeating this step 39 more times, the melting curve is measured by incrementally increasing the temperature by 0.5oC every 5 seconds from 55oC to 95oC. The data can be visualized and converted into a bar graph.

Cellular MTT viability assay

It is also important to validate the compounds inhibitory activities with their selectiveness towards cells overexpressing the targeted proteins. The MTT cellular viability assay is a colorimetric assay that indicates the levels of cellular metabolic activities. In our studies, PCa cell lines at 30-40%

confluence will be incubated with specific concentrations of drugs at 37°C for approximately 72 hours. Prior to performing the MTT assay on the treated cells, MTT solution is made by dissolving MTT powder in 1X PBS at a concentration of 3mg/mL. Afterwards, MTT solution can be directly added to the treated cells, which the final concentration of MTT solution should be 0.5mg/mL. After 50 minutes of incubation at 37°C, cells that are healthy will be noticeably purple in color as only living cells are able to uptake and reduce MTT into formazan from their mitochondria. After the cells are stained for MTT, we can then wash and remove all the media. Then MTT dissolving solution containing 4% 1N HCl in 100% isopropanol can be added so that the formazan can dissociate into the solution, which can be used for colorimetric measurement by a spectrophotometer using the absorbance value of 570nm.

Immunoprecipitation

Immunoprecipitation is a method that determines protein-protein interaction by pulling down specific protein targets via agarose beads and antibodies. Proteins were extracted from treated and non-treated PCa cells via RIPA lysis method as described previously. Approximately 500ug/uL of lysates were obtained from each condition and their volumes were topped off to 2mL with a RIPA buffer containing protease inhibitors. Then the lysates were pre-cleared by adding 40uL of agarose beads and 10ug/mL of normal mouse or normal rabbit antibody of the same species of the antibody used to later pull down the specific protein target. Pre-clearing is important as it helps reduce non-specific binding and reduce background. After 2 hours of inverting at 4oC, the lysates were spun down at 5k rpm at 4oC for 10 minutes, and the supernatants were transferred to a newly labeled centrifuge tube. Specific antibodies (10ug/mL) were added to each tube, while 10ug/mL of normal mouse or normal rabbit antibodies were added to an additional lysate as the IgG control. The lysates were incubated and inverted at 4oC for 1 hour before adding 40uL of agarose beads to then incubate and invert overnight at 4oC. After incubation, the centrifuge tubes were spun down at 5k rpm for 1 minute each, and then the supernatants were discarded. RIPA buffers were added to wash the beads. The centrifugation and washing continues 3 more times. After the final centrifugation, supernatants were removed and 20uL of 2X loading buffer, containing the same ingredient as described previously, were added to the beads to elute the protein complex. The samples were then incubated for 10 minutes at 75oC and then the supernatants were transferred to the Western Blot gel to follow the Western Blotting analysis method as described previously.

Transfection

C42B cell lines were seeded on a 24-well plate in complete RPMI medium incubating at 37oC and 5% CO2 until they reached 50% confluent. Lipofectamine LTX (Thermo Fisher Scientific) were added into a centrifuge tube containing 50uL of Opti-MEM medium. In another centrifuge tube containing 50uL of Opti-MEM medium, 2ug of plasmid DNA and 2uL of Plus Reagent were added. The

two tubes were mixed together and incubated for 5 minutes at room temperature. The plasmid mixtures were then added into the cells and incubated for at least 48 hours. Afterwards, the cells were treated with 2ug/mL of G418 antibiotics.

Transduction

22RV1 cell lines were seeded in a 6-well plate in complete RPMI medium incubating at 37oC and 5% CO₂. Once the cells reach 50% confluent, the cells were media changed with polybrene (5ug/mL, Santa Cruz Biotechnology). Lentivirus were added to the cells and incubated for 24 hours at 37oC with 5% CO₂. Afterwards, the media were changed to complete medium containing 8ug/mL puromycin

Cellular thermal shift assay

PCa cells were trypsinized and aliquoted evenly into two 15-mL tubes. One tube was treated with compounds, while the second tube was treated with 0.1% DMSO as control. After 2 hours of incubation at 37oC, the cells were washed in cold 1X PBS twice, and resuspended in 800uL of 1X PBS containing protease inhibitor. Each tube was equally aliquoted into 8 centrifuge tubes (each containing 100uL of treated cells). The one aliquoted tube from the from each condition were heat shocked for 3 minutes at 40oC, 43oC, 46oC, 49oC, 52oC, 55oC, 58oC, and 61oC, and then cooled at room temperature for 3 minutes before flash freeze in liquid nitrogen. The samples were then lysed via three cycles of thawing-flash freezing. The lysates were then spun down at 13k rpm in a 4oC centrifuge, and then the supernatants were transferred to a newly labeled centrifuge tube. The samples were incubated with 5X loading dye and heated for 5 minutes at 99oC prior to Western Blotting analysis method as described previously.

Cellular isothermal dose response

A single optimal temperature where most of the targeted proteins were insoluble were used for this experiment. PCa cells were trypsinized and aliquoted evenly into 8 centrifuge tubes. Each tube was incubated with different concentrations of drugs for 2 hours at 37oC. Afterwards, the cells were washed three times with cold 1X PBS. The cells were then resuspended in 100uL of cold 1X PBS containing protease inhibitors. Then the cells were heat shocked at a single optimal temperature for 3 minutes, cooled at room temperature for 3 minutes, and finally flash frozen. The samples can then be lysed and analyzed via Western Blotting as described previously.

Surface plasmon Resonance

Surface Plasmon Resonance (SPR) is a label-free method that can study the interaction between protein and ligand binding. Thus, we performed SPR to determine if SNG can bind directly onto LSD1 or AR proteins *in vitro*. Synthesized recombinant LSD1 and recombinant AR proteins with six histidine-tag were purchased from GenScript and diluted to 25ug/mL in 10 mM HEPES, pH 7.4, 150 mM NaCl, 0.005% Tween-20 in RNA-free water. The SPR machine (Biacore S200, GE Healthcare) was used at Chapman University in the Harry and Diane Rinker Health Science Campus, Irvine. To initiate SPR, the

NTA sensor Chip (GE Healthcare) was inserted into the SPR machine, 350 mM EDTA is injected at a flow rate of 30uL/min, and then 0.5mM of NiCl₂ were injected at 10uL/min for a minute through the sensor chip. This will allow the histidine-tagged recombinant proteins to bind to the sensor ship.

Afterwards, 25ug/mL of recombinant protein were injected into the sensor chip at the rate of 10uL/min for a minute, followed by indicated concentrations (0.0625uM to 16uM) of SNG injected into the NTA sensor Chip at a flow rate of 30uL/min for 2 minutes. Finally, 350 mM EDTA can be injected at a flow rate of 30uL/min for one minute to reset the sensor chip back to the baseline to repeat this experiment in triplication.

Recombinant AR protein sequence:

MHHHHHHTSPTEETTQKLTVSHIEGYECQPIFLNVLEAIEPGVVCAGHDNNQPDSFAALLSSLNE
LGERQLVHVVKWAKALPGFRNLHVDDQMAVIQYSWMGLMVFAMGWSFTNVNSRMLYFAP
DLVFNEYRMHKSRMYSQCVRMRHLSQEFQWLQITPQEFLCMKALLFSIIPVDGLKNQKFFDEL
RMNYIKELDRIIACKRKNPTSCSRRFYQLTKLLDSVQPIARELHQFTFDLLIKSHMVSVDPEMMA
EISVQVPKILSGKVKPIYFH

Recombinant LSD1 protein sequence:

MHHHHHHGPLGSPEFAPPEEENESEPEEPSGVEGAAFQSRLPHDRMTSQAACFPDIISGPQQTQK
VFLFIRNRTLQLWLDNPKIQLTFEATLQQLLEAPYNSDTVLVHRVHSYLERHGLINFGIYKRIKPLP
TKKTGKVIIIGSGVSGLAARQLQSFQMDVTLLEARDRVGGRVATFRKGNVYADLGAMVVTGL
GGNPMVAVVSKQVNMELAKIKQKCPLYEANGQAVPKEKDEMVEQEFNRLLEATSYLSHQLDNFN
VLNKPVSLGQALEVVIQLQEKHVKDEQIEHWKIVKTQEELKELLNKMVNLEKIKELHQQY
KEASEVKPPRDITAEFLVSKHRDLTALCKEYDELAETQGKLEEKLELEANPPSDVYLSSDRQ
ILDWHFANLEFANATPLSTLSLKHWDQDDDFEFTGSHLTVRNGYSCVPVALAEGLDIKLNTAVR
QVRYTASGCEVIAVNTRSTSQTFIYKCAVLCTPLGLKQPPAVQFVPLPEWKTSVAVQRMG
FGNLNKVVLCFDRVFWDPVNLFGHVGSTTASRGELFLFWNLYKAPILLALVAGEAAGIMENIS
DDVIVGRCLAILEKIFGSSAVPQKETVVSRRWRADPWARGSYSVAAGSSGNDYDLMAQPITPG
PSIPGAPQPIPRLLFFAGEHTIRNYPATVHGALLSGLREAGRIADQFLGAMYTLPRSGNDYDLMAQP
ITPGPSIPGAPQPIPRLLFFAGEHTIRNYPATVHGALLSGLREAGRIADQFLGAMYTLPRQATPGVPA
QQSPSM

Cryogenic Electron microscopy

Recombinant AR and recombinant LSD1 were diluted in pH 7 Tris(20mM)-NaCl(100mM) buffer to 13ug/mL and 11.4ug/mL, respectively. Negative staining was first performed where the carbon mesh (Electron Microscopy Sciences) were coated in plasma using the CTEM sputter coater 200. Then 2% uranyl acetate were added onto the carbon side of the mesh for 10 second before washing in water. Afterwards, 5uL of the diluted recombinant proteins were added to the mesh and ready for

imaging via CryoEM (JEOL1200). After confirming the right condition for viewable imaging, we next prepare another set of carbon mesh coated in plasma with 5 μ L of diluted recombinant proteins. The proteins are then frozen in liquid nitrogen, and then imaged via the CryoEM. The imaged photos are analyzed using software and 3D rendering of the recombinant proteins were reconstructed.

RESULTS

Sanguinarine inhibits both LSD1 and AR activities

FAD is the only cofactor for LSD1 demethylase activities. Therefore, we have searched for a series of structurally diversified FAD binders or analogs for their potential inhibitory activity on LSD1 enzymatic activity. Supplementary Table 1 showed a list of potential FAD analogs, but only SNG and pacritinib decreased LSD1 mediated demethylation of H3K4 enzymatic activity at IC_{50} of 2.13 μ M and 5.45 μ M, respectively. The IC_{50} of other screened compounds against LSD1 enzymatic activity were more than 16 μ M. In addition, the molecular docking analysis revealed that SNG superimposes FAD and binds to the FAD-binding domain of LSD1 (Figure 1A) and interacts with several important amino acids, including tyrosine 761, valine 811, and valine 333 (Figure 1B). Tyrosine 761 is important for LSD1 demethylation activities, while valine 811 and valine 333 are important for substrate binding [29]. Interestingly, through our LSD1 inhibition assay, SNG was more effective to inhibit LSD1 mediated demethylation of H3K9me2 ($IC_{50} = 1.43 \pm 0.39 \mu\text{M}$) than H3K4me2 ($IC_{50} = 2.13 \pm 0.18 \mu\text{M}$) (Figure 1C). Further, SNG increased cellular levels of In H3K4me2 and H3K9me2 in both CRPC cell lines 22RV1 and LNCaP95 cells (Figure 1D). These results suggested that SNG was a potent cell active LSD1 inhibitor.

In addition, we wanted to determine whether the binding of SNG onto LSD1 would be competitive or covalent. This effort would enable both prospective and retrospective matching of future synthesized compounds with LSD1 targets with enhanced understanding of their mechanism of action. We measured the activities of LSD1 proteins after SNG induction prior to dialysis and 24 hours after dialysis in surrounding LSD1 assay buffer, which contained proprietary concentration (Cayman Chemicals) of noncovalently bound flavin adenine dinucleotide (FAD) cofactor. This method would determine whether SNG can strongly bind to LSD1 and be able to dilute out the bound FAD ligand. As a result, there was a further decrease in LSD1 activities 24-hour post-dialysis after treatment with SNG (Figure 1E), suggesting a strong binding interaction between SNG and LSD1 proteins. We next wanted to determine if SNG can competitively compete with excessive FAD in the dialysis buffer and whether FAD can reverse the binding of excessive SNG within the dialysis buffer. Thus, we treated LSD1 proteins with 2 μ M of FAD or 2 μ M of SNG within the dialysis membrane, and then incubated the membrane for 24

hours with surrounding LSD1 assay buffers containing 2 μ M SNG or 2 μ M FAD, respectively. As a result, SNG was able to reduce LSD1 activities by competing with the excessive FAD in the surrounding solution (Figure 1F, left). In addition, FAD showed to reactivate LSD1 activities even with excessive SNG in the surrounding solution (Figure 1F, right). Overall, these results suggested that SNG is a FAD competitive inhibitor against LSD1.

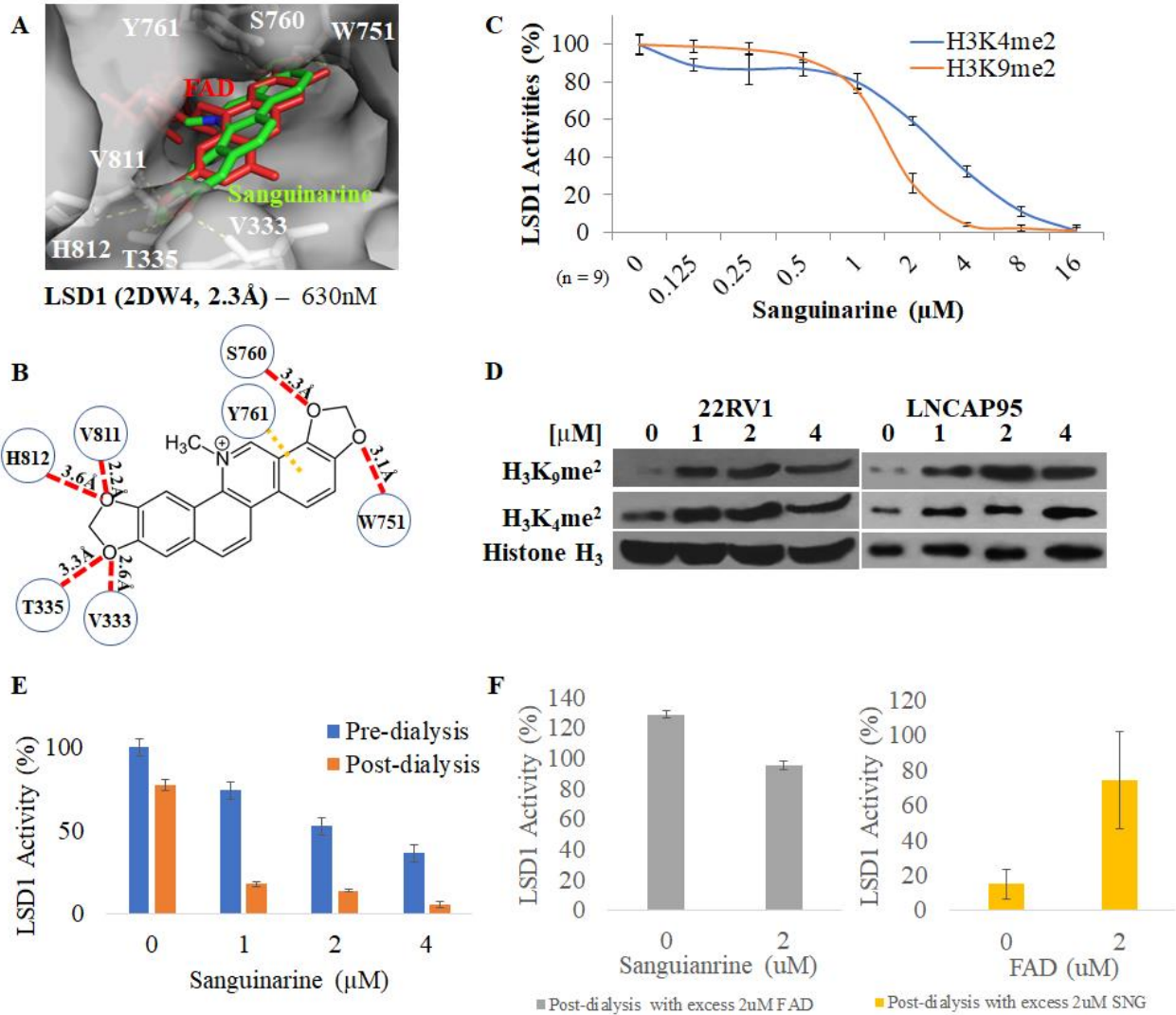


Figure 1: The inhibitory effect of Sanguinarine against LSD1 activities. (A) Surface diagram of the active site of the LSD1 protein (Grey, 2DW4, 2.3 Å) in complex with its ligand FAD (red) and superimposed SNG ligand (Green). (B) 2D representative image of the molecular interaction between SNG within the FAD-binding domain of LSD1. (C) Inhibition of LSD1 demethylase activity. Increasing concentrations of SNG were pre-incubated for 10 minutes with enzymes prior to initiating the demethylase reaction with peptide substrates, H3K4me2 (blue) and H3K9me2 (red), for 60 minutes. Data represent means \pm SD (n=6). (D) H3K9me2 and H3K4me2 protein expressions were analyzed via WB in 22RV1 and LNCaP95 cells after 24 hours of treatment with indicated concentration of SNG. Histone H3 was used as the loading control. (E) LSD1 Competitive binding experiment uses the same LSD1 demethylase activity assay kit. The level of LSD1 demethylation activity under concentration of SNG was measured pre- (blue) and 24 hours post-dialysis (orange) in the surrounding LSD1 assay buffer. Data represent means \pm SD (n=3). (F) LSD1 was treated with (Left) 2 μ M SNG with surrounding FAD (2 μ M) containing buffer or (right) 2 μ M FAD with surrounding SNG(2 μ M) containing buffer for 24 hours post-dialysis. Data represent means \pm SD (n=3).

We next determined whether SNG could inhibit AR signaling by reducing its transcriptional activity and expression of AR target genes. Molecular docking analysis revealed that SNG superimposes DHT and binds to the ligand-binding domain (LBD) of AR (Figure 2A), suggesting SNG to be a dual-inhibitor against both LSD1 and AR. In an AR-luciferase reporter cell line, SNG decreased AR transcriptional activities with an IC_{50} value of $2.07 \pm 0.45 \mu M$ (Figure 2B). Additionally, WB and real-time qPCR analysis demonstrated that 22Rv1 and LNCaP95 cell lines treated with SNG had significantly reduced expression of AR and ARV7 and their target genes (i.e. PSA, UBE2C) at both the protein levels (Figure 2C) and mRNA levels (Figure 2D), respectively. We also looked at the mRNA expression of other AR variants and AR downstream targets, such as AR4, AR5, HSD3B1, HSD3B2, HSD17B6, and AKRIC3 (Supplementary Figures 1A and 1B). These other AR variants and downstream targets were also all downregulated in 22RV1 cells when treated with SNG, although HSD3B1 and AKRIC3 were not significantly downregulated in LNCaP95 cells when treated with SNG. Overall, these results suggested that SNG could inhibit the expression and activities of AR and other AR variants, which is clinically relevant for emerging CRPC therapy.

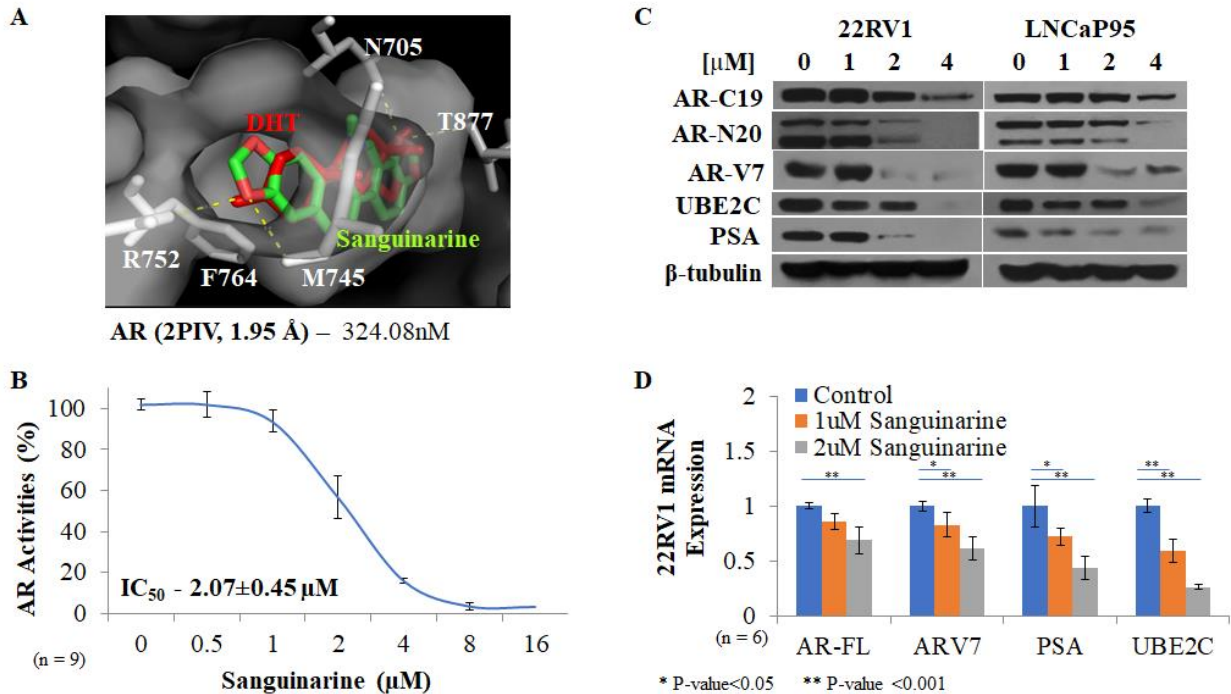
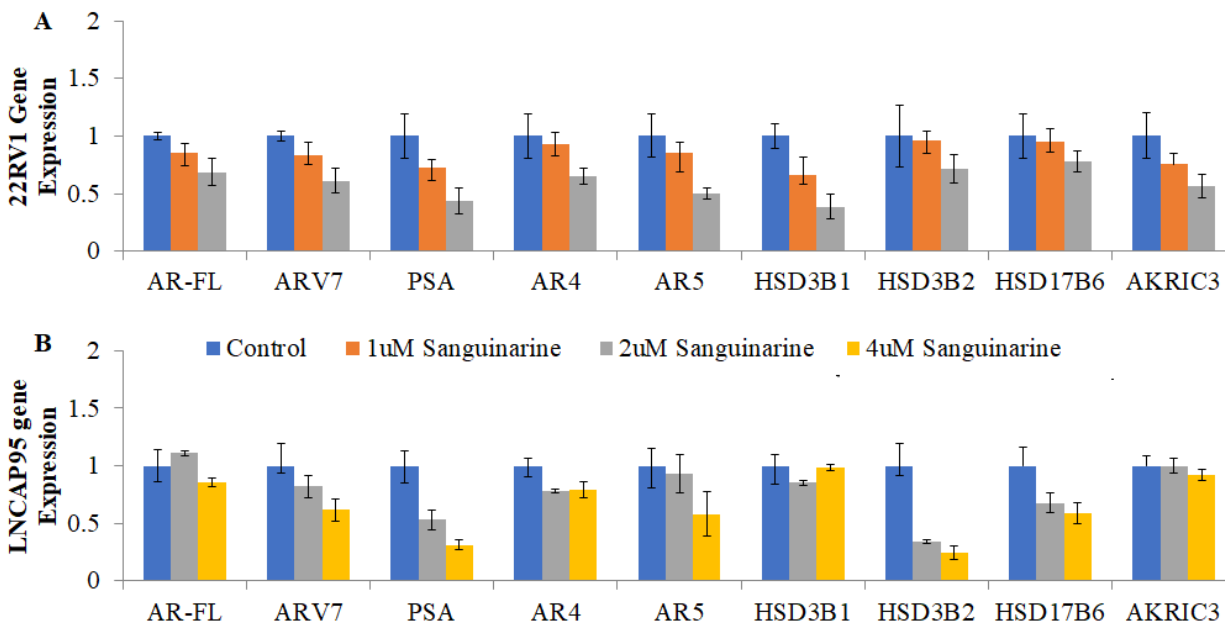


Figure 2: The inhibitory effect of Sanguinarine against AR activities. (A) Surface diagram of active site of the AR protein (Grey, 2PIV, 1.95 Å) in complex with its ligand FAD (red) and superimposed SNG ligand (Green). (B) Transactivation of ARE-LUC by AR in presence of DHT was measured by luciferase reporter assay in terms of RLU (control = 100%) in the presence of indicated concentration of SNG. Data represent means \pm SD (n=6). (C) AR, ARV7, UBE2C, and PSA protein expression were analyzed via WB in 22RV1 and LNCaP95 cells after 24 hours of treatment with indicated concentration of SNG. B-tubulin was used as the loading control. (D) qPCR results for gene expression in 22RV1 cells. Bar graph showing qPCR determined log fold change in expression of AR-FL (full-length), ARV7, PSA, and UBE2C under control (blue), 1 μM (orange), and 2 μM (grey) of SNG for 24 hours. Data represent means \pm SD (n=6). T-test was used to determine statistical significance.



Supplementary Figure 1: Sanguinarine downregulates AR and AR-V7 activities. qPCR results for gene expression in (A) 22RV1 and (B) LNCAP95 cells. Bar graph showing qPCR determined log fold change in expression of AR-FL (full-length), ARV7, PSA, and AR4, AR5, HSD3B1, HSD3B2, HSD17B6, and ARKIC3 under control (blue), 1µM (orange), 2 µM (grey), and 4 µM (yellow) of SNG for 24 hours. Data represent means \pm SD (n=6). T-test was used to determine statistical significance.

Sanguinarine selectively induces the cytotoxicity of LSD1, AR, and ARV7 expressing prostate cancer cells

SNG was shown to have relatively low toxicity to human umbilical vein endothelial cells with an IC_{50} of 23µM [25] and to normal prostate epithelial cells and normal epidermal keratinocytes with an IC_{50} of more than 10µM [26,27]. Whereas, the IC_{50} against prostate cancer cells were between 300nM to 2µM as shown from previous research [27] and our study. Although SNG cytotoxicity against PCa has a relatively small therapeutic window, its ability to inhibit LSD1 becomes very important because prostate cancers overexpress LSD1, having a LSD1 increase of 5 to 15-folds compared to normal tissue [22,23]. In addition, because more than 50% to 75% of CRPC uses AR as the primary driving force for progression [24], the ability that SNG was able to dual-target both LSD1 and AR activities was critical for clinical relevance.

Thus, we wanted to examine whether LSD1 and AR targets were at least in part responsible for the biological consequences of SNG in PCa cell lines. Firstly, protein levels of LSD1, AR, and ARV7 were compared among different PCa cell lines via WB method (Figure 3A), and then the cytotoxicities of 2µM of SNG to different PCa cell lines along with normal prostate epithelial and human mesenchymal stem cells were measured via MTT assay (Figure 3B). As a result, we observed that PCa cell lines with LSD1 overexpression, including CRPC cell lines 22Rv1 and LNCaP95 were more sensitive to SNG's cytotoxic effects compared to those with less LSD1 expression or lack of AR or ARV7 expression.

Interestingly, we observed that PCa neuroendocrine cell line NCI-H6880 were also highly sensitive to SNG-induced cytotoxicity, suggesting that LSD1 alone may be an important target. Furthermore, our observation on normal Prostate Epithelial cells RWPE1 cell lines had an IC₅₀ of 5μM to SNG, and at higher concentrations, RWPE1 cells were relatively less sensitive to SNG compared to the other CRPCs. The lower sensitivity of RWPE1 cells may be due to their low LSD1 expressions or through other unknown mechanisms. Human prostate epithelial cells (PREC) were also observed to have less cytotoxic sensitivity to SNG with an IC₅₀ of 5μM.

We also observed a similar cytotoxic trend with other natural occurring dual inhibitors of similar structure to SNG listed from Figure 4 (Supplementary Figure 3A-D). We next determined the IC₅₀ values for each PCa cell (Figure 3C), and then compared it to the expression of the targeted proteins to obtain the correlation coefficient (Figure 3D). As a result, our results showed strong correlation between PCa cell lines with LSD1 overexpression to be more sensitive to SNG's cytotoxic effects compared to those with less LSD1 expression or lack of AR or ARV7 expression.

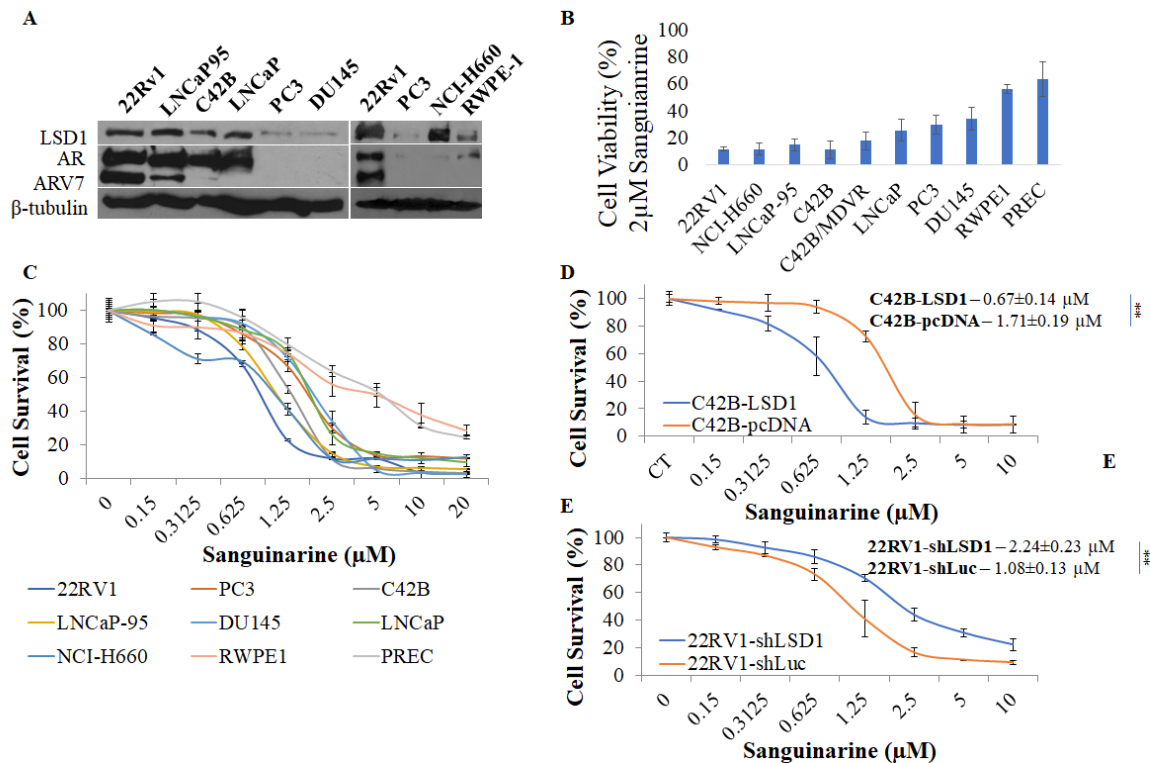
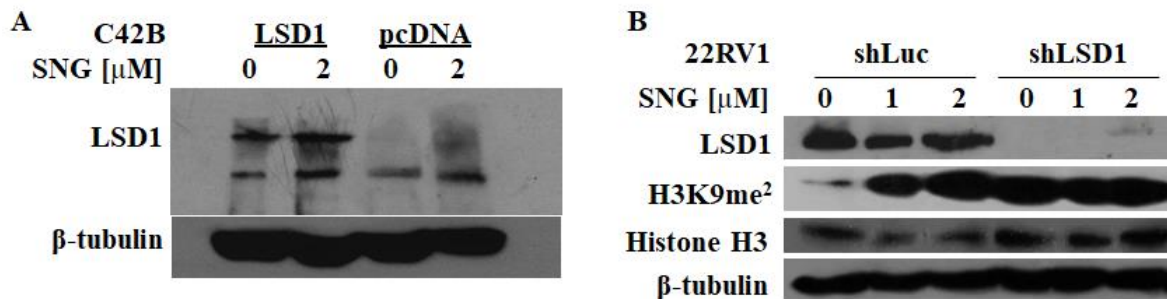


Figure 3: Sanguinarine targets LSD1 and AR/ARV7 to induce cytotoxicity in Prostate Cancer cells. (A) 22RV1, LNCaP95, C42B, LNCaP, PC3, DU145, NCI-H660, RWPE-1, and MSC cells were lysed and LSD1, AR, and ARV7 were observed via WB analysis. β-tubulin was used as loading control. (B) MTT assay was also performed on 22RV1, NCI-H660, LNCaP95, C42B, C42B-MDVR, LNCaP, PC3, and DU145 PCa, RWPE1, and MSC cell lines under 24 hours treatment with 2μM of SNG induction. (C) MTT assay was also performed on these cell lines indicating concentration of SNG for 72 hours. (D) C42B-LSD1 (blue) and C42B-pcDNA (orange) cells or (E) 22RV1-shLSD1 (blue) and 22RV1-shLuc (orange) cells were treated with SNG for 72 hours prior to MTT assay. Each data point for all MTT assays represents the mean of three experiments performed in triplicate. Error bars show the standard error of mean (SD) for the 6 experiments.

Next, we want to determine whether LSD1 directly plays an important role in the cytotoxic sensitivity of SNG. We stably transfected C42B cells to overexpress LSD1 (C42B-LSD1) (Supplementary Figure 2a) or stably transduced 22RV1 cells to suppress LSD1 expression by shRNA knockdown (22RV1-shLSD1) (Supplementary Figure 2b), and then examined the cytotoxic effects of SNG on these LSD1 overexpression or LSD1 knockdown cell lines in comparison with vector control (i.e. pcDNA or shLuc) PCa counterpart cell lines. As a result, C42B-LSD1 cells were more sensitive to the cytotoxic effect of SNG with an estimated IC_{50} value of $0.67 \pm 0.14 \mu M$ compared to C42B-vector control cells with an estimated IC_{50} value of $1.71 \pm 0.19 \mu M$ (Figure 3E). In addition, 22RV1-shLSD1 cells were less sensitive to SNG with an estimated IC_{50} value of $2.24 \pm 0.23 \mu M$ compared to 22RV1-shLuc cells with an estimated IC_{50} value of $1.08 \pm 0.13 \mu M$ (Figure 3F). Similarly, other dual-inhibitor compounds similar structured to SNG listed from Figure 4, 6-methoxydihydrosanguinarine, 6-ethoxydihydrosanguinarine, Oxychelerythrine, and Chelerythrine chloride also showed similar increasing cytotoxic potency trend against LSD1-overexpressing PCa cells compared to non-LSD1-overexpressing PCa cells (Supplementary Figure 3 and Supplementary Figure 4). Overall, we have shown that LSD1 and AR expression could at least in part be required to be responsible for the biological consequences of SNG in PCa cell lines.



Supplementary Figure 2: LSD1 Transduction and Transfection verification. Verification of LSD1 overexpression under indicated concentration of SNG treatment between (A) transfected C42B-LSD1 and C42B-pcDNA cell lines and (B) transduced 22RV1-shLuc and 22RV1-shLSD1 cell lines by Western blotting analysis.

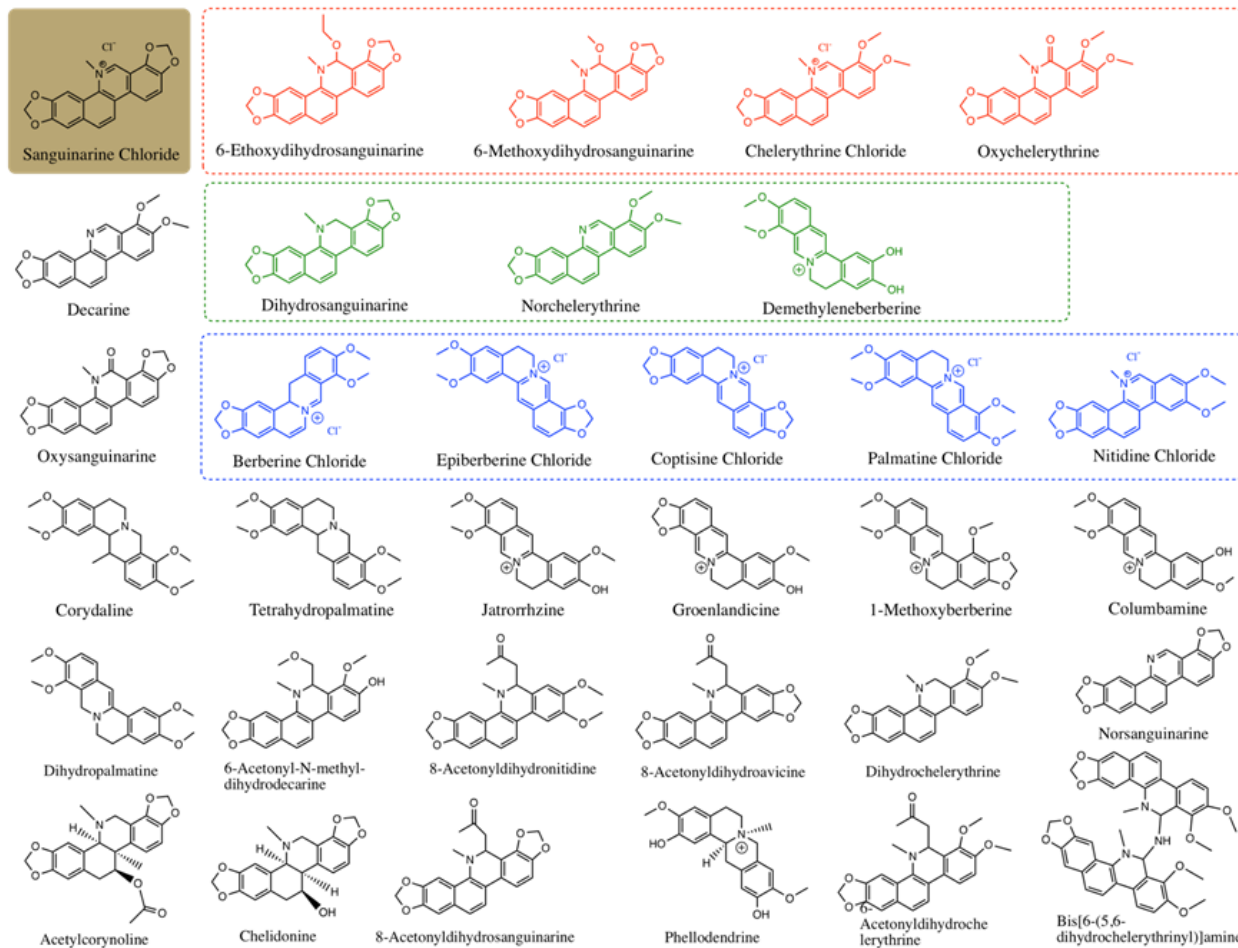
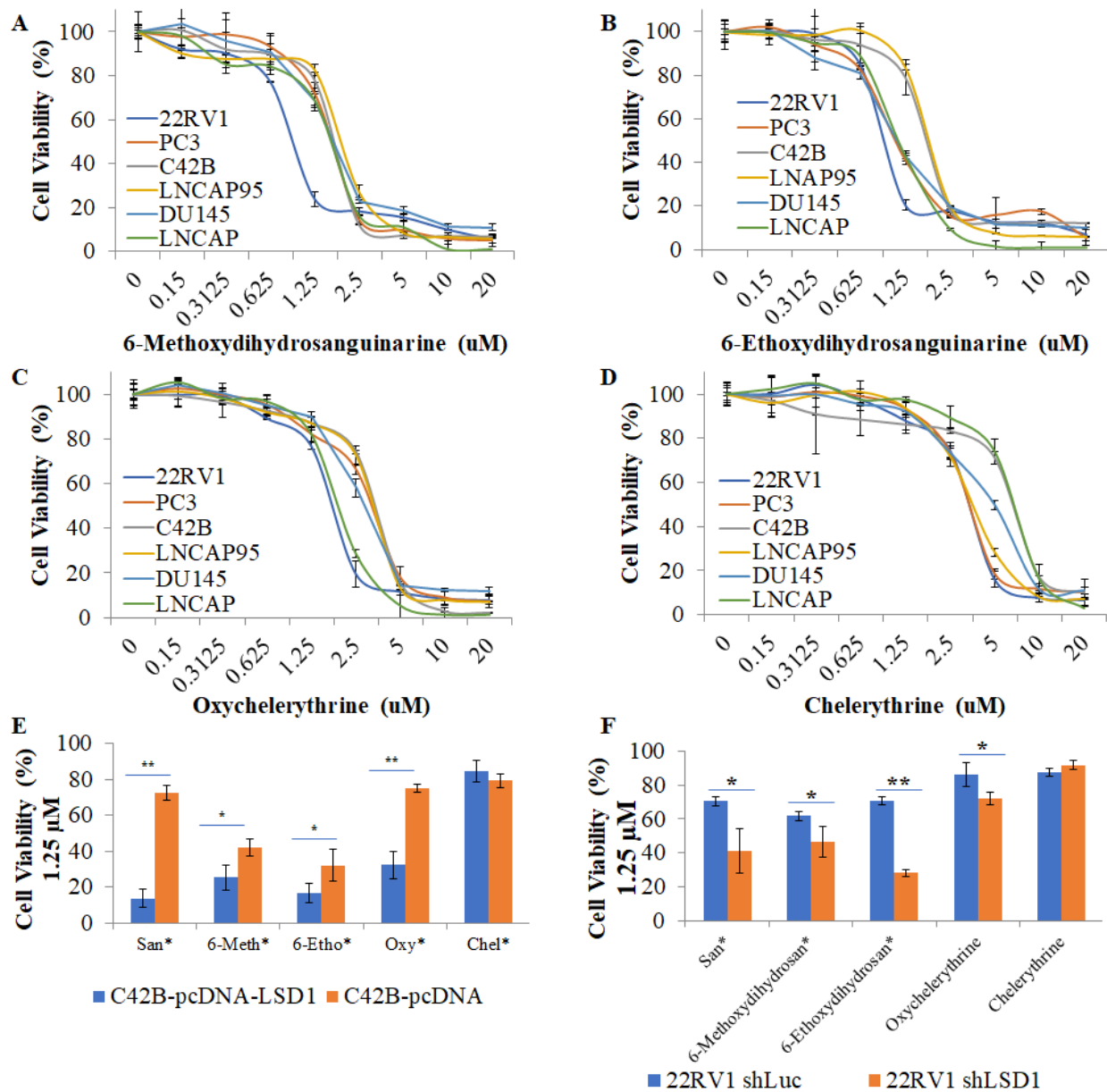
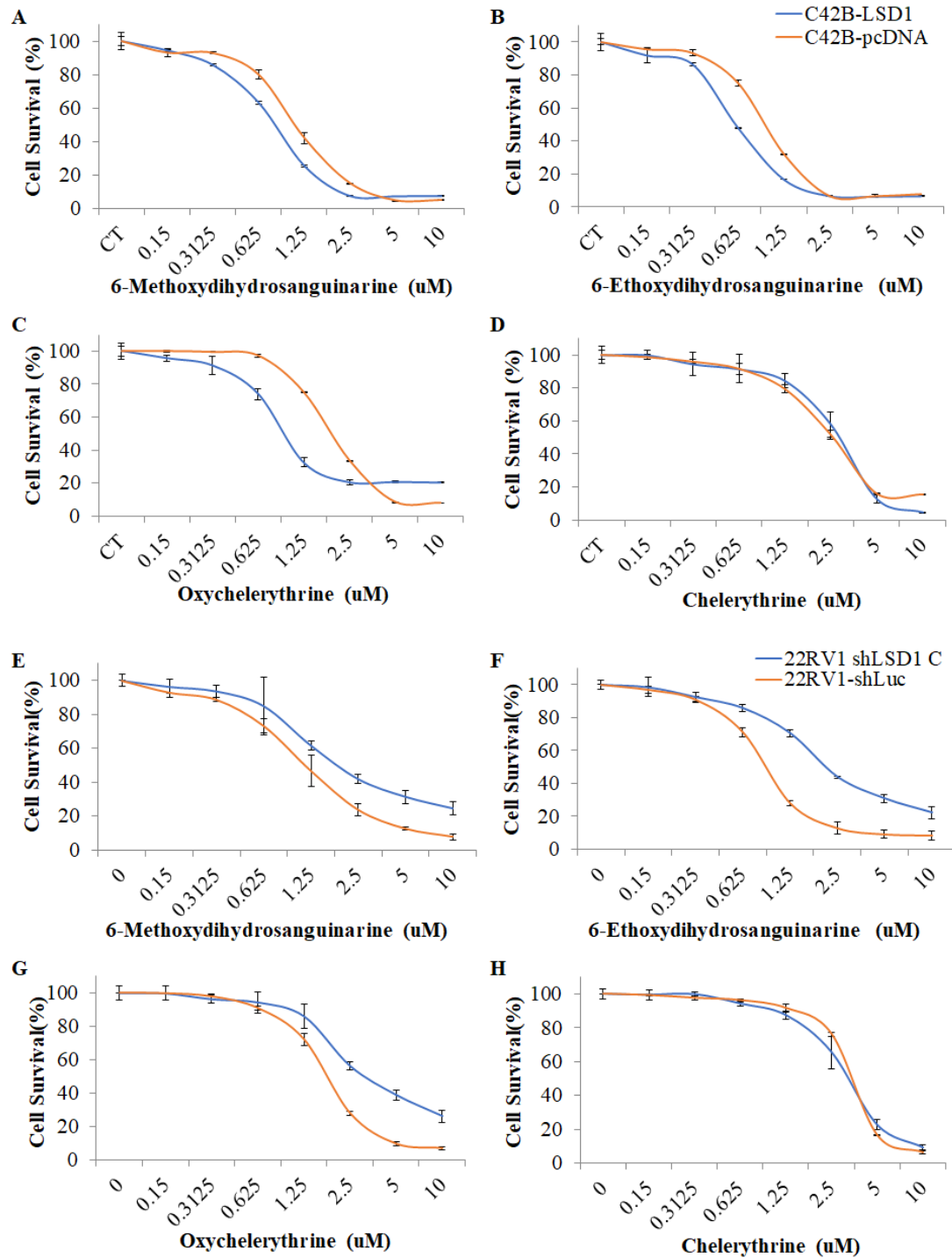


Figure 4. Sanguinarine and its naturally related structures. Indicated in red (top box) are LSD1 and AR dual inhibitors, green (middle box) are LSD1 inhibitors, and blue (bottom box) are AR inhibitors. Non-colored regions have their inhibitory activities above 16µM.



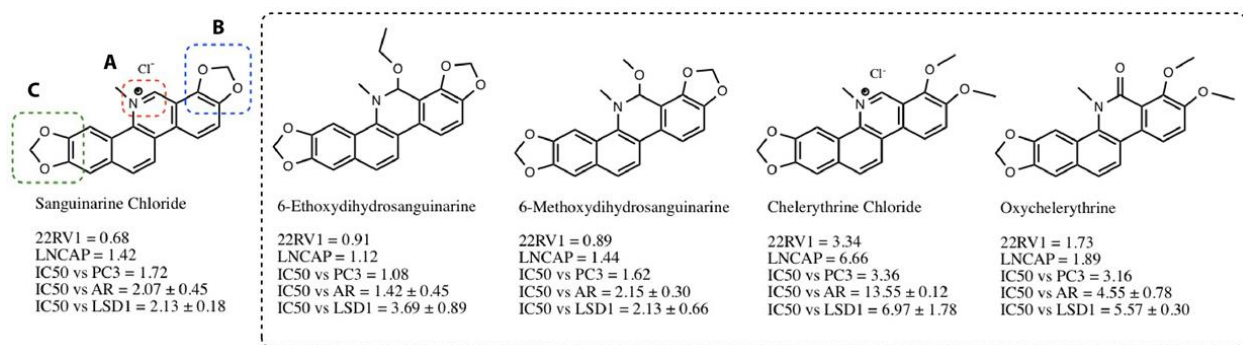
Supplementary Figure 3: Sanguinarine-related dual-inhibitors structures show specificity against LSD1-expressing prostate cancer cell lines. MTT assay was performed on 22RV1, PC3, C42B, LNCAP95, DU145, and LNCAP Pca cell lines treated with indicated concentration of (A) 6-Methoxydihydrosanguinarine, (B) 6-ethoxydihydrosanguinarine, (C) Oxychelerythrine, and (D) Chelerythrine chloride ligand for 72 hours. (E) C42B-LSD1 (blue) and C42B-pcDNA (orange) cells or (F) 22RV1-shLSD1 (blue) and 22RV1-shLuc (orange) cells were treated with SNG, 6-methoxydihydrosanguinarine (6-Meth), 6-ethoxydihydrosanguinarine (6-Etho), Oxychelerythrine (Oxy), and Chelerythrine chloride (Chel) for 72 hours prior to MTT assay. Each data point for all MTT assays represents the mean of three experiments performed in triplicate. Error bars show the standard error of mean (SD) for the 3 experiments.



Supplementary Figure 4: LSD1 expression is required at least in part for LSD1 and AR dual inhibitors to induce cytotoxicity. [Top] C42B-LSD1 (blue) and C42B-pcDNA (orange) cells or [Bottom] 22RV1-shLSD1 (blue) and 22RV1-shLuc (orange) cells were treated with (A,E) 6-Methoxydihydrosanguinarine, (B,F) 6-ethoxydihydrosanguinarine, (C,G) Oxychelerythrine, and (D,H) Chelerythrine chloride for 72 hours prior to MTT assay. Each data point for all MTT assays represents the mean of three experiments performed in triplicate. Error bars show the standard error of mean (SD) for the 3 experiments.

Sanguinarine and its structure activity relationship against LSD1 and AR activities

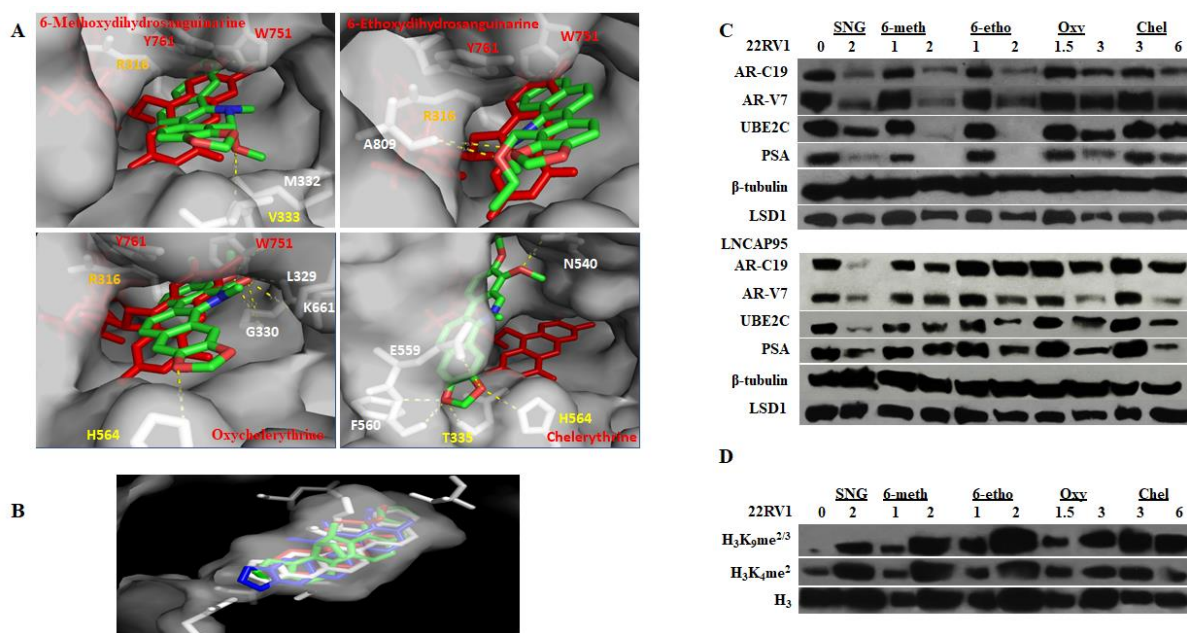
SNG itself is a novel structure derived from nature. Investigating the binding potential of SNG to LSD1 and AR is very crucial, as SNG could be developed as a template for future synthesis of potent LSD1 and AR dual-inhibitors with larger therapeutic indexes for specificity. Further structure activity comparison analysis of more than 32 naturally occurring SNG analogs indicates that SNG is the most potent dual inhibitor of LSD1 and AR (Figure 4). The antiproliferative activity against 22Rv1, LNCaP, and PC3 cell lines for 72 hours are tested by the MTT method. In addition, as shown from Figure 3A, 22Rv1 cells are very important in this study for their expression of LSD1, AR, and ARV7, while LNCaP cells express only AR and LSD1, and PC-3 cells express relatively low level of LSD1, AR, and ARV7.



Supplementary Table 2: Sanguinarine vs. dual inhibitors. Sanguinarine vs. 6-methoxydihydrosanguinarine, 6-ethoxydihydrosanguinarine, Oxychelerythrine, and Chelerythrine.

Among all the 32 natural products, 6-methoxydihydrosanguinarine, 6-ethoxydihydrosanguinarine, Oxychelerythrine, and Chelerythrine chloride display similar, but slightly lower dual inhibitory activity against AR and LSD1 activities compared to that of SNG (Supplementary Table 2). Against 22Rv1 cells, SNG displays an IC_{50} value of $0.68\mu M$, while 6-methoxydihydrosanguinarine, 6-ethoxydihydrosanguinarine, Oxychelerythrine, and Chelerythrine chloride display the IC_{50} value of $0.89\mu M$, $0.91\mu M$, $1.73\mu M$, and $3.34\mu M$, respectively. In addition, against LNCaP cells, SNG displays an IC_{50} value of $1.42\mu M$, while 6-methoxydihydrosanguinarine, 6-ethoxydihydrosanguinarine, Oxychelerythrine, and Chelerythrine chloride display the IC_{50} value of $1.44\mu M$, $1.12\mu M$, $1.89\mu M$, and $6.66\mu M$, respectively. Also, SNG displays an IC_{50} of $2.07\pm 0.45\mu M$ against AR protein activities, and $2.13\pm 0.18\mu M$ against LSD1 activities, whereas 6-methoxydihydrosanguinarine, 6-ethoxydihydrosanguinarine, Oxychelerythrine, and Chelerythrine chloride displays an IC_{50} of $2.15\pm 0.30\mu M$, $1.42\pm 0.45\mu M$, $4.55\pm 0.78\mu M$, and $13.55\pm 0.12\mu M$ against AR protein activities, respectively, and $2.13\pm 0.66\mu M$, $3.69\pm 0.89\mu M$, $5.57\pm 0.30\mu M$, $6.97\pm 1.78\mu M$ against LSD1 protein activities, respectively. Furthermore, molecular docking analysis revealed that these dual-inhibitors also

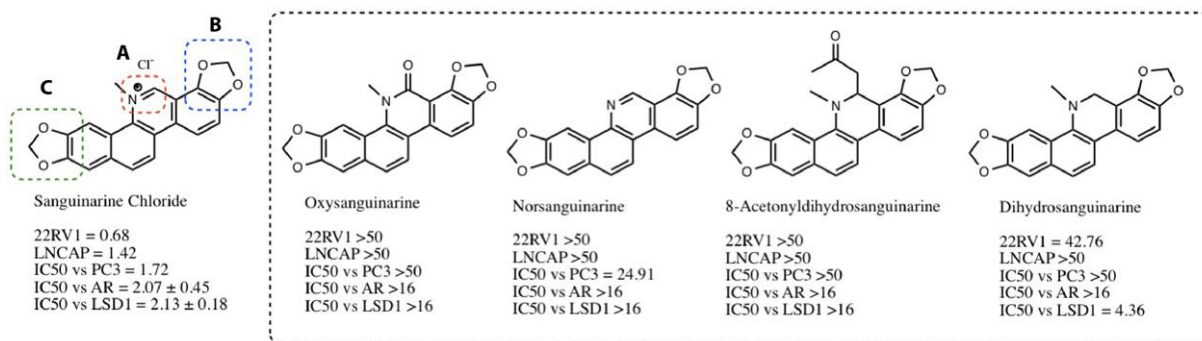
superimpose FAD and bind to the FAD-binding domain of LSD1 (Supplementary Figure 5A) as well as superimpose DHT and bind to the ligand-binding domain of AR (Supplementary Figure 5B). Additionally, WB analysis demonstrates that 22Rv1 and LNCaP95 cell lines treated with these dual inhibitors had significantly reduced the protein expression of AR, ARV7, and PSA (Supplementary Figure 5C). Further, these dual inhibitors increase cellular levels of In H3K4me2 and H3K9me2 in 22Rv1 cells (Supplementary Figure 5D). These results suggest the structure of SNG plays a relevant role in the dual inhibition of both LSD1 and AR activities.



Supplementary Figure 5: Dual-inhibitors binding and inhibiting LSD1 and AR activities. Surface diagram of the active site of the (A) LSD1 protein (Grey, 2DW4, 2.3 Å) in complex with its ligand FAD (red) and superimposed 6-methoxydihydrosanguinarine (Top left), 6-ethoxydihydrosanguinarine (Top right), Oxychelerythrine (Bottom left), or Chelerythrine ligand (Bottom right) (Green). (B) Surface diagram of the active site AR proteins (Grey, 2PIV, 1.95Å) in complex with its ligand DHT (red) and superimposed with 6-methoxydihydrosanguinarine, 6-ethoxydihydrosanguinarine, Oxychelerythrine, and Chelerythrine ligand altogether. (C) AR, ARV7, UBE2C, and PSA protein expression were analyzed via WB in 22RV1 and LNCaP95 cells after 24 hours of treatment with indicated concentration of SNG. B-tubulin was used as the loading control. (D) H3K9me2 and H3K4me2 protein expressions were analyzed via WB in 22RV1 and LNCaP95 cells after 24 hours of treatment with indicated concentration of SNG. Histone H3 was used as the loading control.

Next, we compare the chemical structures of SNG to that of 6-methoxydihydrosanguinarine, 6-ethoxydihydrosanguinarine, Oxychelerythrine, and Chelerythrine chloride. These structures have a similar orientation of the 4 aromatic rings and 1 methylenedioxy group. Both SNG and Chelerythrine chloride have the 5-methylbenzo[c]phenanthridine moiety, Chelerythrine chloride has one of the methylenedioxy groups changed to dimethoxy group (Supplementary Table 2, B region). This alteration reduces the cytotoxic sensitivity of Chelerythrine chloride against 22Rv1 cells and against LNCaP cells down by 5-fold, and reduces the inhibition efficacy against AR protein activities by 10-fold and against LSD1 protein activities by 3-fold. This suggests that the methylenedioxy group in the B region is required for the dual inhibitory activity. Additionally, although Oxychelerythrine also has the methylenedioxy group replaced with dimethoxy group, it has the amide bond (Supplementary Table 2, A region) compared to SNG's

structure. This only brings its cytotoxic sensitivity down by 2-fold against 22Rv1 and LNCaP cells, and its activities down by 2.5-fold against AR and LSD1 protein compared to those of SNG. Moreover, both 6-methoxydihydrosanguinarine and 6-ethoxydihydrosanguinarine's chemical structures are different with that of SNG in which they have the nitrogen atom in sp³ hybridized orbital while SNG has a nitrogen atom in sp² hybridized orbital. This change slightly decreases the cytotoxic sensitivity of 6-methoxydihydrosanguinarine against 22Rv1 and LNCaP cells and decrease those of 6-ethoxydihydrosanguinarine against 22Rv1 cells and the inhibitory activities against LSD1 protein. In fact, those IC₅₀ of 6-ethoxydihydrosanguinarine against LNCaP cells and AR protein activities showed better cytotoxic and inhibitory activity compared to SNG. These results suggest that the changing of sp²-hybridized nitrogen to sp³-hybridized nitrogen together with having a methoxy group or an ethoxy group as the substituent is not required for the dual inhibitory activity.

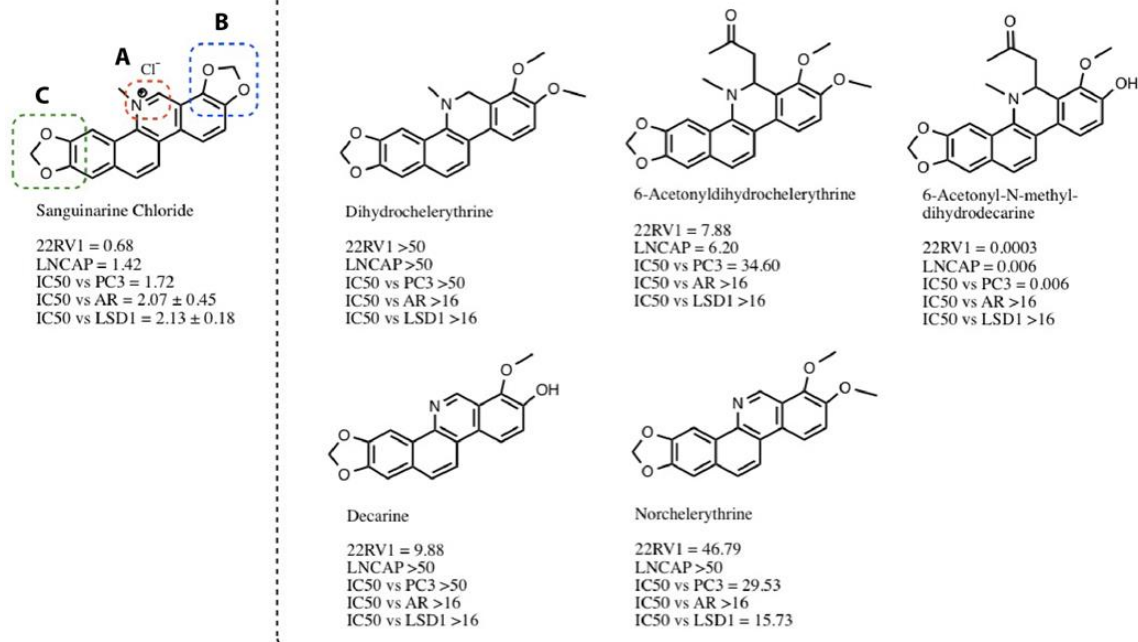


Supplementary Table 3: Sanguinarine vs. A motif changes. Sanguinarine vs. Oxysanguinarine, Norsanguinarine, 8-acetyldihydrosanguinarine, and Dihydrosanguinarine.

The other 28 natural products show either very low inhibitory activity or not show the dual inhibitory effect. For example, as in Supplementary Table 3, Oxysanguinarine, Norsanguinarine, 8-acetyldihydrosanguinarine, and Dihydrosanguinarine have similar orientation of the 4 aromatic rings and 1 methylenedioxy group but have alternatives in A region compared to the chemical structure of SNG. The IC₅₀ of Oxysanguinarine, Norsanguinarine, and 8-acetyldihydrosanguinarine show low inhibitory activity on all the cell lines and AR/LSD1 proteins, and the IC₅₀ of Dihydrosanguinarine shows inhibitory activity only against LSD1 proteins. The chemical structure of Oxysanguinarine is similar to that of Oxchelerythrine in which they both have the amide bond. However, in region B, Oxysanguinarine has the methylenedioxy group while Oxchelerythrine has dimethoxy group. This change is perhaps the reason for the decrease in activity of Oxysanguinarine against all cell lines and AR protein compared to that of Oxchelerythrine. Similarly, 8-acetyldihydrosanguinarine has similar chemical structure with 6-methoxydihydrosanguinarine and 6-ethoxydihydrosanguinarine. However, in the A region, 8-acetyldihydrosanguinarine has an acetyl group, while 6-methoxydihydrosanguinarine and 6-ethoxydihydrosanguinarine have the methoxy and ethoxy group, respectively. The significant decrease in activity against all cell lines and AR/LSD1 proteins of 8-acetyldihydrosanguinarine presumably is a result of the bulkiness of the substituent group. In addition, in the A region, although both

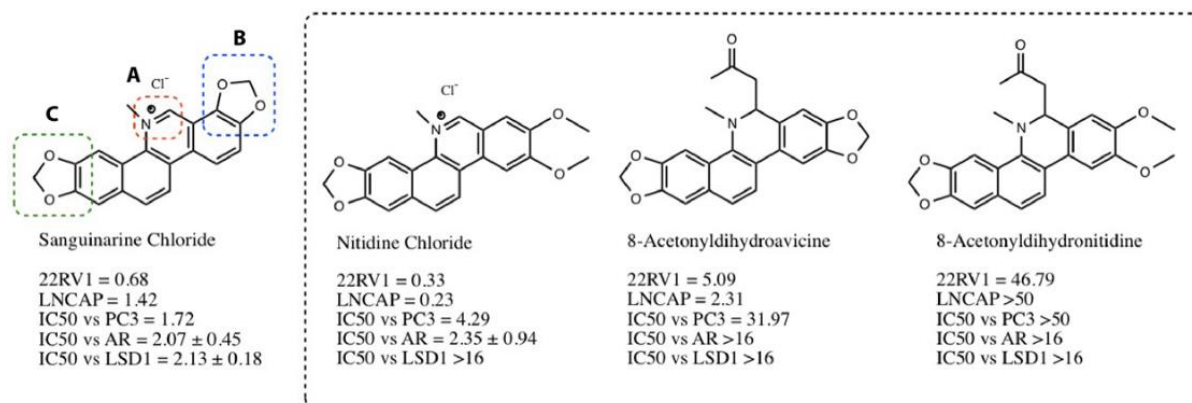
Norsanguinarine and SNG have the nitrogen atom in sp²-hybridized orbital, the absence of a methyl group to the nitrogen atom of Norsanguinarine is probably the reason for its inactive effect on all the cell lines and AR/LSD1 proteins. Additionally, the IC₅₀ of Dihydrosanguinarine shows inhibitory activity only against LSD1 proteins but goes down by 2-fold compared to that of SNG. This presumably is a result of the change from sp²-hybridized nitrogen of sanguinarine to the sp³-hybridized nitrogen of Dihydrosanguinarine. In summary, these results suggest that the sp²-hybridized orbital of nitrogen atom and the methyl group to the nitrogen atom are required for the dual inhibitory activity.

Supplementary Table 4 shows that Dihydrochelerythrine, 6-acetyldihydrochelerythrine, Decarine, 6-acetyl-N-methyl-dihydrodecarine, and Norchelerythrine have similar orientation of the 4 aromatic rings and 1 methylenedioxy group, but have alternatives in the A and B regions compared to the chemical structure of SNG. The IC₅₀ of Dihydrochelerythrine, 6-acetyldihydrochelerythrine, Decarine, and 6-acetyl-N-methyl-dihydrodecarine show very low inhibitory activity on all the cell lines and AR/LSD1 proteins, and the IC₅₀ of Norchelerythrine shows inhibitory activity only against LSD1. Besides the alternatives in region A that can significantly decrease their inhibitory activities as we discussed above, changes in region B can also alter their inhibitory effect. For example, Norchelerythrine has similar chemical structure to that of Norsanguinarine, but having the methylenedioxy group replaced with dimethoxy group. This change is probably the reason Norchelerythrine has its inhibitory activity against LSD1 (although 7-fold lower than that of SNG), while Norsanguinarine is almost inactive against LSD1. Moreover, 6-acetyldihydrochelerythrine, Decarine, and 6-acetyl-N-methyl-dihydrodecarine have similar chemical structures and show low inhibitory activity against AR/LSD1. However, while 6-acetyldihydrochelerythrine and Decarine also show very low inhibitory activity against all cell lines, 6-acetyl-N-methyl-dihydrodecarine has high potency against 22RV1, LNCAP, and PC3 cells. This suggests that the acetyl substituent (A region) and the change from methylenedioxy group to a methoxy group and a hydroxyl group (B region) can potentially inhibit one or more enzyme(s) in these cell lines, and can become a potential subject for future study against PCa cells.



Supplementary Table 4: Sanguinarine vs. A/B motif changes. Sanguinarine vs. Dihydrochelerythrine, 6-acetyl-dihydrochelerythrine, Decarine, 6-acetyl-N-methyl-dihydrodecarine, and Norchelerythrine.

Supplementary Table 5 shows that both 8-Acetyl-dihydroavicine and 8-Acetyl-dihydro-nitidine have very low inhibitory activity against all cell lines and AR/LSD1 proteins. They both have the addition of acetyl substituent (A region), and 8-Acetyl-dihydroavicine has the methylenedioxy group changed in orientation, and 8-Acetyl-dihydro-nitidine has the methylenedioxy group changed in orientation as well as changed to dimethoxy groups. These changes are presumably the reason for the decreases in their inhibitory activities. Additionally, Nitidine chloride has the same 5-methylbenzo[c]phenanthridine moiety with SNG but having the methylenedioxy group changed in orientation as well as changed to dimethoxy group. These alternatives significantly decrease the inhibitory of Nitidine chloride against LSD1, but still keep its inhibitory potency against AR protein, and cytotoxic potency against 22Rv1, LNCaP, PC3 cells. Nitidine chloride also has the same 5-methylbenzo[c]phenanthridine moiety with Chelerythrine chloride but having the dimethoxy group changed in orientation (Supplementary Table 2 and 5). This change brings the IC₅₀ of Nitidine chloride against AR up by nearly 6-fold compared to that of Chelerythrine chloride, but significantly decreases the inhibitory of Nitidine chloride against LSD1. These results suggest that the orientation of the B region is critical to the dual inhibitory activity.

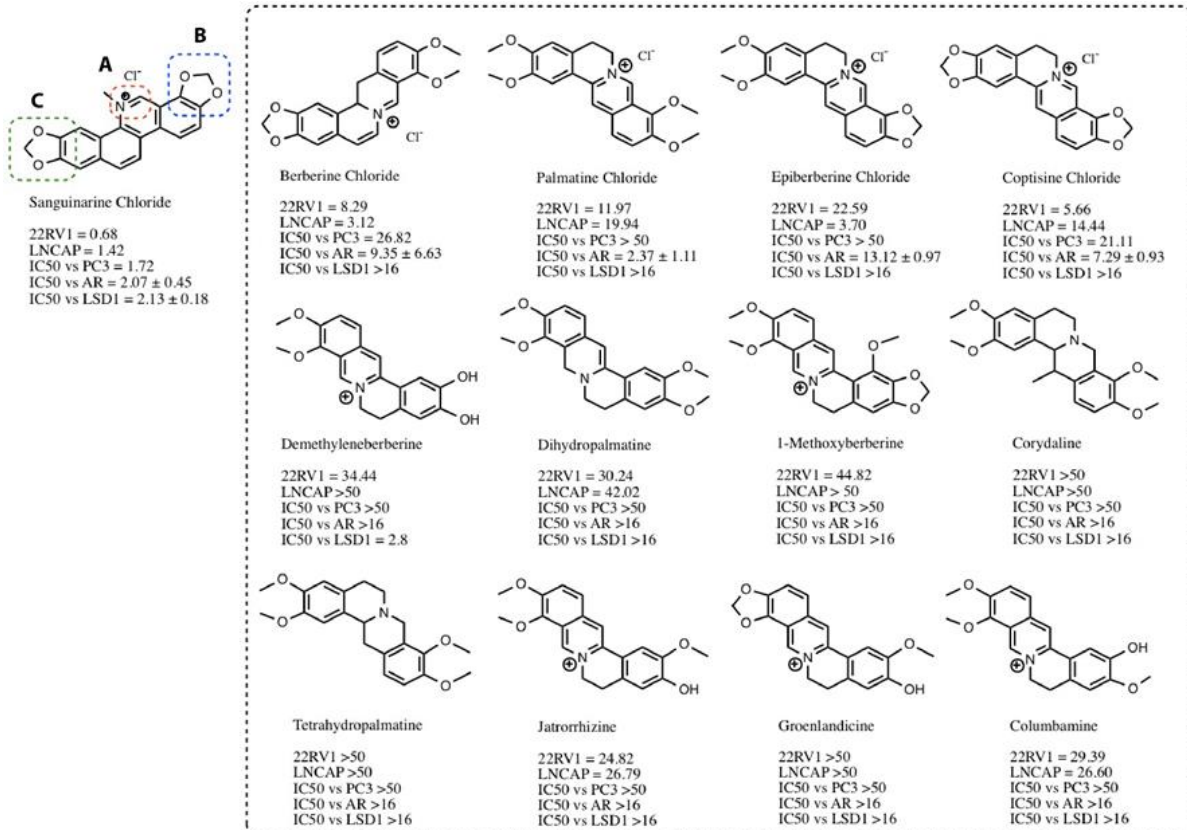


Supplementary Table 5: Sanguinarine vs. A/B motif changes. Sanguinarine vs. Nitidine chloride, 8-Acetyldihydroavicine, and 8-Acetyldihydrontidine

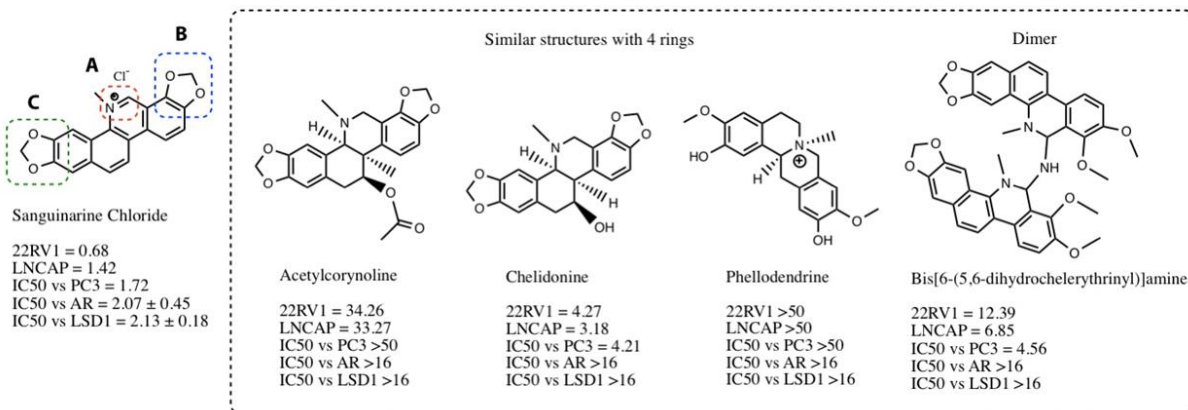
Supplementary Table 6 shows all compounds that have alternatives in B and/or C regions as well as in the orientation of the aromatic rings and the position of the nitrogen atom. The nitrogen atoms are shared between different rings and might cause the chemical structure of the compounds to bend and not planar, which affects the aromaticity and the binding of the compounds to the active sites of AR/LSD1 enzymes. The IC₅₀ of Berberine chloride, Palmatine chloride, Epiberberine chloride, and Coptisine chloride show high inhibitory activity against AR proteins, but weak inhibitory activity against LSD1 proteins and all cell lines. Demethyleneberberine shows high inhibitory activity against LSD1 proteins, but weak inhibitory activity against AR proteins and all cell lines. Dihydropalmatine, 1-Methoxyberberine, Corydaline, Tetrahydropalmatine, Jatrorrhizine, Groenlandicine, and Columbamine show low inhibitory activity against all cell lines and AR/LSD1 proteins. The decreases in their inhibitory activities suggest that the orientation of the aromatic rings and the position of the nitrogen atom in region A are important for the dual inhibitory activity.

Acetylorynoline, Chelidonine, and Phellodendrine have the 4-ring structure similar to SNG and have various substituents. Bis[6-(5,6-dihydrochelerythrinyl)] amine is a dimer (Supplementary Table 7).

Overall, this structural comparison analysis shows the fundamental changes to SNG in effect to its activities against PCa cells and against AR and LSD1 proteins.



Supplementary Table 6: Sanguinarine vs. Berberine chloride, Palmatine chloride, Epiberberine chloride, Coptisine chloride, Demethyleneberberine, Dihydropalmatine, 1-Methoxyberberine, Corydaline, Tetrahydropalmatine, Jatrorrhizine, Groenlandicine, and Columbamine.



Supplementary Table 7: Sanguinarine vs. Acetylornoline, Chelidonine, Phellodendrine, and Bis[6-(5,6-dihydrochelerythryl)]amine.

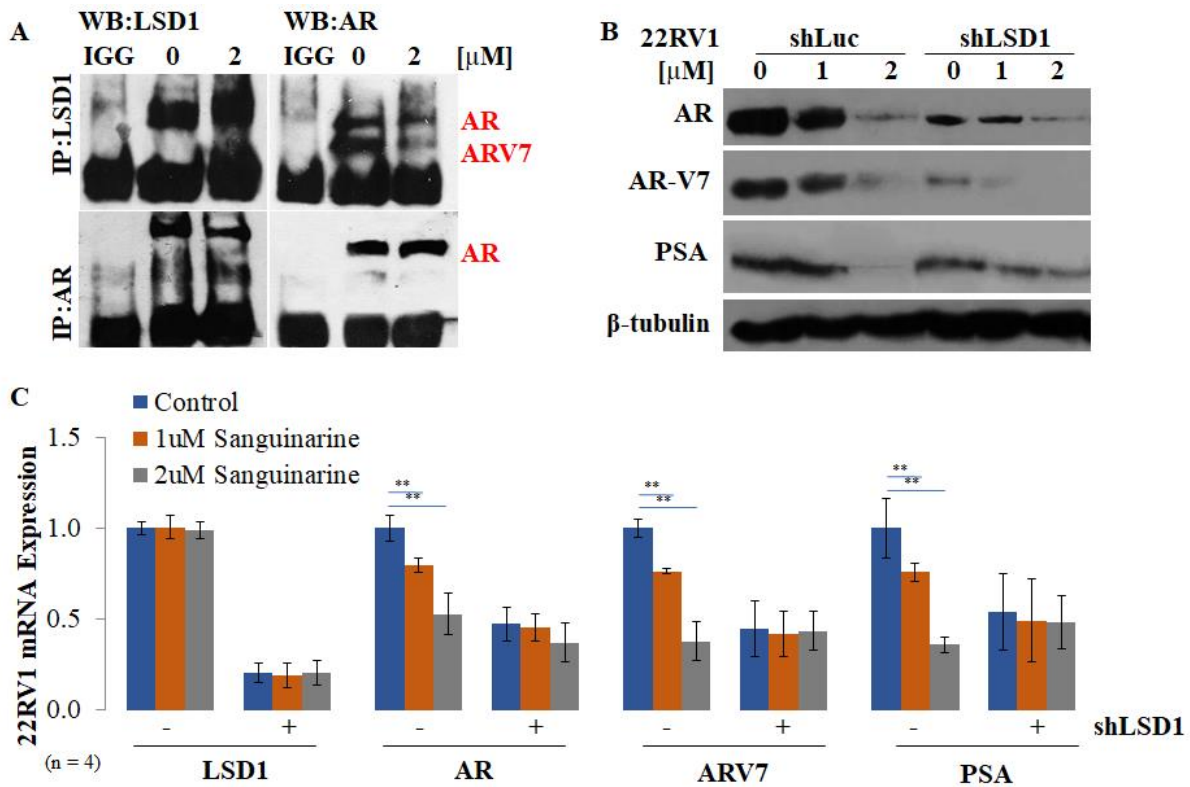
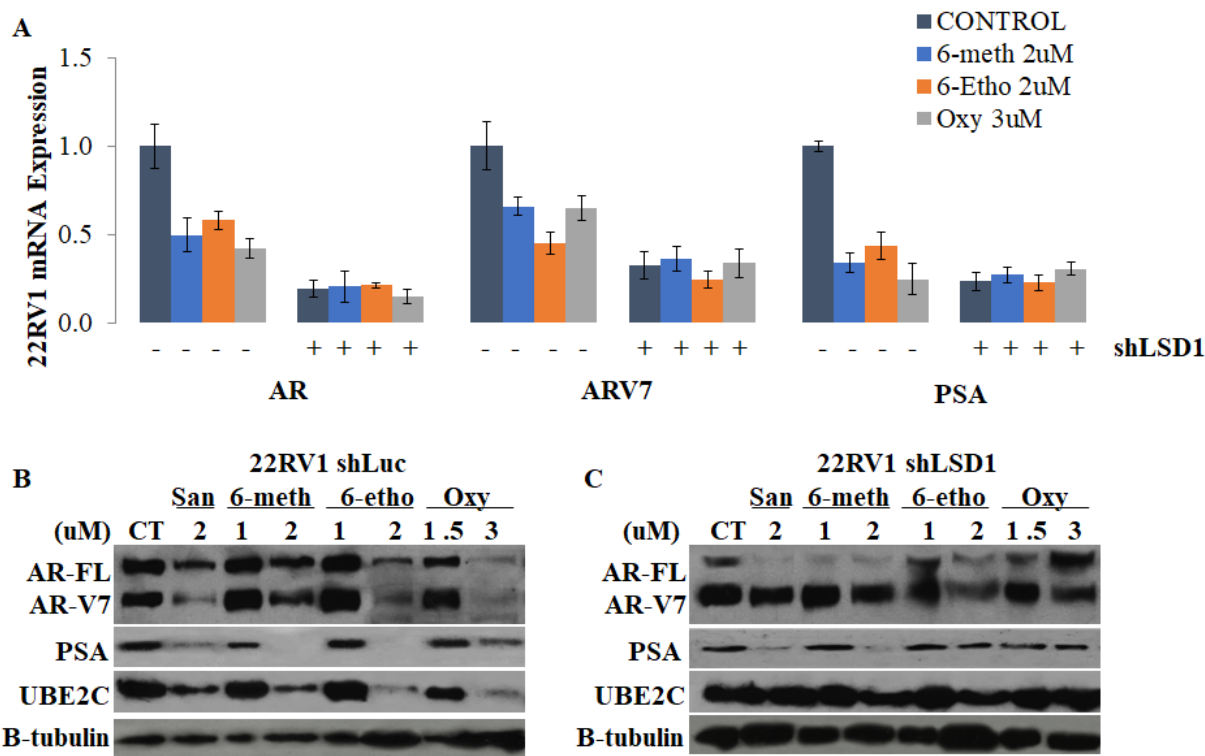


Figure 5: Sanguinarine downregulates AR and ARV7 through in an LSD1 dependent manner. (A) 22RV1 cells were treated with or without SNG for 24 hours. LSD1 (left) and AR (right) were observed after immunoprecipitation WB, pulling down with LSD1 (top) or AR (bottom). (B) WB and (C) qPCR was performed to evaluate the expression levels of AR, ARV7, and their activities in 22RV1- shLuc and 22RV1-shLSD1 cells after 24 hours treatment with SNG.

Sanguinarine inhibits AR and ARV7 through the LSD1-dependent manner

Previous research suggests that LSD1 regulates AR transcriptional activity through direct LSD1 to AR interaction [6]. To determine whether SNG can disrupt the LSD1-AR interaction, we performed immunoprecipitation with anti-LSD1 or anti-AR antibodies, and then WB analysis of their binding partners using corresponding antibodies. Figure 5A upper right panel and lower left panel showed that SNG reduced the complex formation of LSD1 with AR and ARV7 after pulling down LSD1 and staining for AR and vice versa. This result indicated that the interaction between LSD1 and AR or ARV7 was disrupted by SNG. To determine whether the effect of SNG on AR signaling was mediated through LSD1 inhibition, we performed real-time qPCR and WB analysis and looked at the expression of AR, ARV7 and their target genes (i.e. PSA) in 22Rv1 cells with and without LSD1 suppression by shLSD1 transduction. We observed significantly attenuated effects on the inhibition of AR and ARV7 signaling at both protein (Figure 5B) and mRNA (Figure 5C) levels regardless of SNG induction in the 22Rv1-shLSD1 knockdown cells compared to shLuc knockdown control cells. This suggests that LSD1 knockdown alone downregulates AR and ARV7 signaling in 22Rv1 cells. Similarly, treatment with 6-methoxydihydroanguinarine, 6-ethoxydihydroanguinarine, and Oxycelerythrine also did not further

attenuated the mRNA level of AR, ARV7, and PSA in the 22Rv1-shLSD1 knockdown cells (Supplementary Figure 6A), but did continue to affect AR, ARV7, and PSA at the protein levels similar to SNG (Supplementary Figure 6B and 6C), suggesting another enzymatic or protein pathway to decrease AR/ARV7 protein expression level. Overall, these results suggest SNG reduced the complex formation of LSD1 with AR and ARV7, and that SNG reduced AR and ARV7 signaling partly through LSD1-dependent inhibition.



Supplementary Figure 6: Natural LSD1 and AR dual-inhibitors inhibit AR and ARV7 through an LSD1-dependent manner (A) qPCR was performed to evaluate the expression levels of AR, ARV7, and their activities in 22RV1- shLuc and 22RV1-shLSD1 cells after 24 hours treatment with 6-methoxydihydroanguinarine (6-Meth), 6-ethoxydihydroanguinarine (6-Etho), or Oxychelyerythrine (Oxy). WB was performed to evaluate the protein levels of AR, ARV7, and their activities in (B) 22RV1- shLuc and (C) 22RV1-shLSD1 cells after 24 hours treatment with 6-Meth, 6-Etho, or Oxy.

Sanguinarine competitively and directly interact with LSD1 and AR

To determine whether SNG could directly interact with LSD1 and AR proteins, we conducted two novel binding-assays: Cellular thermal shift assay (CETSA) and surface plasmon resonance (SPR). LSD1 (Figure 6A) and AR (Figure 6B) protein remained stable as temperatures were increased by increments of 3°C under SNG treatment in 22Rv1 cells compared to those treated with vehicle control (0.1% DMSO). Furthermore, we performed a CETSA isothermal dose response (ITDR_{CETSA}), where the cells were treated under increasing increment concentrations of SNG under single high temperature that targeted protein were degraded under no treatment conditions. The lower panels of the ITDR_{CETSA} curves

for LSD1 proteins at 50°C (Figure 6C) and AR proteins at 52°C (Figure 6D) showed that SNG binding at an estimated K_m values of 520 nM and 400 nM, respectively. These results suggested SNG might interact with both complexes of LSD1 and AR proteins to increase their thermal stabilities. In addition, 6-methoxydihydrosanguinarine, 6-ethoxydihydrosanguinarine, and Oxychelerythrine was shown to stabilize both the LSD1 and AR complex compared to 0.1% DMSO control (Supplementary Figure 7A-C), whereas Chelerythrine did not show any changes (Data not shown).

Both CESTA and ITDR_{CESTA} could only suggest that SNG binds to the LSD1 and AR complex, but does not indicate whether SNG could directly bind to them individually. Thus, to determine whether SNG could directly bind to LSD1 and AR proteins, SPR assay was performed using recombinant His-tagged containing LSD1 or AR proteins. The recombinant LSD1 or AR proteins were fixed on a NTA-containing gold film layer with SNG ligands being injected to flow over proteins. Any binding of the protein and ligand would result in a signal, measured as a response unit (RU). As a result, the K_D and k_d values of SNG binding was measured to be $1.10 \pm 0.42 \mu\text{M}$ and 0.0086 1/s on LSD1 proteins (Figure 6E and 6G) and $2.54 \pm 0.89 \mu\text{M}$ and 0.0075 1/s on AR proteins (Figure 6F and 6H). Overall, these results demonstrated that SNG could directly bind to LSD1 and AR proteins individually to inhibit their enzymatic activities.

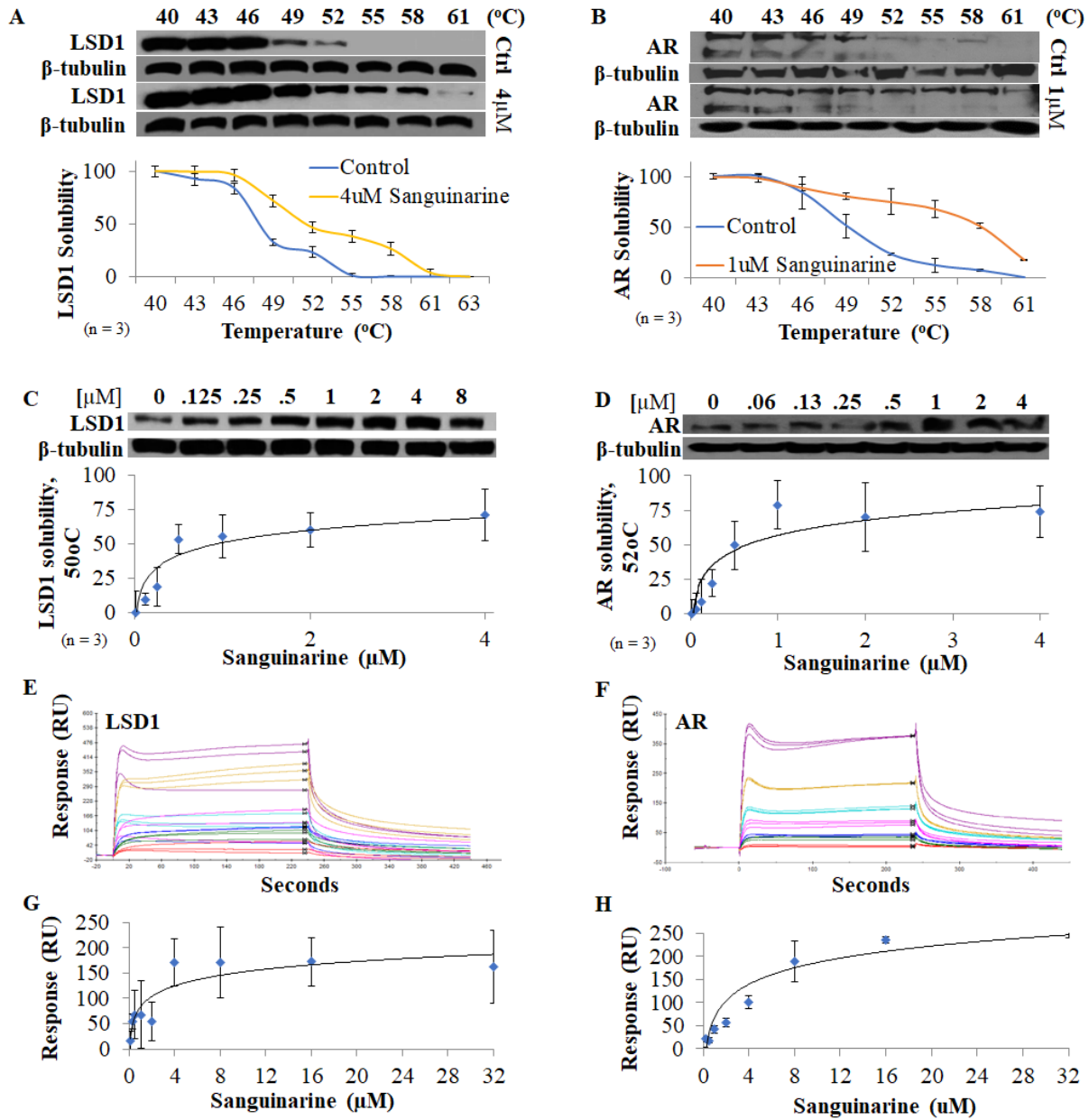
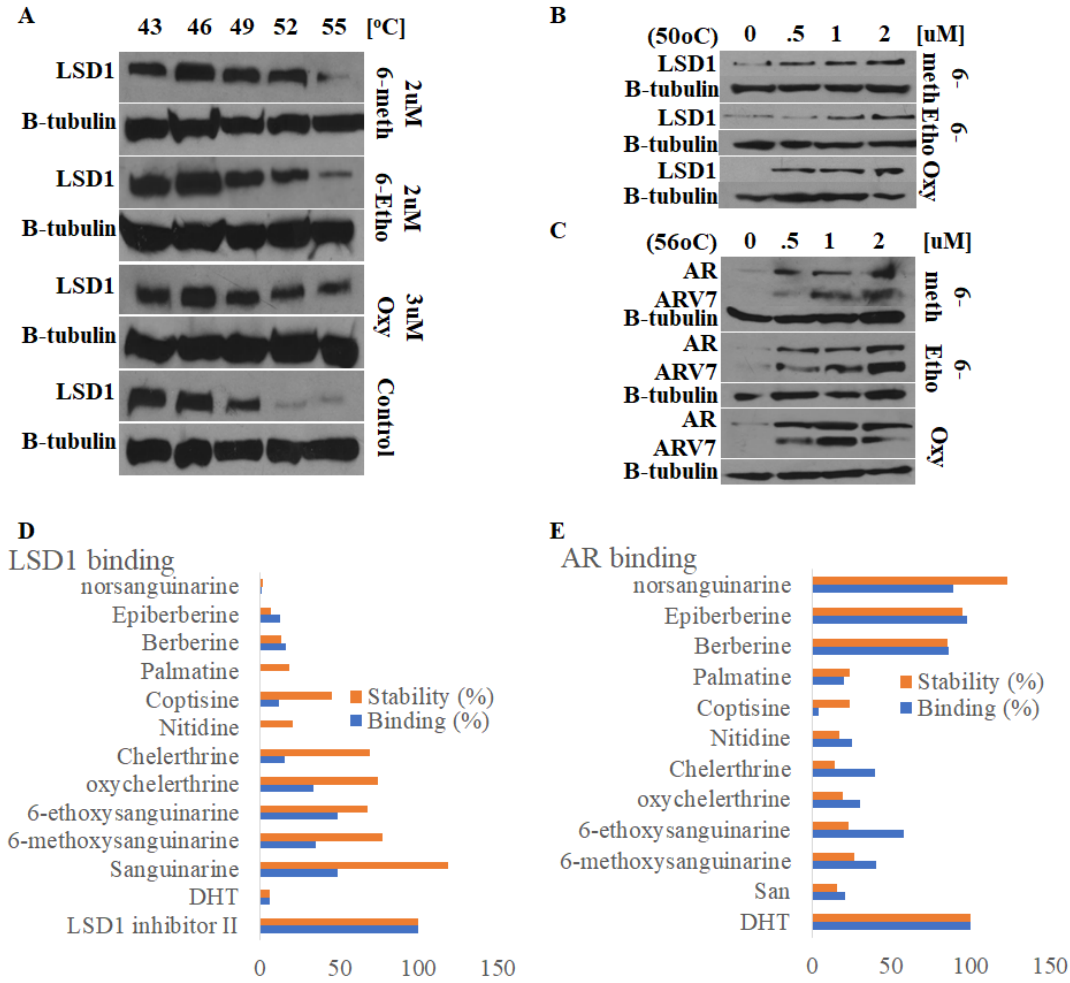


Figure 6: Sanguinarine directly interacts with LSD1 and AR proteins. CESTA was performed using (A) 22RV1 cells treated with 4 μM SANG looking at LSD1 and (B) C42B cells treated with 1 μM SNG looking at AR under a range of temperatures from 40 °C to 61 °C. β-tubulin antibody was used as loading control, and 0.1% DMSO was used as treatment control. ImageJ program was used to measure the density of bands between control and SANG treatment. CITDR CESTA experiment was performed to determine the potency of SNG engagement to (C) LSD1 at 50 °C and to (D) AR at 50 °C. SNG K_m to LSD1 = 520 nM and K_m Sensorgrams of SPR analysis of (E) LSD1 recombinant protein and (F) AR recombinant protein at different concentrations of SANG. 8 μM (purple), 4 μM (orange), 2 μM (baby blue), 1 μM (pink), 0.5 μM (blue), 0.25 μM (Green), and 0.125 μM (red), to AR = 400 nM. Data is the mean ± SD of one replicate, n=3. Binding curves of SNG conjugated to the immobilized (G) LSD1 and (H) AR and results of one-site binding fitting. The calculated dissociation constant and the maximum RU value that was reached and theoretically possible can be found within the individual graphs.



Supplementary Figure 7: LSD1 and AR dual-inhibitors engage in LSD1 and AR complexes. CESTA was performed using (A) 22RV1 cells treated with 2µM 6-methoxydihydrosanguinarine, 2µM 6-ethoxydihydrosanguinarine, and 3µM Oxychelerythrine looking at LSD1 under a range of temperatures from 43oC to 55oC. β-tubulin antibody was used as loading control, and 0.1% DMSO was used as treatment control. CITDR CESTA experiment was performed with 22Rv1 cells to determine the potency of 6-methoxydihydrosanguinarine, 6-ethoxydihydrosanguinarine, and Oxychelerythrine engagement to (B) LSD1 at 50oC and to (C) AR at 56oC. Binding and stability screening of several SNG-related compounds conjugated to the immobilized (D) LSD1 and (E) AR.

The correlation of LSD1 and AR under Sanguinarine treatment shown by RNA-sequencing analysis.

To further investigate the correlation and the overall effect of SNG on LSD1 and AR, we analyzed the RNA-sequencing data from 22Rv1-shLuc and 22Rv1-shLSD1 cell lines. Unfortunately, we were not able to complete this last experiment by the time this dissertation was submitted.

DISCUSSION

Castration-resistant prostate cancer (CRPC) has still been immensely lethal up to the present despite many newly developed therapies such as chemotherapy, hormone therapy, and immunotherapy [30-37]. The CRPC mechanism underlying AR signaling, includes mutation, amplification and diminishment in activity, and truncating splice variants such as ARV7. Therefore, targeting AR and its abnormal forms such as ARV7 is a strategic approach as therapy for CRPC.

Studies have shown many epigenetic mechanisms involved in the development of prostate cancer, leading to the CRPC progression. In prostate cancer, tumor suppressor genes are silenced through hyper-methylation of promoter and DNA hypo-methylation that leads to epigenetic aberrations [38]. Similarly, genes resulting in aggressive PCa can be epigenetically modified through histone methylation and altered gene expression. LSD1, a histone demethylase that interacts with AR in prostate cancer, could promote AR-dependent gene expression and progress the disease into more advanced levels [39-41]. Therefore, suppressing both LSD1 and AR is our new approach to establish further advanced treatments.

We examined whether SNG, which is our molecule candidate, could play a role in dual inhibition of LSD1 and AR. Through LSD1 inhibition assay and dialysis assay, SNG was shown to potentially bind to LSD1 and inhibit LSD1-mediated demethylation by competing with FAD, an only cofactor for LSD1 methylase activities. In addition, we determined that SNG would reduce the expression and transcriptional activities of AR and its variants and downstream genes. By examining the effects of SNG in LSD1-overexpressed, LSD1-suppressed, AR-lacked PCa cell lines, we explored that SNG would be more sensitive to cells that have moderate-to-strong LSD1 and AR expressions. This would imply that LSD1 and AR are partially responsible for the biological consequences of SNG. We further investigated into the mechanism of inhibition, and evidence has shown that SNG might potentially induce the LSD1-mediated suppression on AR and its variant (AR-V7) signaling. Overall, our results suggest that SNG could play a dual-inhibitory role against LSD1 and AR and be a potential compound for further therapeutic development.

The proposed dual-inhibitory function of SNG against LSD1 and AR was not only crucial to its clinical relevance for treatment of CRPC but also as a scaffold for future derivative synthesis. According to our molecular modeling results, SNG's ability of targeting LSD1 and AR relied on its relatively planar structure as an analog of the cofactor FAD. As verified by CESTA and SPR, SNG could be a good candidate for future investment on research regarding the synthesis of isoquinoline derivatives with high clinical value. FAD-analog inhibitors presented the possibility of off-target effects onto other FAD-dependent enzymes. Consequently, developing next-generation derivatives of SNG while retaining and magnifying its dual inhibition of both LSD1 and AR is crucial. Whether SNG-derived inhibitors bind

only to either LSD1 or AR, future experiments need focus on elucidating how the singular binding results in the dual inhibition. Clinical relevance of SNG for treatments of CRPC was also dependent on its pharmacokinetics and pharmacodynamics properties, as well as the abilities to prevent the progression of CRPC. Overall, the significance of this study demonstrated that SNG was a novel structure that could hinder CRPC progression through a dual-target inhibition of LSD1 and AR.

REFERENES

1. Xie SW, Wang YQ, Dong BJ, Xia JG, Li HL, Zhang SJ, Li FH, Xue W (2018) A Nomogram Based on a TRUS Five-Grade Scoring System for the Prediction of Prostate Cancer and High Grade Prostate Cancer at Initial TRUS-Guided Biopsy. *Journal of Cancer* 9 (23):4382-4390. doi:10.7150/jca.27344
2. Barry MJ, Simmons LH (2017) Prevention of Prostate Cancer Morbidity and Mortality: Primary Prevention and Early Detection. *Medical Clinics of North America* 101 (4):787-806. doi:https://doi.org/10.1016/j.mcna.2017.03.009
3. Gucalp A, Traina TA (2017) The Androgen Receptor: Is It a Promising Target? *Annals of Surgical Oncology* 24 (10):2876-2880. doi:10.1245/s10434-017-5961-9
4. Culig Z, Santer FR (2014) Androgen receptor signaling in prostate cancer. *Cancer and Metastasis Reviews* 33 (2):413-427. doi:10.1007/s10555-013-9474-0
5. He Y, Hooker E, Yu E-J, Cunha GR, Liao L, Xu J, Earl A, Wu H, Gonzalgo ML, Sun Z (2018) Androgen signaling is essential for development of prostate cancer initiated from prostatic basal cells. *Oncogene*. doi:10.1038/s41388-018-0583-7
6. Tatsumi K, Hirotsu A, Daijo H, Matsuyama T, Terada N, Tanaka T (2017) Effect of propofol on androgen receptor activity in prostate cancer cells. *European Journal of Pharmacology* 809:242-252. doi:https://doi.org/10.1016/j.ejphar.2017.05.046
7. Thadani-Mulero M, Portella L, Sun S, Sung M, Matov A, Vessella RL, Corey E, Nanus DM, Plymate SR, Giannakakou P (2014) Androgen receptor splice variants determine taxane sensitivity in prostate cancer. *Cancer research* 74 (8):2270-2282. doi:10.1158/0008-5472.CAN-13-2876
8. Guo C, Yeh S, Niu Y, Li G, Zheng J, Li L, Chang C (2017) Targeting androgen receptor versus targeting androgens to suppress castration resistant prostate cancer. *Cancer Letters* 397:133-143. doi:https://doi.org/10.1016/j.canlet.2017.03.022
9. Ho Y, Dehm SM (2017) Androgen Receptor Rearrangement and Splicing Variants in Resistance to Endocrine Therapies in Prostate Cancer. *Endocrinology* 158 (6):1533-1542. doi:10.1210/en.2017-00109
10. Battaglia S, Karasik E, Gillard B, Williams J, Winchester T, Moser MT, Smiraglia DJ, Foster BA (2017) LSD1 dual function in mediating epigenetic corruption of the vitamin D signaling in prostate cancer. *Clinical epigenetics* 9:82-82. doi:10.1186/s13148-017-0382-y
11. Chen Z-Y, Chen H, Qiu T, Weng X-D, Guo J, Wang L, Liu X-H (2016) Effects of cisplatin on the LSD1-mediated invasion and metastasis of prostate cancer cells. *Molecular medicine reports* 14 (3):2511-2517. doi:10.3892/mmr.2016.5571
12. Wang M, Liu X, Jiang G, Chen H, Guo J, Weng X (2015) Relationship between LSD1 expression and E-cadherin expression in prostate cancer. *International Urology and Nephrology* 47 (3):485-490. doi:10.1007/s11255-015-0915-2
13. Ketscher A, Jilg CA, Willmann D, Hummel B, Imhof A, Rüsseler V, Hölz S, Metzger E, Müller JM, Schüle R (2014) LSD1 controls metastasis of androgen-independent prostate cancer cells through PXN and LPAR6. *Oncogenesis* 3 (10):e120-e120. doi:10.1038/oncsis.2014.34
14. Achkar IW, Mraiche F, Mohammad RM, Uddin S (2017) Anticancer potential of sanguinarine for various human malignancies. *Future Medicinal Chemistry* 9 (9):933-950. doi:10.4155/fmc-2017-0041
15. Ma Y, Chu J, Ma J, Ning L, Zhou K, Fang X (2017) Sanguinarine protects against ovariectomy-induced osteoporosis in mice. *Molecular medicine reports* 16 (1):288-294. doi:10.3892/mmr.2017.6574
16. Zhang R, Wang G, Zhang P-F, Zhang J, Huang Y-X, Lu Y-M, Da W, Sun Q, Zhu J-S (2017) Sanguinarine inhibits growth and invasion of gastric cancer cells via regulation of the DUSP4/ERK pathway. *Journal of cellular and molecular medicine* 21 (6):1117-1127. doi:10.1111/jcmm.13043
17. Ma Y, Sun X, Huang K, Shen S, Lin X, Xie Z, Wang J, Fan S, Ma J, Zhao X (2017) Sanguinarine protects against osteoarthritis by suppressing the expression of catabolic proteases. *Oncotarget* 8 (38):62900-62913. doi:10.18632/oncotarget.17036
18. Li X, Li T, Chen D, Zhang P, Song Y, Zhu H, Xiao Y, Xing Y (2015). Overexpression of lysine-specific demethylase 1 promotes androgen-independent transition of human prostate cancer LNCaP cells through activation of the AR signaling pathway and suppression of the p53 signaling pathway. *Oncology Report*
19. Ricq E. (2016) Chemical Neurobiology of the histone Lysin demethylase KDM1A. Harvard dissertation defense.
20. Yadav S, Li J1, Stockert J, Herzog B, O'Connor J, Garzon-Manco L, Parsons R, Tewari A, Yadav K (2017) .Induction of Neuroendocrine Differentiation in Prostate Cancer Cells by Dovitinib (TKI-258) and its Therapeutic Implications. *Translational Oncology*
21. Mota S, Bailey S, Strivens RA, Hayden AL, Douglas LR, Duriez PJ, Borrello T, Benelkebir H, Ganesan A, Packham G and Crabb S. (2018) LSD1 inhibition attenuates androgen receptor V7 splice variant activation in castration resistant prostate cancer models. *Cancer Cell International*.
22. Hayami, S., Kelly, J. D., Cho, H., Yoshimatsu, M., Unoki, M., Tsunoda, T., . . . Hamamoto, R. (2010, November 27). Overexpression of LSD1 contributes to human carcinogenesis through chromatin regulation in various cancers.
23. Li, Xuechao, Li, Tao, Chen, Dehong, . . . Yifei. (2016, January 01). Overexpression of lysine-specific demethylase 1 promotes androgen-independent transition of human prostate cancer LNCaP cells through activation of the AR signaling pathway and suppression of the p53 signaling pathway.
24. (2018) Association of androgen receptor (AR) copy number gain with ARV7 expression and response to chemotherapy. *Journal of Clinical Oncology*
25. (2017) Activity of sanguinarine against *Candida albicans* biofilms
26. (2010) Sanguinarine Suppresses Prostate Tumor Growth and Inhibits Survivin Expression
27. (2000) Differential Antiproliferative and Apoptotic Response of Sanguinarine for Cancer Cells versus Normal Cells
28. (2012) LSD1/CoREST is an allosteric nanoscale clamp regulated by H3-histone-tail molecular recognitio
29. <https://www.genecards.org/cgi-bin/carddisp.pl?gene=KDM1A>
30. Beer TM, Armstrong AJ, Rathkopf DE, Loriot Y, Sternberg CN, Higano CS, Iversen P, Bhattacharya S, Carles J, Chowdhury S, et al. Enzalutamide in metastatic prostate cancer before chemotherapy. *N Engl J Med*. 2014;371(5):424–33.
31. de Bono JS, Logothetis CJ, Molina A, Fizazi K, North S, Chu L, Chi KN, Jones RJ, Goodman OB Jr, Saad F, et al. Abiraterone and increased survival in metastatic prostate cancer. *N Engl J Med*. 2011;364(21):1995–2005.
32. Ryan CJ, Smith MR, de Bono JS, Molina A, Logothetis CJ, de Souza P, Fizazi K, Mainwaring P, Piulats JM, Ng S, et al. Abiraterone in meta-static prostate cancer without previous chemotherapy. *N Engl J Med*. 2013;368(2):138–48.
33. Scher HI, Fizazi K, Saad F, Taplin ME, Sternberg CN, Miller K, de Wit R, Mulders P, Chi KN, Shore ND, et al. Increased survival with enzalutamide in prostate cancer after chemotherapy. *N Engl J Med*. 2012;367(13):1187–97.
34. Smith MR, Saad F, Chowdhury S, Oudard S, Hadaschik BA, Graff JN, Olmos D, Mainwaring PN, Lee JY, Uemura H, et al. Apalutamide Treatment and Metastasis-free Survival in Prostate Cancer. *N Engl J Med*. 2018;378:1408–18.

35. de Bono JS, Oudard S, Ozguroglu M, Hansen S, Machiels JP, Kocak I, Gravis G, Bodrogi I, Mackenzie MJ, Shen L, et al. Prednisone plus cabazitaxel or mitoxantrone for metastatic castration-resistant prostate cancer progressing after docetaxel treatment: a randomised open-label trial. *Lancet*. 2010;376(9747):1147–54.
36. Kantoff PW, Higano CS, Shore ND, Berger ER, Small EJ, Penson DF, Redfern CH, Ferrari AC, Dreicer R, Sims RB, et al. Sipuleucel-T immunotherapy for castration-resistant prostate cancer. *N Engl J Med*. 2010;363(5):411–22.
37. Parker C, Nilsson S, Heinrich D, Helle SI, O’Sullivan JM, Fossa SD, Chodacki A, Wiechno P, Logue J, Seke M, et al. Alpha emitter radium-223 and survival in metastatic prostate cancer. *N Engl J Med*. 2013;369(3):213–23.
38. Graca I, Pereira-Silva E, Henrique R, Packham G, Crabb SJ, Jeronimo C. Epigenetic modulators as therapeutic targets in prostate cancer. *Clin Epigenetics*. 2016;8:98. doi: 10.1186/s13148-016-0264-8.
39. Wissmann M, Yin N, Muller JM, Greschik H, Fodor BD, Jenuwein T, Vogler C, Schneider R, Gunther T, Buettner R, et al. Cooperative demethylation by JMJD2C and LSD1 promotes androgen receptor-dependent gene expression. *Nature Cell Biol*. 2007;9(3):347–353. doi: 10.1038/ncb1546.
40. Cai C, He HH, Gao S, Chen S, Yu Z, Gao Y, Chen S, Chen MW, Zhang J, Ahmed M, et al. Lysine-specific demethylase 1 has dual functions as a major regulator of androgen receptor transcriptional activity. *Cell Rep*. 2014;9(5):1618–1627. doi: 10.1016/j.celrep.2014.11.008.
41. Cai C, He HH, Chen S, Coleman I, Wang H, Fang Z, Chen S, Nelson PS, Liu XS, Brown M, et al. Androgen receptor gene expression in prostate cancer is directly suppressed by the androgen receptor through recruitment of lysine-specific demethylase 42. *Cancer Cell*. 2011;20(4):457–471. doi: 10.1016/j.ccr.2011.09.001.

CHAPTER 5

Nitidine induces toxicity to Castration-resistant prostate cancer (CRPC) by degrading AR/AR-V7 mediated by Hsp70/STUB1 pathway

Victor Pham† and Vinh X. Le†, Erik D. Tran, Thanh NH Le, Matthew Tippin, and Xiaolin Zi

ABSTRACT

Castration-resistant prostate cancer (CRPC) is a lethal type of late-stage prostate cancer (PCa) due to developing resistance to androgen deprivation therapy (ADT) and treatments with the second-generation of anti-androgen medications (i.e. Enzalutamide, Abiraterone). Androgen receptor (AR) has been a main driver and therapeutic target, which has been established from various studies on ADT resistance whose mechanisms include androgen-independent AR activation, AR mutation, and AR variants (i.e. AR-V7). Hence, suppressing AR and its variants (AR-V7) is one of new potential approaches to inhibit PCa progression. Previously, we discovered that Sanguinarine had inhibitory activities in AR and AR-V7. For further investigation on the mechanism of degrading AR and AR-V7 proteins, here we show Nitidine (Ni), an analog of Sanguinarine, suppresses AR and AR-V7 protein expression through the machinery of the Hsp70/STUB1 pathway, which could potentially be the novel template for therapeutic drugs treating CRPC.

BACKGROUND

Proteostasis is modulated through an extensive network which includes molecular chaperone proteins, ubiquitin–proteasome system, and autophagy system. Recently, target protein degradation via ubiquitin–proteasome pathway has been considered as the new approach for CRPC [1]. The Ubiquitin/Proteasome System (UPS) is a highly regulated mechanism of intracellular protein degradation and turnover. Through the concerted actions of a series of enzymes, proteins are marked for proteasomal degradation by being linked to the polypeptide co-factor, ubiquitin. Several studies demonstrated AR degradation could be mediated by this pathway with some typical E3 enzymes (MDM2, SKP2, CHIP).

Heat shock proteins are the members of the chaperone protein family which regulates the activity and stability of many oncogenes that control cancer cell survival and progression^{3,13,14,15}. The HSP70s family, including stress inducible member HSP70 (HSPA1A/HSPA1B) and constitutively expressed member HSC70 (HSPA8), plays important roles for protein maturation and correct folding in cancer cell signal transduction and regulation^{16,17,18}. STUB1 is a co-chaperone protein and functional E3 ubiquitin

ligase that links HSP70's polypeptide-binding activity to the ubiquitin proteasome system. HSP70 interacts with STUB1 and controls protein stabilization. Binding of STUB1 to HSP70 can halt the proper folding of HSP70 substrate proteins and concomitantly facilitate the U-box-dependent ubiquitination of HSP70-bound substrates^{19,20,21}. As AR's co-chaperone protein, HSP70 assists the folding and maturation of AR protein^{22,23,24}. However, understanding of the interaction among AR-V7, HSP70, and STUB1 in next generation anti-androgen resistance remains elusive.

RESULTS

Nitidine (Ni) attenuates androgen receptor (AR) activities

This study was initiated with the screening of 32 natural compounds which are analogous to Sanguinarine (Pham et al., 2020) in respect to their influences on Lysine-specific Demethylase 1A (LSD1) and androgen receptor (AR) activity. To further discover the pathway of Sanguinarine on down-regulating AR, we selected compounds analogous to the screened Sanguinarine-related analogs from Pham et al., 2020 that were only targeting AR. Among the selected molecules, we observed that Nitidine, a structural analog of Sanguinarine, was shown to have the highest potential of AR inhibitory activities. Then, we compared the chemical structure, cytotoxicity, and AR activities of Nitidine to Berberrubine, Dihydropalmatine, 13-methylberberine, Palmatrubine, and Pseudopalmatine (Figure 1A). Using AR-Luciferase Reporter Assay, among these compounds, only Nitidine was shown to considerably attenuate the activities of androgen receptor (AR) with an approximate IC_{50} value of 5.65 μ M, whereas the other five compounds insignificantly affected AR activity at very high dosages with the approximate IC_{50} values $> 16 \mu$ M (Figure 1B). In addition, Nitidine is the only compound that possesses the strong antiproliferative activity on prostate cancer cell 22Rv1, PC3, and C4-2B (Figure 1C-E). Based on these observations, we detected that Nitidine has a unique 5-methylbenzo[c]phenanthridine moiety, which contains the 4 aromatic rings in a different orientation from the 4 aromatic rings of the other five compounds. The low inhibitory activity of the five compounds against AR suggested that the 5-methylbenzo[c]phenanthridine moiety is required for the inhibitory activity against AR. Therefore, Nitidine could potentially be the only hit molecule in the screened compound library since it would contain high potency against AR activity in prostate cancer.

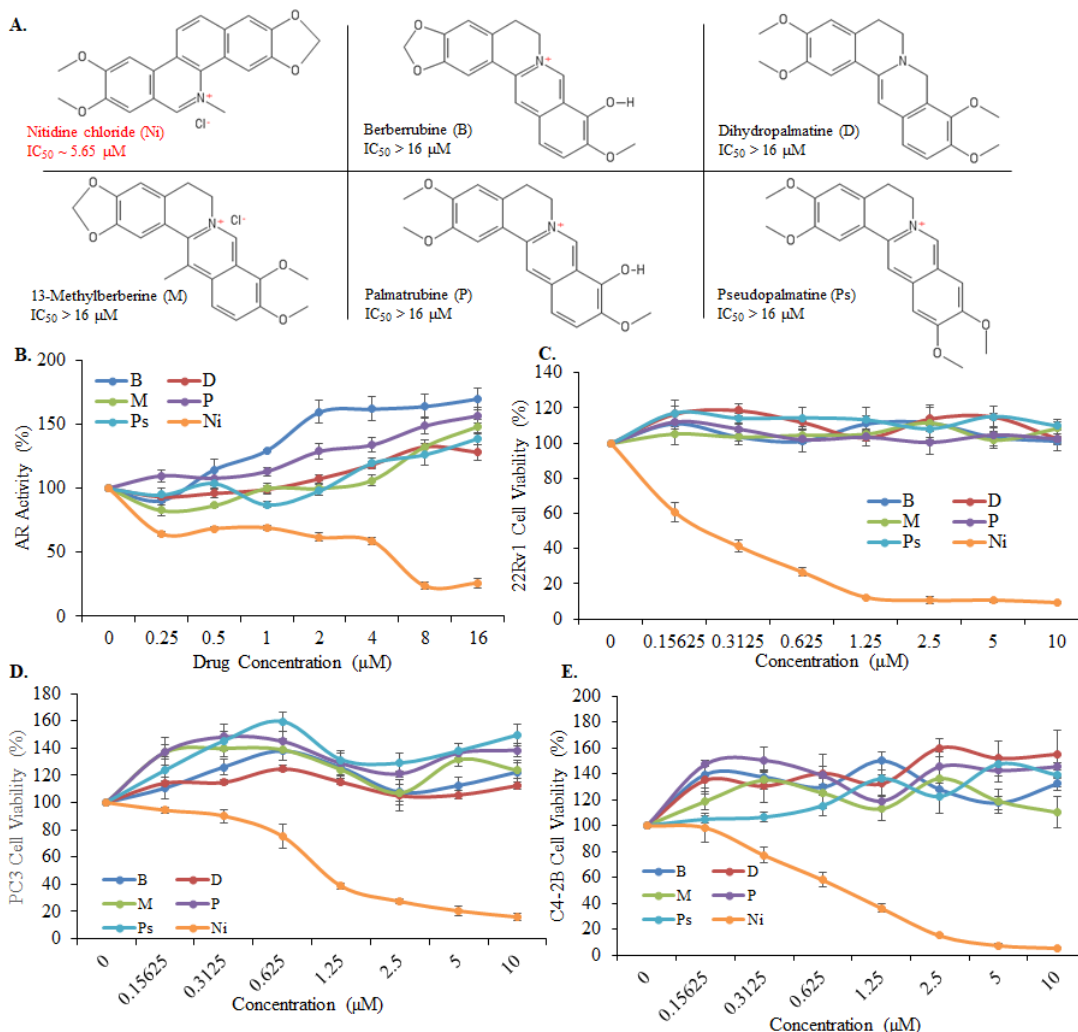


Figure 1. Structure-related analogs and their influences on AR activities. (A) These structure-related analogs were chosen based on our previous publication for their relative inhibition of AR activities, [Pham et al., 2020](#). These structures include Nitidine, Berberubine, Dihydropalmitine, 13-Methylberberine, Palmatrubine, and Pseudopalmitine (B) The influence of these analogs on AR activities was detected by AR-Luciferase Reporter Assay, where DHT-pretreated MDA-MB-453 cells were treated for 8 hours with indicated concentration of each compound. MTT assay was performed on (C) 22Rv1, (D) PC3, and (E) C4-2B under 72 hours treatment with indicated concentration of the analogs.

Nitidine (Ni) induces cytotoxicity and apoptosis in CRPC cells

Several studies demonstrated that 22Rv1, C4-2B MDVR, C4-2B, and LNCaP are AR-positive with the respectively decreasing level, while PC3 and DU145 are considered as AR-negative cell lines [2-7]. Following the identification of Nitidine (Ni) as our candidate molecule, we next examined and compared the potential cytotoxicity of Nitidine on the normal prostate epithelial RWPE-1 cell line to various PCa cell lines using MTT Assay. Our MTT results showed that Nitidine was more cytotoxic to these PCa cells such as 22Rv1, C4-2B MDVR, LNCaP, C4-2B, PC3, DU145 with an IC_{50} value of $0.2333 \pm 0.0696 \mu M$, $2.4352 \pm 0.3118 \mu M$, $0.4802 \pm 0.1621 \mu M$, $0.7917 \pm 0.1434 \mu M$, $1.1496 \pm 0.1385 \mu M$ and $0.5615 \pm 0.0759 \mu M$, respectively, than the normal prostate epithelial RWPE-1 cell line with the

estimated IC₅₀ value > 20 μM (Figure 2A). This outcome suggests that AR and its variants (e.g. AR-V7) could be the potential therapeutic targets of Nitidine, as 22Rv1 was most influenced by the cytotoxicity of Nitidine than all of the other PCa cell lines. Besides, even though C4-2B MDVR has high expression of AR and its variant (AR-V7), it was surprisingly more resistant to Nitidine among those cell lines above, suggesting that C4-2B MDVR growth and progression could be through different mechanisms, for example, the neuroendocrine-like pathway as suggested in Pham et al., 2020. Altogether, Nitidine may potentially be a novel structure for developing new therapeutic drugs with low side effects against CRPCs, as its cytotoxicity was relatively low against the normal prostate epithelial cell and high against CRPCs.

Thereafter, we examined whether the cytotoxicity of Nitidine was potentially induced through the apoptosis of PCa cell lines such as 22Rv1 and C4-2B MDVR. The cleavages of Caspase 3 (Casp3) and PARP are the important markers indicating the apoptosis. Through Western Blotting analysis, both 22Rv1 and C42B-MDVR achieved the increase in cleaved-PARP and cleaved-Casp3 levels and the decrease in full-length PARP and full-length Casp3 levels, as the concentration of Ni was enhanced (Figure 2B). For more detailed verification, flow cytometry (FACS) was applied to investigate the potential apoptosis in 22Rv1 cells by staining the apoptotic markers using Propidium iodide and Annexin V-FITC. Damaged plasma membranes of apoptotic cells allow Propidium iodide to easily pass through, intercalate into the nucleic acids, and exhibit red fluorescence [23-25]. Annexin V-FITC is the protein that binds to phosphatidylserine, an apoptotic marker which has been translocated to the outer leaflet of the plasma membrane, in a calcium-dependent manner to produce green fluorescence. As a result, an increasing level of apoptotic cells was shown after 4-hour treatment with increasing concentration of Ni (Figure 2C). These results suggested that apoptosis can be triggered in the presence of Ni, which potentially could be a structural model to induce cytotoxicity and apoptosis in CRPC cells.

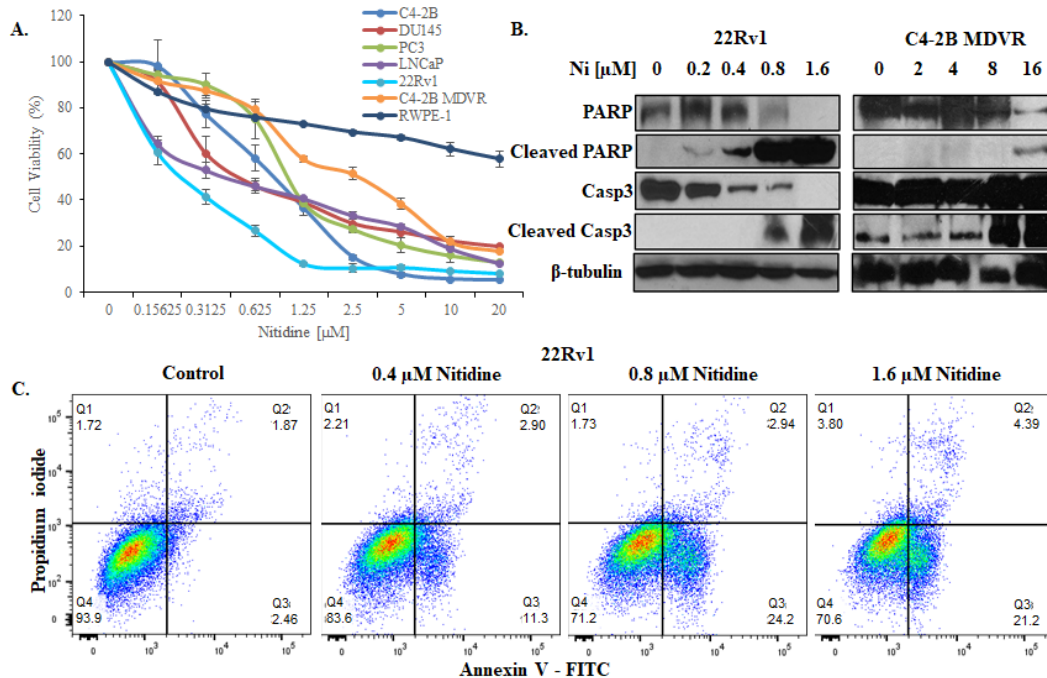


Figure 2. Nitidine induces cytotoxicity and apoptosis in CRPC cells. (A) MTT assay was performed to determine the cell viability of the normal prostate epithelial cell and CRPC cells, including C4-2B, DU145, PC3, LNCaP, 22Rv1, C4-2V MDVR, and RWPE-1 under 72-hour treatment of indicated concentration of Ni. (B) 22Rv1 and C42B-MDVR cells were treated with 0.1% DMSO or with indicated concentration of Ni for 24 hours. Apoptotic markers PARP and Casp3 were detected by WB analysis. β-tubulin was used as loading control. (C) 22Rv1 cells were treated with 0.1% DMSO as control or with indicated concentration of Ni for 4 hours. The cells were stained for 30 minutes with propidium iodide and annexin V-FITC, and then detected by flow cytometry (FACS).

Nitidine (Ni) inhibits AR and AR-V7 expressions and activities in CRPC cells

In addition to the cytotoxicity of Nitidine, we next wanted to discover the inhibitory mechanism of Nitidine starting with examination how Nitidine played a role in affecting AR and AR-V7 expression and activities. Through Western Blotting and real-time qPCR, we detected the protein and mRNA levels of AR, AR-V7, and their downstreams in 22Rv1 and C4-2B MDVR under various-dose treatment of Nitidine. As a result, AR, AR-V7, and their downstream (PSA, UBE2C) expressions in both cell lines were significantly suppressed at protein level as Nitidine concentration increased (Figure 3A-B). Furthermore, Nitidine was shown to attenuate the mRNA expression of AR, AR-V7, and their downstream in both cell lines (Figure 3C-D). Overall, Nitidine could potentially downregulate and suppress AR, AR-V7, and their downstream expressions and activities.

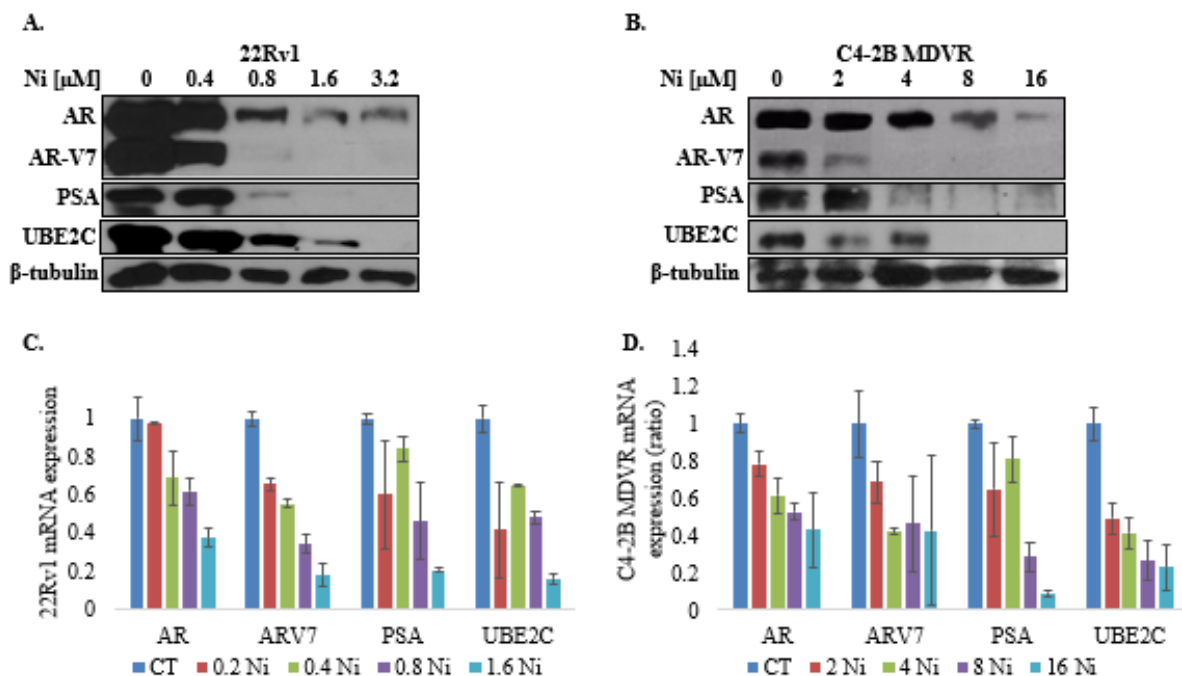


Figure 3. Nitidine inhibits AR and AR-V7 expressions and activities in CRPC cells. Western Blotting analysis was performed on (A) 22Rv1 and (B) C42B-MDVR cell lines, and AR and AR-V7 protein levels were detected after 24-hour treatment with 0.1% DMSO or with indicated concentration of Nitidine. β -tubulin was used as loading control. Real-time qPCR was performed on (C) 22Rv1 and (D) C42B-MDVR to detect AR and AR-V7 mRNA levels under the 24-hour treatment of 0.1% DMSO or indicated concentration of Nitidine. Actin was used as loading control.

Nitidine (Ni) induces AR and AR-V7 degradation through ubiquitin-proteasome pathway

According to Pham et al., 2020, when LSD1 was knocked down in 22Rv1, Sanguinarine was shown to further downregulate AR and AR-V7 at the protein level, whereas the mRNA level of AR and AR-V7 stayed unaffected. This would suggest that along with the LSD1-dependent pathway, Sanguinarine may downregulate AR and AR-V7 at their protein level in a different pathway. Hence, as a structural comparison, we wanted to discover the inhibitory mechanism of both Nitidine and Sanguinarine towards AR and AR-V7 proteins. To investigate whether both molecules could induce AR and AR-V7 protein degradation, we pretreated 22Rv1 with 10 μ g/mL cycloheximide (a protein-synthesis inhibitor) for 4 hours, followed by 2 μ M of Nitidine or 2 μ M of Sanguinarine treatment. Through Western Blotting analysis, AR and ARV7 proteins were further downregulated under the treatment of Nitidine and Sanguinarine than the correspondingly untreated groups, (Figure 4A and Supplementary Figure 1A, respectively), suggesting that these compounds may induce AR and AR-V7 protein degradation. Several studies revealed through specific molecules, the ubiquitin-proteasome system could significantly induce AR protein degradation as the more highly potential alternative therapeutic approach for CRPC [A-G]. Hence, we further investigated whether Nitidine and Sanguinarine could induce AR and AR-V7 protein

degradation through the ubiquitin-proteasome pathway. Firstly, we pretreated 22Rv1 with a proteasome inhibitor MG132 followed by Nitidine treatment. As a result, AR and AR-V7 expressions were unaffected in the presence of MG132, whereas their expressions were downregulated in the absence of MG132 (Figure 4B). Next, since Sanguinarine was shown to influence mRNA level of AR and AR-V7 through LSD1-dependent pathway (Pham et al., 2020), we pretreated normal 22Rv1 with 10 µg/mL cycloheximide (CHX) to see the potential direct effect of Sanguinarine at protein level, followed by the treatment of proteasome inhibitors and lastly Sanguinarine. As a result, the inhibitors (MG132 and Bortezomib) alleviated the AR and AR-V7 degradation induced by Sanguinarine (Supplementary Figure 1B). These results demonstrated that Nitidine and Sanguinarine could induce AR and AR-V7 proteasomal degradation. To determine whether AR and AR-V7 proteasomal degradation was mediated by ubiquitination, immunoprecipitation (IP) was performed and analyzed by Western Blotting. We pulled down AR/AR-V7 and stained for ubiquitin (Ub) and vice versa. The results showed an increasing level of ubiquitin binding to AR/AR-V7 under the treatment of Nitidine (Figure 4C-D) or Sanguinarine (Supplementary Figure 1C), suggesting that Nitidine and Sanguinarine could induce AR and AR-V7 degradation through the ubiquitin-proteasome pathway.

Ubiquitin-proteasome pathway (UPP) is a sequence of enzymatic actions that couple Ub chains onto the protein designated for proteasomal degradation. Three enzymes are involved in the pathway. E1 enzyme activates ubiquitin molecules through ATP-requiring reaction, then passes them to E2 enzyme which later complexes with E3 enzyme. The E3 enzyme is the key enzyme in the process, which binds to and transfers ubiquitin chain from E2 enzyme to the target protein [H-J]. MDM2, FBXW2 and STUB1 are reported to be typical E3 enzymes interacting with AR, according to several studies [K-O]. In addition, some UPP-implicated factors would also be taken into consideration. For example, CDH1 is a co-activator protein that regulates the activities of APC/c - an ubiquitin E3 ligase which induces proteasomal degradation of the targets in a cell cycle regulated manner [O-Q]. CDT1, a licensing factor which regulates and restricts DNA from replicating more than one time per cell cycle, is reported to interact with Skp2 - an E3 ubiquitin ligase [R-T]. Since both Sanguinarine and Nitidine were shown to induce AR and AR-V7 degradation through the UPP, we next screened those E3 enzymes and cell cycle regulation factors under the various-dosed treatment of both compounds to determine the potential machinery for the ubiquitination. We observed that FBXW2 and STUB1 were the only proteins that increased under the treatment of Nitidine (Figure 4E-F). Sanguinarine showed STUB1 to remain the same (Supplementary Figure 1D). These results suggested that STUB1 may potentially be the crucial E3 enzyme that regulates AR degradation by the induction of Nitidine and Sanguinarine.

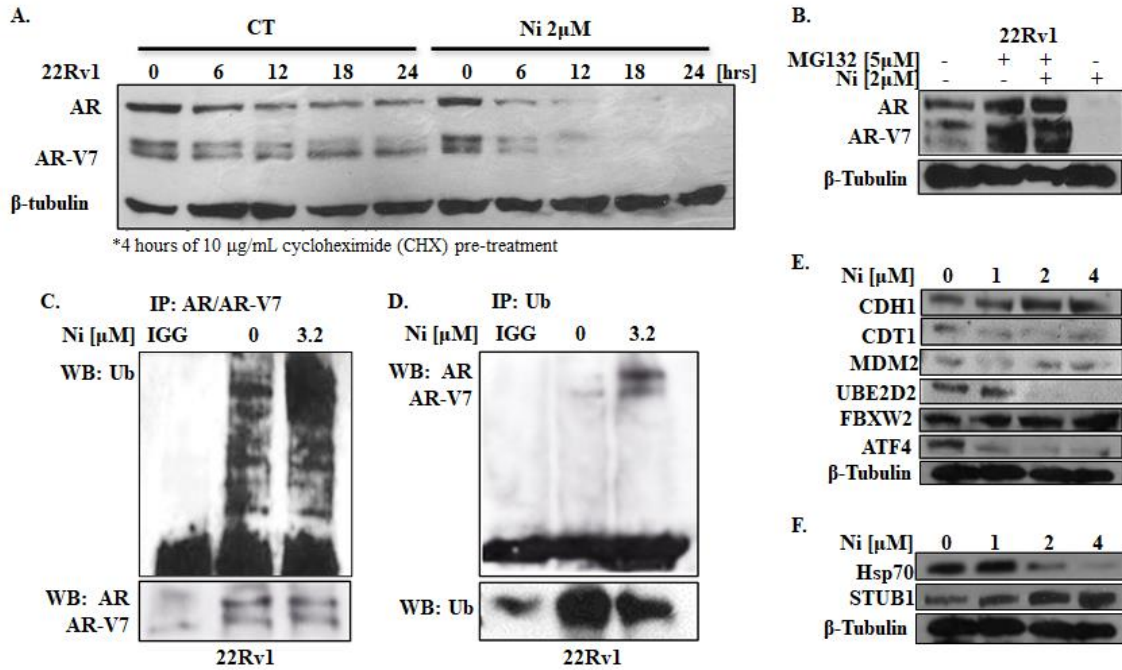
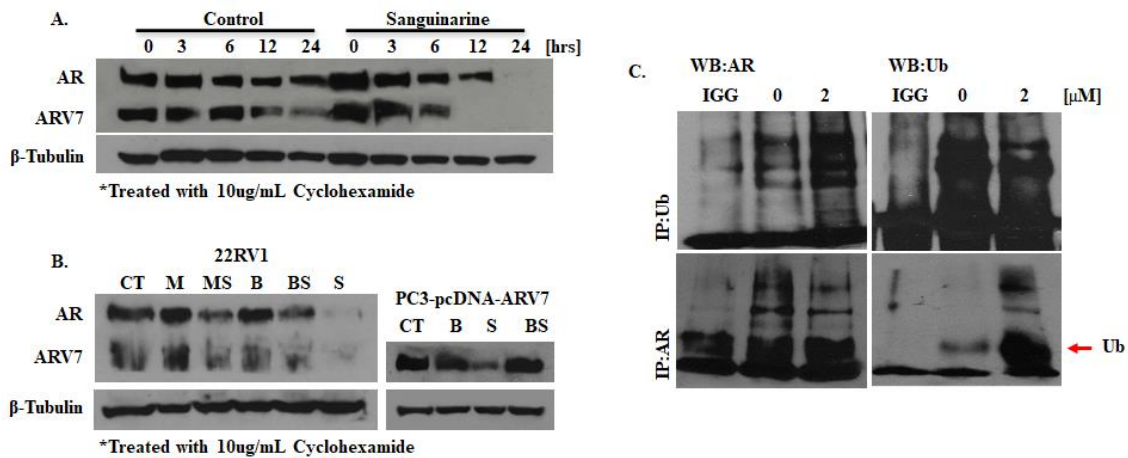


Figure 4. Nitidine induces AR and AR-V7 degradation in UPP manner. Immunoprecipitation (IP) was performed and followed by Western Blotting analysis to detect (C) the presence of Ub upon AR and AR-V7 and (D) vice versa. IGG was used as loading control. (E-F) Expressions of indicated factors and E3 enzymes under various-dosed Nitidine treatment were detected by Western Blotting. β -tubulin was used as loading control.



Supplementary Figure 1. Sanguinarine induces AR and AR-V7 degradation in UPP manner. (C) Immunoprecipitation (IP) was performed and followed by Western Blotting analysis to detect the presence of Ub upon AR and AR-V7 and vice versa. IGG was used as loading control.

Nitidine (Ni) induces AR degradation through a potential binding to AR and Hsp70

Heat-shock protein 70 (Hsp70) has been known as one of the key components that stabilize the inactive conformation of steroid hormone receptors including AR [a-c]. Hsp70 was shown to bind to and interact with AR protein, thus, it could play a significant role in AR expression and activities [9]. So, we then investigated whether Nitidine may influence the Hsp70 binding ability on AR. Based on the molecular

docking prediction, we observed that Nitidine binds to AR with an IC_{50} of 553.02 nM (Figure 5A) and to Hsp70 with an IC_{50} of 6.55 μ M (Figure 5B), which suggested that Nitidine may potentially bind to AR and Hsp70. For further investigations, we performed Cellular Thermal Shift Assay (CETSA) which was then analyzed by Western Blotting. Under the treatment of Nitidine, AR, AR-V7, and Hsp70 expressions were stabilized as the temperature rose compared to non-treatment groups (Figure 5C and 5E). In addition, we performed isothermal dose response CESTA (ITDR_{CESTA}) at 61°C which was the optimal temperature determined from the previous CETSA results were presented the noticeable difference in AR/AR-V7/Hsp70 expressions between non-treatment and treatment conditions. At the same temperature, AR and AR-V7 expressions were strengthened as the concentration of Nitidine was building up (Figure 5D and 5F). These outturns pointed out that AR, AR-V7, and Hsp70 were thermally stabilized under high temperature with different drug concentrations due to potential binding to Nitidine. Overall, these assays supported our hypothesis that Nitidine may potentially bind to AR and Hsp70 to induce AR degradation through the ubiquitin-proteasome pathway.

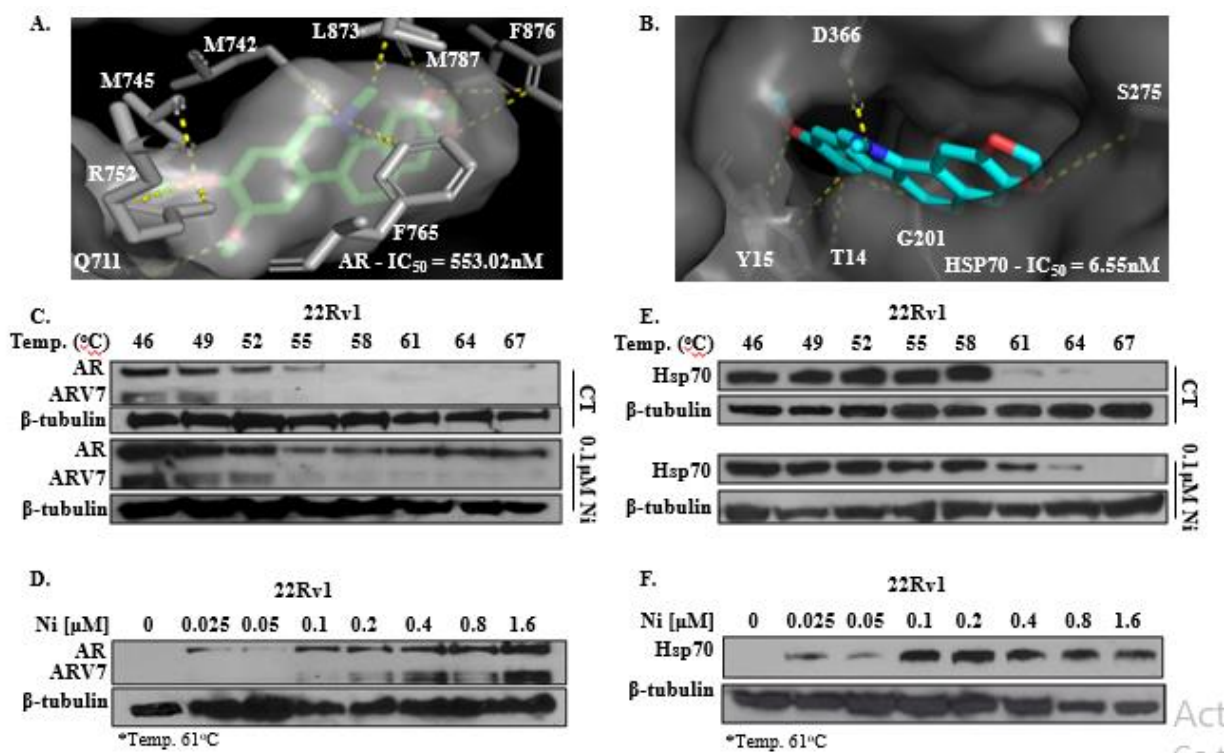


Figure 5. Nitidine induces AR degradation through the potential binding to AR and Hsp70. Nitidine binding to AR and Hsp70 were predicted and illustrated by Molecular Docking (A-B). CETSA and (ITDR_{CESTA}) of Nitidine on AR and Hsp70 were performed and detected by Western Blotting (C-F). β -tubulin was used as loading control.

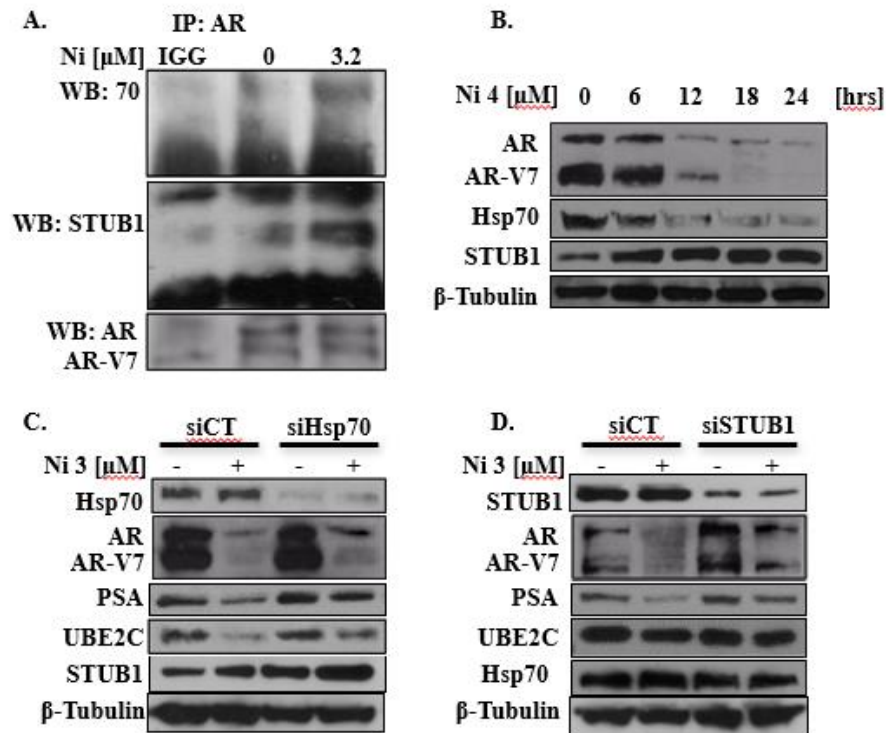


Figure 6 Nitidine induces STUB1-HSP70 interaction

Nitidine (Ni) degrades AR and AR-V7 through Hsp70/STUB1 mediations.

STUB1, an E3 ubiquitin ligase, has been known for being capable of integrating Hsp70's protein-binding function to the ubiquitin-proteasome system. The interaction between STUB1 and Hsp70 would enable the ubiquitination of Hsp70-attached substrate [d-f].

Next, we inspected whether Ni induced AR degradation through the Hsp70/STUB1-mediated pathway. HSP70 was shown to modulate AR function by binding to the AR [9]. Based on these studies, we performed IP and WB to pull down AR and stained for STUB1 and HSP70. As a result, both STUB1 and HSP70 had increased binding to AR after an induction of Ni treatment (Figure 6A), suggesting that Ni may directly mediate AR expression through the STUB1/HSP70 pathway. Because STUB1 was shown to increase and HSP70 was shown to decrease as the concentration of Ni increases, we wanted to determine whether there were consistent results under a timepoint experiment. Thus, we did a 6-hour interval time point Ni-treatment to 22Rv1 cells up to 24 hours. We observed that AR degradation occurred approximately the same time as HSP70 expression decreases and STUB1 expression increases (Figure 6B). The fact that HSP70 is bound to AR, there may be a relation between AR degradation and HSP70 expression. To determine whether HSP70 or STUB1 play a role in AR protein expression and

whether Ni is dependent on HSP70 or STUB1 to induce AR degradation, we knock-down HSP70 or STUB1 protein expression via siRNA 48-hour prior to Ni treatment. As a result, knockdown of HSP70 and STUB1 attenuated the degradation effect of Ni on AR and ARV7 protein level, suggesting that Ni may partly degrade AR and ARV7 in a STUB1/HSP70-dependent pathway (Figure 6C-D).

DISCUSSION

These observations suggest that Ni may downregulate and degrade AR and ARV7 through the induction of STUB1/HSP70. It is possible that Ni induced HSP70 to strongly bind to AR and ARV7, preventing the dissociation and nucleolization of AR and ARV7 from entering the nucleus for their transcriptional activity. At the same, the binding of HSP70 to AR may activate STUB1 activity leading to AR and ARV7 ubiquitination for degradation.

CRPC has still been immensely lethal up to the present despite many newly developed therapies such as chemotherapy, hormone therapy, and immunotherapy [10-17]. The underlying mechanism of many CRPCs is still through AR signaling. Studies have shown many epigenetic mechanisms, including the overexpression of LSD1 are involved in the progression of CRPC progression. In addition, many studies showed that AR-V7 is the key factor that creates the resistance to enzalutamide due to its lacking ligand-binding domain (LBD) which is the main target of this second-generation drug [18-21]. Therefore, targeting AR and its abnormal forms such as AR-V7 is a new approach to novel therapies for CRPC. As shown from our previous studies, inhibiting LSD1 with Sanguinarine subsequently led to the downregulation of AR and ARV7, but partly. The other mechanism that further downregulated the remainder of AR and ARV7 remains unknown. Thus, we wanted to study other similar structured compounds that only affected AR and not LSD1.

After screening various related compounds, we determined Ni is our candidate molecule, and so we did an in-depth investigation to determine its activities against AR protein expression level. Through the AR-luciferase assay, WB analysis, and qPCR, Ni was shown to repress the protein expression of and the activities of AR and AR-V7. Thus, the downregulation of AR and AR-V7 by Ni might be partly involved in prostate cancer cell deaths. As we observed through the MTT assay, 22Rv1 was most sensitive to Ni induction. These 22Rv1 cells are AR-independent cell lines that contain ARV7, which may lead to their progression. Interestingly, C42B-MDVR cells, which also contain ARV7, were least sensitive to Ni. As suggested from several papers, C42B-MDVR are neuroendocrine like CRPC, which may progress through a different mechanism, such as LSD1-dependent mechanism. Even with these outcomes, our focus was not to determine Ni's cytotoxicity against CRPC, but to uncover the protein downregulation activities of AR and AR-V7.

In our investigation through WB analysis, IP, and several knockdown experiments, we identified that the principal mechanism of AR and ARV7 downregulation induced by Nitidine was through the STUB1/HSP70 ubiquitin-proteasome pathway. It is possible that Ni binds directly to AR/AR-V7 as well as to HSP70 to create a stronger Hsp70 to AR/AR-V7 binding. This complex can signal STUB1 to accumulate, hence, increased protein level of STUB1; and thus, leading to the ubiquitination and downregulation of AR and AR-V7. Subsequently, the degradation of AR and ARV7 will also lead to the downregulation of HSP70 as reflected from our WB analysis. We also suggest that CRPC with active STUB1/HSP70 could be more cytotoxic sensitive to Ni.

The mechanism of Ni against AR and AR-V7 is significant for its clinical relevance for treatment of CRPC and important for creating scaffolds for future anti-resistance therapies. Going back to our previous study, we can suggest that sanguinarine may also induce AR and ARV7 degradation through the STUB1/HSP70 pathway. In addition, Ni was shown to have relatively low cytotoxicity against normal epithelial prostate cells, which is structurally relationship for development of novel therapeutic drugs against CRPC with low adverse effects. Clinical relevance of Ni for the treatments of CRPC will also depend on its pharmacokinetics and pharmacodynamics properties, as well as its abilities to prevent CRPC progression. Overall, the significance of this study demonstrated that Ni was a novel structure that could hinder CRPC progression through degrading AR and AR-V7 protein expression and activities.

REFERENCES

1. Chandrasekar T, Yang JC, Gao AC, Evans CP. Mechanisms of resistance in castration-resistant prostate cancer (CRPC). *Transl Androl Urol.* (2015) 4:365–80. 10.3978/j.issn.2223-4683.2015.05.02
2. Proteostasis by STUB1/HSP70 complex controls sensitivity to androgen receptor targeted therapy in advanced prostate cancer.
3. Alimirah F, Chen J, Basrawala Z, Xin H, Choubey D. DU-145 and PC-3 human prostate cancer cell lines express androgen receptor: implications for the androgen receptor functions and regulation. *FEBS Lett.* 2006;580:2294–2300. doi: 10.1016/j.febslet.2006.03.041.
4. Z. Culig, H. Klocker, J. Eberle, F. Kaspar, A. Hobisch, M.V. Cronauer, G. Bartsch, DNA sequence of the androgen receptor in prostatic tumor cell lines and tissue specimens assessed by means of the polymerase chain reaction. *Prostate*, 22, (1993), 11– 22.
5. R.A. Edelstein, M.C. Carr, R. Caesar, M. Young, A. Atala, M.R. Freeman, Detection of human androgen receptor mRNA expression abnormalities by competitive PCR. *DNA Cell Biol.*, 13, (1994), 265– 273.
6. W.D. Tilley, J.M. Bentel, J.O. Aspinall, R.E. Hall, D.J. Horsfall, Evidence for a novel mechanism of androgen resistance in the human prostate cancer cell line, PC-3. *Steroids*, 60, (1995), 180– 186.
7. G. Buchanan, P.S. Craft, M. Yang, A. Cheong, J. Prescott, L. Jia, G.A. Coetzee, W.D. Tilley, PC-3 cells with enhanced androgen receptor signaling: a model for clonal selection in prostate cancer. *Prostate*, 60, (2004), 352– 366.
8. Saraon P, Musrap N, Cretu D, Karagiannis GS, Batruch I, Smith C, Drabovich AP, Trudel D, van der Kwast T, Morrissey C, Jarvi KA, Diamandis EP. Proteomic profiling of androgen-independent prostate cancer cell lines reveals a role for protein S during the development of high grade and castration-resistant prostate cancer. *J Biol Chem.* 2012; 287:34019–31. 10.1074/jbc.M112.384438
9. Dong J, et al. Hsp70 binds to the androgen receptor N-terminal domain and modulates the receptor function in prostate cancer cells. *Mol. Cancer Ther.* 2019;18:39–50. Doi: 10.1158/1535-7163.MCT-18-
10. Beer TM, Armstrong AJ, Rathkopf DE, Loriot Y, Sternberg CN, Higano CS, Iversen P, Bhattacharya S, Carles J, Chowdhury S, et al. Enzalutamide in metastatic prostate cancer before chemotherapy. *N Engl J Med.* 2014;371(5):424–33.
11. de Bono JS, Logothetis CJ, Molina A, Fizazi K, North S, Chu L, Chi KN, Jones RJ, Goodman OB Jr, Saad F, et al. Abiraterone and increased survival in metastatic prostate cancer. *N Engl J Med.* 2011;364(21):1995–2005.
12. Ryan CJ, Smith MR, de Bono JS, Molina A, Logothetis CJ, de Souza P, Fizazi K, Mainwaring P, Piulats JM, Ng S, et al. Abiraterone in meta-static prostate cancer without previous chemotherapy. *N Engl J Med.* 2013;368(2):138–48.
13. Scher HI, Fizazi K, Saad F, Taplin ME, Sternberg CN, Miller K, de Wit R, Mulders P, Chi KN, Shore ND, et al. Increased survival with enzalutamide in prostate cancer after chemotherapy. *N Engl J Med.* 2012;367(13):1187–97.
14. Smith MR, Saad F, Chowdhury S, Oudard S, Hadaschik BA, Graff JN, Olmos D, Mainwaring PN, Lee JY, Uemura H, et al. Apalutamide Treatment and Metastasis-free Survival in Prostate Cancer. *N Engl J Med.* 2018;378:1408–18.
15. de Bono JS, Oudard S, Ozguroglu M, Hansen S, Machiels JP, Kocak I, Gravis G, Bodrogi I, Mackenzie MJ, Shen L, et al. Prednisone plus cabazitaxel or mitoxantrone for metastatic castration-resistant prostate cancer progressing after docetaxel treatment: a randomised open-label trial. *Lancet.* 2010;376(9747):1147–54.
16. Kantoff PW, Higano CS, Shore ND, Berger ER, Small EJ, Penson DF, Redfern CH, Ferrari AC, Dreicer R, Sims RB, et al. Sipuleucel-T immunotherapy for castration-resistant prostate cancer. *N Engl J Med.* 2010;363(5):411–22.
17. Parker C, Nilsson S, Heinrich D, Helle SI, O’Sullivan JM, Fossa SD, Chodacki A, Wiechno P, Logue J, Seke M, et al. Alpha emitter radium-223 and survival in metastatic prostate cancer. *N Engl J Med.* 2013;369(3):213–23.
18. Longo DL. New therapies for castration-resistant prostate cancer. *N Engl J Med.* 2010;363:479–81.
19. Ryan CJ, Tindall DJ. Androgen receptor rediscovered: the new biology and targeting the androgen receptor therapeutically. *J Clin Oncol.* 2011;29:3651–8.
20. Tran C, Ouk S, Clegg NJ, et al. Development of a second-generation antiandrogen for treatment of advanced prostate cancer. *Science.* 2009;324:787–90
21. Scher HI, Beer TM, Higano CS, et al. Antitumour activity of MDV3100 in castration-resistant prostate cancer: a phase 1-2 study. *Lancet.* 2010;375:1437–46.

CHAPTER 6

Sanguinarine hinders Dovitinib-induced Neuronal-like differentiation through an LSD1-dependent mechanism

Victor Pham, Erik Dan Tran, Vinh X. Le, Merci Mino, Thanh Le, and Xiaolin Zi

ANSTRACT

Neuroendocrine prostate cancer (NEPC) is regarded as the most aggressive form of the disease and appears to develop as a means of resistance to Androgen Deprivation Therapy (ADT). In our study, we used dovitinib (DOV) to induce neuroendocrine differentiation and observed the levels of LSD1 expression to determine a possible mechanism of differentiation. Sanguinarine (SNG), a novel inhibitor of LSD1, was shown to inhibit DOV-induced neuronal-like morphology in vitro as shown from its downregulation of NE markers, such as chromogranin A (CgA), synaptophysin (Syn), and neuron specific enolase (NSE). In mice studies, SNG in combination with DOV was seen to synergistically inhibit tumor growth drastically. DOV was seen to upregulate LSD1, while in groups that were treated in combination of DOV and SNG, LSD1 was downregulated and displayed lower levels of neuroendocrine differentiation as measured by neuroendocrine markers. Our study shows that SNG can reduce neuroendocrine differentiation. Thus, exploring the effectiveness of a combination therapy of both SNG and DOV could be promising treatment against NEPC.

BACKGROUND

Prostate cancer (PCa) accounts for 1 in 5 new diagnoses and is the second leading cause of cancer related deaths in men in the United States.(1,2) In 2020, it has been estimated that there will be 191,930 new cases of PCa and 33,330 PCa-related deaths, and it is only expected to increase in the coming decades. One common therapy involves medical and surgical castration or androgen deprivation therapy (ADT) that involves the suppression of the synthesis of androgens (i.e. abiraterone) or directly inhibiting the androgen receptor (AR) (i.e.enzalutamide) (3). These methods are successful in treating early stages as well as metastatic prostate cancer, but several patients eventually relapse (Reference).

One form of relapse may be the development of neuroendocrine prostate cancer (NEPC), which appears to develop as a means of resistance to ADT and has been regarded as one of the most invasive forms of prostate cancer(Clinical features of neuroendocrine prostate cancer). Neuroendocrine markers such as chromogranin A (CgA), synaptophysin (Syn), and neuron-specific enolase/gamma enolase (NSE) have been used as a method to detect NEPC, and their increasing protein levels in tissue and blood serum

have been associated with a poor prognosis and the progression of the disease. (Neuroendocrine Differentiation in Prostatic Carcinoma, Neuroendocrine cells in tumour growth of the prostate). Given that such a large percentage of patients eventually relapse, understanding the mechanisms of NEPC is a main priority.

Current research has shown that inducing NE differentiation is possible through the addition of a variety of different chemical agents (Reference). In a study conducted by Yadav et al., treatment of prostate cancer cells with dovitinib (DOV) was able to induce NEPC differentiation after 3 weeks of treatment, although the mechanism for their differentiation is unclear (Induction of Neuroendocrine Differentiation in Prostate Cancer Cells by Dovitinib (TKI-258) and its Therapeutic Implications). NEPC contains morphology like neuronal stem cells, and they lack AR expression and exhibit a dense cell body with long branching processes extending out. In a study conducted by Tofollo et al. (2013), Lysine-specific demethylase 1A (LSD1) and its isoform, LSD1-8a, was shown to be central to neuronal differentiation and maturation in the mammalian central nervous system (Phosphorylation of neuronal Lysine-Specific Demethylase 1LSD1/KDM1A impairs transcriptional repression by regulating interaction with CoREST and histone deacetylases HDAC1/2). LSD1 is also involved in neural stem cell development and proliferation as well as a variety of other processes (Histone Demethylase LSD1 Regulates Neural Stem Cell Proliferation). Although NEPC exhibits androgen independence, targeting both AR and LSD1 may be important since prostate tumors are often heterogeneous. A percentage of the tumor may show the neuronal-like phenotype while other areas are not.

Thus, Sanguinarine (SNG) may be an ideal candidate in this scenario through its dual inhibition of both the AR and LSD1 (Pham et al., 2020). Our preliminary studies had shown that DOV-induced PCa cells had increased LSD1 expression, suggesting a possible mechanism between LSD1 and NEPC differentiation. In the present study, we have shown SNG to hinder neuronal-like phenotypes from DOV-induced NEPC differentiation *in vitro* and *in vivo*, suggesting that LSD1 to be an important therapeutic target for future studies. By determining the pathway in which NEPC disease develops, it is possible to reduce the occurrence of NEPC differentiation.

METHODS

Culturing Methods

Human prostate cancer cell lines used for this study include: 22RV1, DU145, and 22RV1 LSD1 knockdown. Cells were cultured in RPMI media supplemented with 10% fetal bovine serum (FBS) and penicillin(10U/mL). Cells were kept in a warm, humidified environment containing CO₂.

Cells were cultured until they reached about 50% confluence at which point treatment began. Cells were treated in media containing either 2 μ M of SNG, 6 μ M of DOV, or a combination of both. Cells were treated with drug media for two days, switched to drug-free media for one to two days, and then switched back to drug media again. At the end of the 21 day study, the cells were lysed and cell lysates were subjected to western blot and qPCR. A subset of cells were also grown in the same way but had cells harvested every three days.

Western Blotting Analysis

Proteins are extracted from cells via RIPA lysis buffer supplemented with protease inhibitors. 100 μ L to 150 μ L are added to each plate after two washes with 1xPBS. Plates were then set to incubate on ice for 15 minutes. Afterwards, lysate is collected and transferred into microcentrifuge tubes and centrifuged for 15 minutes at 13,000 RPM at 4°C. Protein content is then quantified using a lowry assay. Samples of equal protein concentration are then combined with B-mercaptoEthanol and loaded into polyacrylamide gels, ranging from 6% to 12%. Loading buffer is added and gel electrophoresis is run for 80V for approximately 20 minutes and then 100V for 40 minutes. After gel electrophoresis is complete, proteins are then transferred to a PVDF membrane by electrophoresis at 100V for 45 minutes. The PVDF membrane is blocked in 5% nonfat milk diluted in 1xTBST for one hour to prevent antibodies from binding to non-specific antibodies. Membrane is then washed in 1xTBST three times for three minutes each rinse to wash off any excess antibodies. Antibodies are diluted in the blocking buffer and left to probe overnight at 4°C. Afterwards, excess antibodies are washed off using 1xTBST leaving only bound antibodies which are then detected using horseradish peroxidase (HRP) labeled antibodies. Developing film is then used to capture the signal on x-ray film.

RNA Extraction

RNA is extracted by incubating cells in RNA-Bee solution for 5 minutes on ice after washing cells with 1xPBS twice. Lysate is transferred into microcentrifuge tubes and 600 μ L of chloroform is added to the mixture and inverted vigorously 20 times to ensure mixing, then allowed to settle on ice for 5 minutes. Afterwards, tubes are spun down for 20 minutes at 6000RPM at 4°C. There will be two layers,

one nonpolar and one aqueous which contains the nucleotides. The aqueous layer is carefully pipetted into another microcentrifuge tube and 600uL of isopropanol is mixed into it and allowed to incubate overnight at 4°C. The next day the aqueous layer is again transferred to another microcentrifuge tube and spun down at 6000 RPM for 10 minutes at 4°C after an addition of absolute ethanol. Ethanol is removed from the solution via air drying and once completely dry, RNA-free water is added and nanodrop is performed to determine its concentration.

Reverse Transcription Polymerase Chain Reaction

Reverse transcription polymerase chain reaction (RT-PCR) is performed after RNA extraction and nanodrop analysis. This technique converts RNA into cDNA and amplifies specific cDNA sequences. 2 ug of extracted RNA were combined with 500ng/ug Oligo DT primers and random primers and then filled with nuclease free water until the total volume of the mixture is 10uL. In order to allow annealing of the primers, mixtures are heated to 70°C for 5 minutes then cooled at 4°C for at least 10 minutes. While waiting, a mastermix of MgCl₂, dNTP mix, 1X reaction buffer, reverse transcriptase, and RNasin inhibitor was prepared. Once cooling is complete, the mastermix is added into the RNA mixture and RT-PCR can now be run. The new mixture is heated to 40°C for one hour, then 70°C for 15 minutes, and then cooled at 4°C. The newly synthesized cDNA can then be stored or used in future experiments.

Quantitative Polymerase Chain Reaction

Quantitative polymerase chain reaction (qPCR) is a method of characterizing and quantifying gene sequences. cDNA samples obtained from RT-PCR are now diluted in nuclease free water and combined with SYBR green and 50uM of forward and reverse primers. The mixture is then run using a qPCR machine with preset settings of: 95°C for 10 seconds, 55°C for 30 seconds, 72°C for 30 seconds, and then read. After the initial run, this process is repeated 39 more times until the melting curve of the sample is able to be quantified via a gradual increase in temperature of 0.5°C increments every 5 seconds beginning at 55°C and ending at 95°C.

Cellular MTT Viability Assay

MTT assay is a colorimetric assay that portrays the level of cellular metabolism. For our study, we cultured cells until they reached 30-40% confluence before incubating them with a drug at specific concentrations for 72 hours. Just before incubation is completed, the MTT reagent solution is made by dissolving MTT powder in 1x PBS at a concentration of 3mg/mL. Once the 72-hour incubation is complete, the MTT solution is added directly onto cells so that the final concentration will be 0.5mg/mL. This mixture can incubate at 37°C for 50 minutes at which point cells that are healthy will appear purple

due to the reduction of MTT to formazan. After the cells have been stained, they can then be washed and have their media removed. They then have isopropanol that contains 4% 1N HCl added into the cells to dissolve the formazan that has stained the cells. The formazan that is now dissociated into the solution can be used for analysis using a spectrophotometer using the absorbance level of 570nm.

Transfection

C42B cells could grow in 24 well plates until they reached approximately 50% confluence. Cells were cultured in complete RPMI medium at 37°C with 5% CO₂. Lipofectamine LTX (Thermo Fisher Scientific) is then added into centrifuge tubes that contain 50uL of Opti-MEM medium. In a separate centrifuge tube, which contains 50 uL of Opti-MEM medium, 2 ug of plasmid DNA and 2 uL of Plus reagent are added. The two tubes are then combined and allowed to incubate for 5 minutes at room temperature. The mixture is then added to the cells in the 24 well plates and allowed to incubate for at least 48 hours. After treatment, cells are treated with 2 ug/mL of G418 antibiotics.

Mice Xenograft Study

All mice experiments in this study were completed in line with IACUC protocol. Five million 22RV1 cells, mixed in Matrigel, were injected subcutaneously into one flank of a six-week-old BALB/c nod skid mouse. Mice are “naired” around the site of tumor injection and tumor volume was measured every two days until volume reached 200mm³. Tumor measurements were completed by measuring length(L) and width(W) of the tumor and height(H) was taken as the average of length and width. Tumor volume was calculated using the formula: LxWxHx0.52. At this point, mice were either treated with saline, DOV (30 mg/kg), SNG (8 mg/kg), or a combination of the two every day by oral gavage. Once the study had run for seven weeks, mice were sacrificed, and tumors and organs were collected. Tumors were stored at -80 °C and organs were placed into formalin for preservation.

Immunofluorescence Staining

To observe the inhibitory effect of SNG on NE differentiation, immunofluorescence (IF) staining was utilized on tumors extracted from the mice study and included the LSD1, NE markers, and various other proteins. First, tumor samples were cut, and slides were prepared by the pathology department. Since our target proteins were intracellular, we began by permeabilizing the cell membrane. Tumor samples were incubated for 10 minutes in PBS that contained 0.1-0.25% Triton x-100 and subsequently washed 3 times with PBS for 5 minutes each after incubation. To block non-specific antibodies, samples were incubated with 1% BSA, 22.52 mg/mL glycine in PBST (PBS+0.1% Tween 20) for 30 minutes. Afterwards, samples were incubated with diluted antibody in 1% BSA in PBST overnight at 4°C. The

next day, decant the solution and wash the sample three times in PBS for 5 minutes each wash then incubate the sample with the secondary antibody in 1% BSA at room temperature for 1 hour in the dark. Afterwards, decant the solution and wash the sample 3 times in PBS, 5 minutes each wash and in the dark. Next, samples are incubated on 0.1-1 $\mu\text{g}/\text{mL}$ Hoechst or DAPI (DNA stain) for 1 min and then washed with PBS. To mount the coverslip, use a drop of mounting medium and then seal the coverslip with nail polish to prevent drying and movement and store in the dark at -20°C or at $+4^{\circ}\text{C}$.

RESULTS

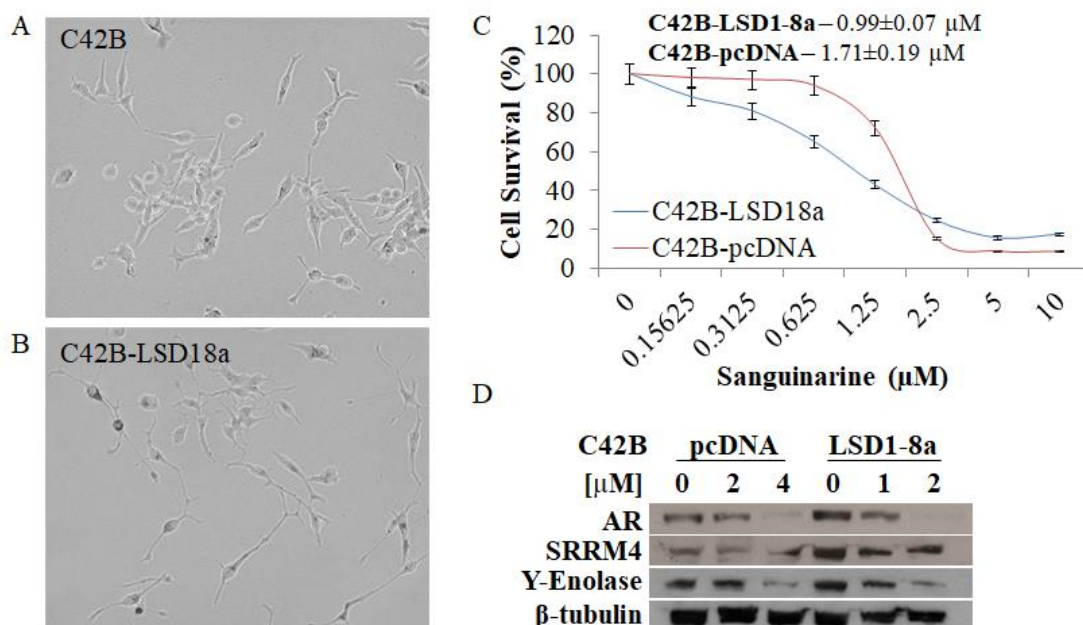


Figure 1. Transfection with LSD1-8a results in sensitization of prostate cancer cells to SNG. Light microscope images of (A) C42B cells and (B) C42B cells that have been transfected with LSD1-8a at 20X magnification. (C) MTT assay was performed on C42B-LSD1-8a and C42B-pcDNA at varying concentrations of SNG. (D) After treatment with SNG at varying concentrations, C42B-LSD1-8a and pcDNA cells were lysed and subjected to western blot analysis in order to detect expression levels of AR, SRRM4, and γ -enolase. β -tubulin was used as loading control.

Transfection of LSD1-8a into prostate cancer cells results in NE differentiation and sensitivity to SNG

A study conducted by Toffollo et al. (2013) found that LSD1-8a is upregulated in neuronal stem cells. They also stated that LSD1-8a in combination with LSD1 is able to enhance neurite growth as well and morphogenesis in mammalian central nervous systems (Phosphorylation of neuronal Lysine-Specific Demethylase 1LSD1/KDM1A impairs transcriptional repression by regulating interaction with CoREST and histone deacetylases HDAC1/2). In addition, upregulation of LSD1 has also been implicated in the progression of CRPC, particularly neuroendocrine prostate cancer (LSD1: A single target to combat lineage plasticity in lethal prostate cancer). To confirm whether LSD1-8a and LSD1 is important towards neuroendocrine differentiation in PCa, we transfected it into C42B cells with LSD1-8a pcDNA plasmids.

Intriguingly, unlike the C42B vector control (Figure 1A), C42B cells transfected with LSD1-8a showed neuronal-like phenotypes, which includes long extending arms (Figure 1B). In addition, because our candidate drug, SNG, is an LSD1 inhibitor, we wanted to determine whether PCa cells that overexpress LSD1-8a would be more sensitive to SNG treatment through MTT assay. As a result, C42B cells transfected with LSD1-8a were shown to be more sensitive to SNG compared to C42B vector control cells (Figure 1C). To verify whether LSD1-8a affected the expression of neuronal phenotypes, Western blot (WB) analysis was performed, and as a result, C42B-LSD18a cells revealed an upregulation of neuronal markers γ -enolase and neural alternative splicing factor SRRM4 when compared to C42B-vector control cells (Figure 1D). Sanguinarine was previously shown to target LSD1, but is still effective against cells that upregulate LSD1-8a, suggesting its potential to inhibit neuroendocrine differentiation in PCa. Interestingly, AR was shown to be upregulated in LSD1-8a overexpressing C42B, which AR is not normally expressed in neuroendocrine cells. Since SNG was previously studied to inhibit LSD1, which exhibits similar function to its variant LSD1-8a, we suggest that SNG may inhibit LSD1-8a through a similar pathway.

SNG reduces DOV-induced neuroendocrine differentiation over time In Vitro

We wanted to determine whether SNG can inhibit neuroendocrine differentiation, and so we investigated a method that can induce CRPC to differentiate into neuroendocrine in a clinical setting that involves chemotherapy. Dovitinib, or DOV, is currently in phase 2 clinical trials for prostate cancer and phase 3 for treatment of renal cancer, and is expected to gain FDA approval as it has been shown to be potent in treatment of numerous cancer types, including renal cell carcinoma (RCC) than the current methods. In a study conducted by Yadav et al. (2017), DOV was shown to have the capability of differentiating PCa to have neuronal-like phenotype, including neuronal-like morphology and upregulated neuronal markers. In our study, we utilized DOV in combination with SNG to elucidate SNG's ability to inhibit NE differentiation. Although the mechanism through which NE differentiation occurs is unclear, our data suggests that it could be through an LSD1 mediated pathway. To compare the neuronal differentiation phenomenon among these two drugs, we treated 22Rv1 cell lines with SNG alone, with dovitinib (DOV) alone, or with both SNG and DOV (Combination) for 21 days with images taken every 3 days. We observed that DOV-treated 22Rv1 cells developed an elongated neuronal-like body with long extending arms over the period of treatment (Figure 2), while SNG-treated and combination-treated 22Rv1 cells showed little to no neuronal-like phenotype. Although the combination treatment group showed some level of neuronal-like phenotype, it seems that SNG was able to prevent the cells from full differentiation, suggesting that neuronal-like differentiation may be due to the blocking of LSD1 by SNG. Thus, to verify this phenomenon, we treated 22Rv1 with down regulated levels of LSD1 through viral

shLSD1 transduction with DOV. As a result, DOV-treated 22Rv1-shLSD1 cells exhibited little to no neuronal-like phenotype, like the combination-treatment group for 22Rv1. These results emphasize the potential relevance of LSD1 overexpression in neuroendocrine differentiation.

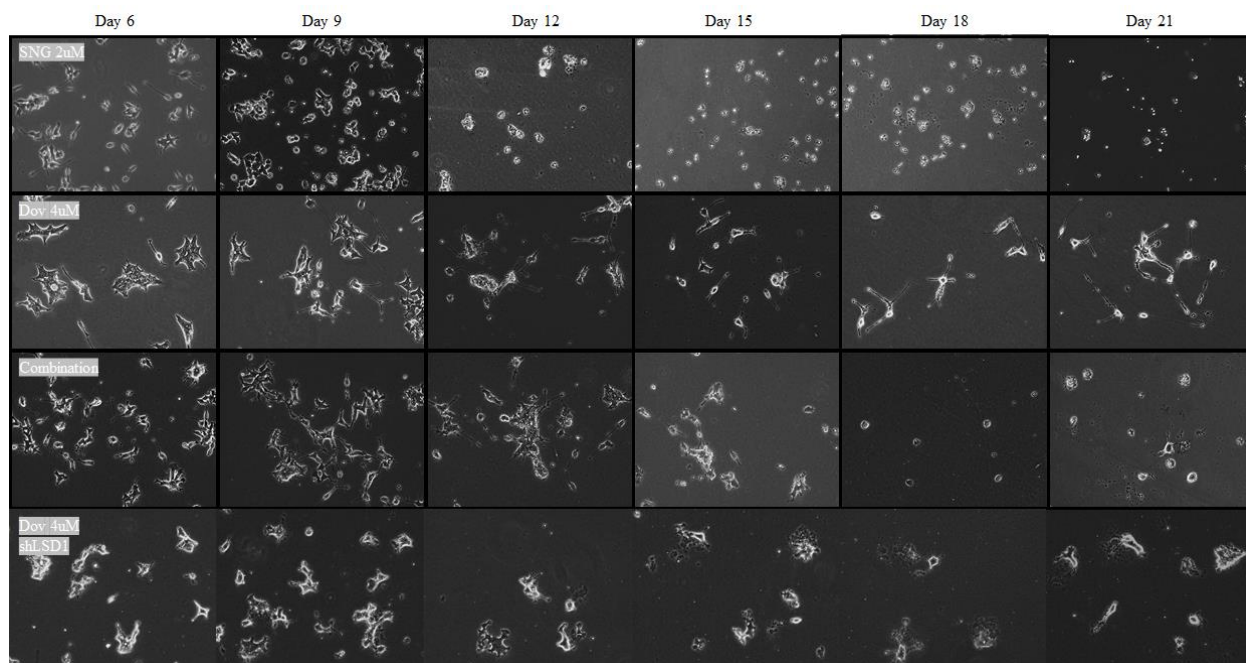


Figure 2. DOV-induced neuroendocrine differentiation is inhibited by SNG. 22Rv1 cells were treated with DOV (4uM), SNG (2uM), or a combination (4uM DOV and 2uM SNG) every three days over 21 days. Every three days images were taken of the cells at 20X magnification. 22Rv1 cells that had knocked down levels of LSD1 expression were also subjected to the same conditions.

SP2509 treatment reduces neuroendocrine differentiation via LSD1 inhibition

To further determine whether DOV-induced neuroendocrine differentiation is mediated through LSD1, 22Rv1 cells were subjected to a combination treatment between DOV and SP2509. SP2509 is another LSD1 inhibitor that blocks LSD1 through an allosteric inhibition (REfERENCE). Cells were treated and imaged every three days for three weeks, and then subjected to WB analysis at the end of the treatment period. From images taken over the three-week study, neuronal-like features were observed in the DOV treatment group, like the previous experiment. SP2509 alone and combination treatment with DOV and SP2509 treated groups appeared to have similar morphology to the untreated group (Figure 4A). Western blot analysis revealed that LSD1 was upregulated in DOV but downregulated in SP2509 and combo treated groups (Figure 4B). Neuroendocrine markers are seen to be upregulated in the DOV treatment group but downregulated in all other conditions. These results and the previous results suggest that LSD1 may in part be the pathway in which DOV induces neuroendocrine differentiation in prostate cancer cells.

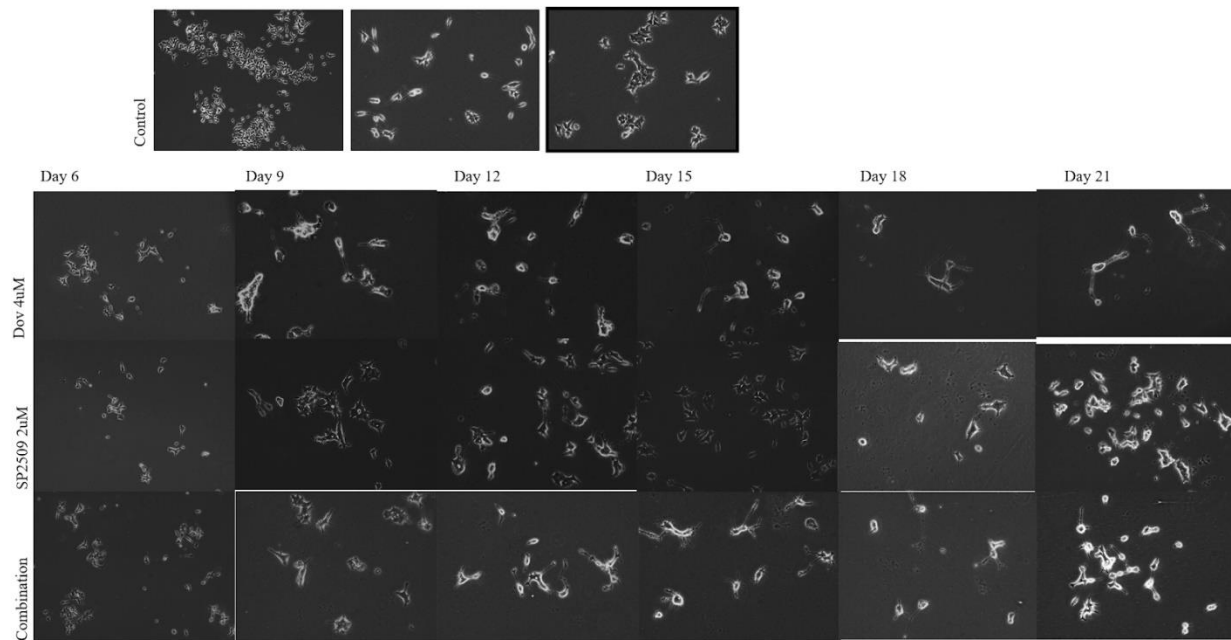


Figure 3. DOV-induced NE differentiation reduced by LSD1 inhibitor, sp2509. 22Rv1 cells were treated with DOV (4uM), sp2509 (1uM), or a combination (4uM DOV and 1uM sp2509) of the two every three days for 21 days.

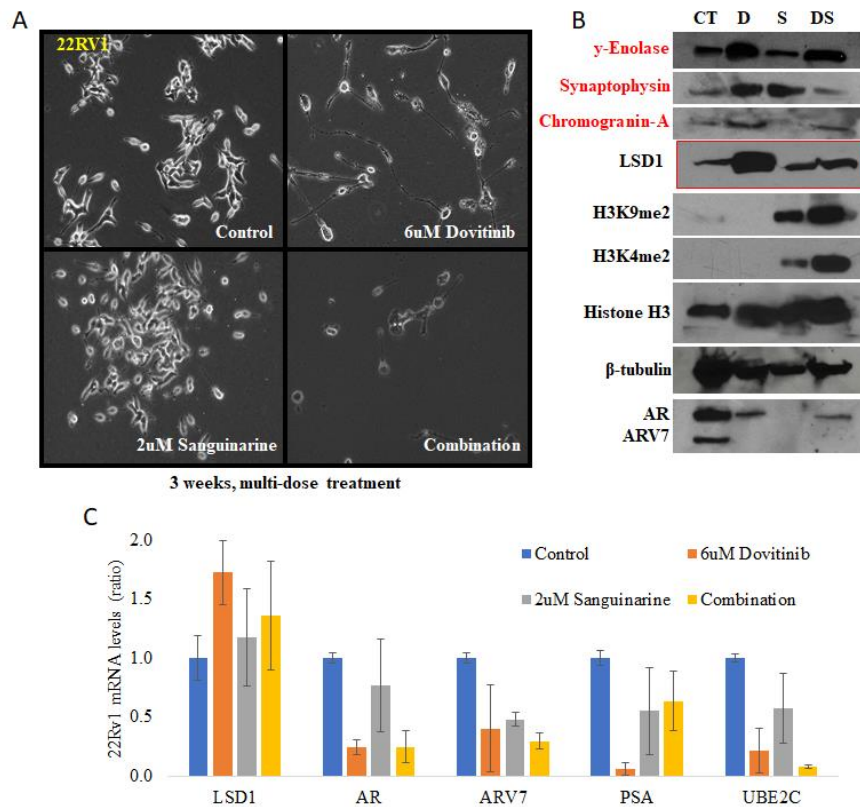


Figure 4. End result of the three-week study and western blot and qPCR results. At the end of the three-week study DOV, SNG, or combination treatment, (A) representative images were taken using a light microscope at 20X, cells were lysed, and protein and RNA were extracted from each condition. (B) Extracted protein from each condition were subjected to western blot analysis and γ -enolase, synaptophysin, chromogranin A, LSD1, H3K9me2, H3K4me2, Histone H3, AR, and ARV7 were observed. β -tubulin was used as loading control. (C) Extracted RNA from each condition were subjected to qPCR analysis and expression levels of LSD1, AR, ARV7, PSA, and UBE2C were observed.

At the end of the 21-days of treatment, there was a noticeable morphological distinction between the different treatment groups under 0.1% DMSO, SNG alone, DOV alone, or Combination (Figure 4A). To reveal whether these treatment groups affected neuronal phenotypes, these 22Rv1 cells were lysed and subjected to WB analysis and Real-time qPCR. Neuroendocrine differentiation may be shown by observing a decreased expression of AR and an increased expression of neuronal markers, which include γ -enolase, synaptophysin, and chromogranin A. WB analysis showed 21-days of DOV treatment induced the overexpression of the three neuronal markers in 22Rv1 cells, whereas the 0.1% DMSO, SNG treatment, and Combination treatment did not show noticeable increase (Figure 4B). Although γ -enolase showed an increase in the combination treated group and synaptophysin increased in the SNG treated group, it is more relevant if all three neuronal markers increase to indicate actual neuronal-like differentiation. Prognostic tools are subject to error and capturing only one neuronal marker, including only Chromogranin A, γ -enolase, or Synaptophysin may have their drawbacks and may be susceptible to false positives. Thus, an assay including all three neuronal markers for detection is more likely to have significant results. In addition to our results, LSD1 protein expression and activity (i.e. H3K9 and H3K4 methylation) was observed to be upregulated in DOV treated 22Rv1 cells, while SNG and combination treated 22Rv1 cells decreased in LSD1 and its activity, suggesting that LSD1 inhibition may partly play a role to prevent neuronal-like differentiation. Interestingly, under all the treatments (except for the control group), the protein expression level of AR and ARV7 were decreased. The decreased of AR and ARV7 in the DOV treated group may be due to the neuronal-like differentiation phenomenon, whereas the decrease in AR and ARV7 in the SNG and Combination treated groups may be due to SNG's ability to inhibit AR and ARV7 at both protein and mRNA level (Pham et al., 2020, and Le and Pham et al., 2020). Consistently, Real-time qPCR results showed that expression of LSD1 was increased and AR and its downstream targets were decreased after 21-days of DOV treatment in 22Rv1 cells when compared to untreated 22Rv1 cells (Figure 4C). Similarly, the mRNA expression of AR and its downstream targets were also lowered in 21-days treatment with SNG and with Combination treated 22Rv1 cells. Overall, these results suggest that DOV induces neuronal-like differentiation partly through the LSD1 pathway, and SNG may hinder neuronal-like differentiation in these cells.

SNG inhibits Neuroendocrine Differentiation in vivo

After verifying the importance of LSD1 for DOV-induced neuronal-like differentiation in 22Rv1 cells, we next wanted to determine the therapeutic potential of treating 22Rv1 xenografts with DOV and SNG. Nodskid/balb/c, mice were subcutaneously injected with 5 million 22Rv1 cells in Matrigel. After the tumor size reached 200 mm³, the mice were treated with 1XPBS, SNG alone, DOV alone, or SNG+DOV combination daily via oral gavage. As a result, all three mice treatment groups did not show

significant weight loss compared to the PBS control group (Figure 5A). Furthermore, after 42 days, the Kidney and liver weight were found to be similar among all mice groups (Figure 5B-C), suggesting that even under combination treatment, there is an insignificant level of induced-toxicity. In addition, DOV treatment alone and SNG treatment alone were shown to reduce tumor volume at similar rates, and when under combination treatment, tumor growth was significantly hindered (Figure 5D). The tumor size and tumor weight were measured after 42-days of treatment, and consistently, the combination treatment had significantly smaller weight and size compared to control and the single drug treatment alone (Figure 5E-G). These results suggest that the combination therapy of DOV and SNG may have a synergistic effect in treating tumors. This is further evidenced by the PSA results. PSA levels of combo treated mice were lower than either treatment alone or significantly lower than control groups. Possibly DOV may induce strong cytotoxic effect against 22Rv1 cells, while SNG also induces cytotoxic effect and prevent the DOV from inducing neuroendocrine differentiation in 22Rv1 cells to become more aggressive.

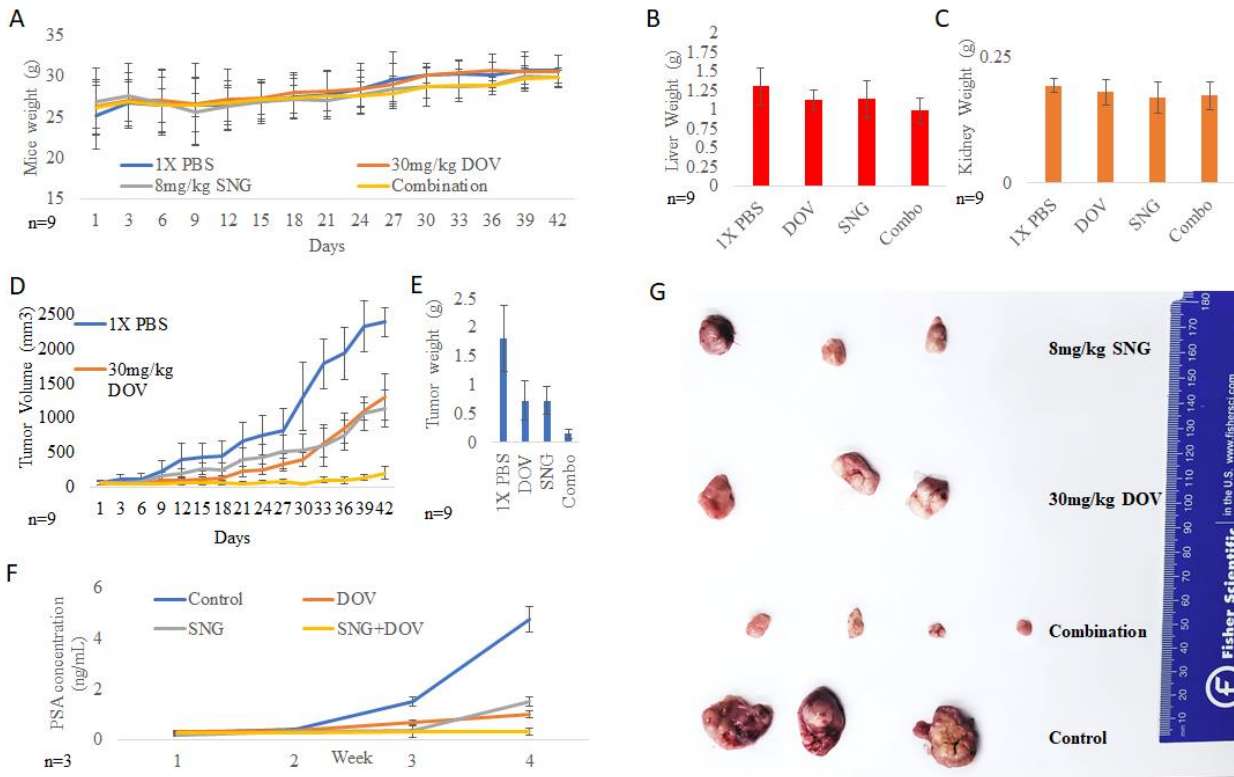


Figure 5. Combination treatment resulted in a significant reduction in tumor growth. Mice were given either DOV (30mg/kg), SNG (8mg/kg), or a combination of (30mg/kg DOV and 8mg/kg SNG) every day for 42 days. (A, D) Mice tumor and weight were measured every three days. (F) Blood samples were collected at the end of every week and subjected to ELISA analysis. (B, C, G) At the end of the 42 day study, mice were sacrificed and tumors and organs were collected, weighed, and used in further analysis.

To further investigate the effect of the drug after 42-days of treatment, the protein and mRNA of the tumors were extracted, and then subjected to WB analysis and Real-time qPCR,

respectively. Neuronal markers γ -enolase, synaptophysin, and chromogranin A protein expression levels were upregulated in DOV treated 22Rv1 tumor xenograft and downregulated in SNG and combination treated 22Rv1 tumor xenograft (Figure 6A). As expected, LSD1 protein expression level and activities were upregulated in DOV treated 22Rv1 tumor xenograft but remain relatively lower in the other groups. The difference in expression of LSD1 and its downstream targets suggest that SNG was able to hinder neuroendocrine differentiation through the inhibition of LSD1 activities. Moreover, our qPCR consistently showed LSD1 mRNA level was increased in DOV treated 22Rv1 tumor xenograft and decreased in SNG and combination treated 22Rv1 tumor xenograft (Figure 6B). Expression of AR, ARV7, PSA, and UBE2C is decreased in all drug treatment groups compared to the control. Blood collected weekly from the mice study were also subjected to an enzyme-linked immunosorbent assay (ELISA) in order to determine serum prostate specific antigen (PSA) levels. Tumors from each condition were also stained for a variety of proteins such as synaptophysin and AR (Supplementary Figure 1). Similar to our western blot and qPCR results, combination treatment displayed reduced levels of the NE marker, synaptophysin. AR level was also seen to be significantly reduced in SNG and combination treated mice. The neuronal marker, E-Cadherin, was also seen to be reduced in combination treated mice when compared to DOV treated mice (Supplementary Figure 2). Ki67 and P63 were also seen to be reduced in groups treated by SNG and a combination of the two.

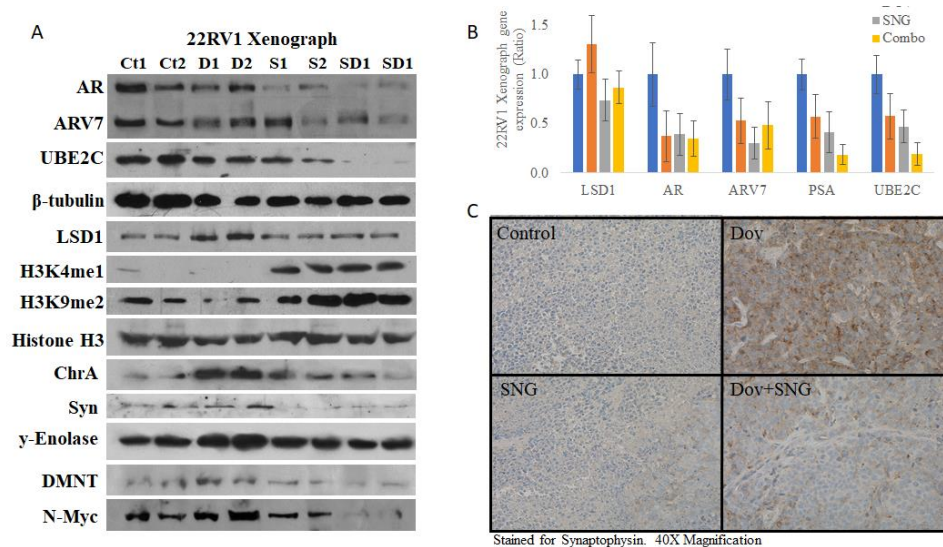
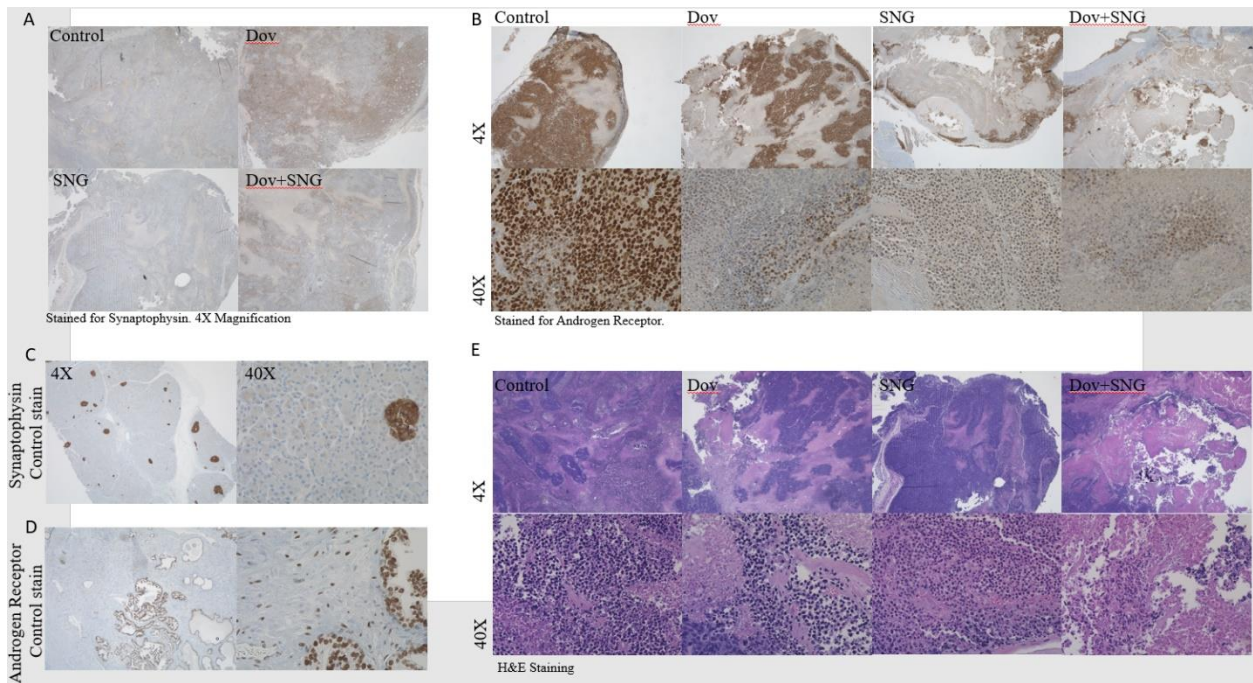
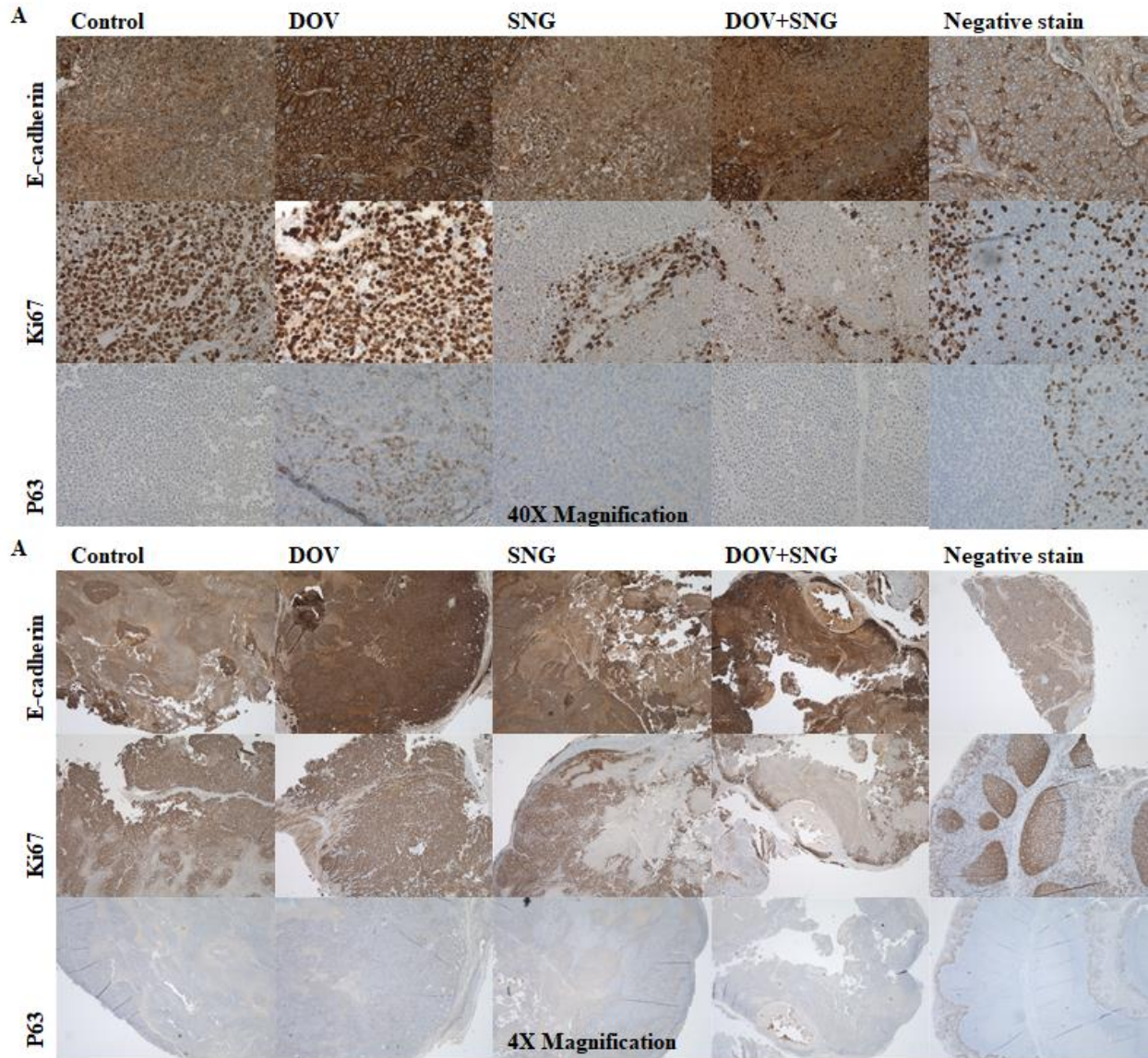


Figure 6. SNG inhibits DOV-induced neuroendocrine differentiation *in vivo*. Protein and RNA from mice xenograft study were extracted and subjected to western blot and qPCR analysis. (A) Western blot analysis observed levels of AR, ARV7, UBE2C, β -tubulin, LSD1, H3K4me1, H3K9me2, Histone H3, Chromogranin A, Synaptophysin, γ -enolase, DMNT, and N-Myc in mice treated with saline, DOV, SNG, or a combination. (B) RNA from tumors were subjected to qPCR analysis in order to observe expression levels of LSD1, AR, ARV7, PSA, and UBE2C in all the same four conditions. (C) Tumors from each condition were also stained for synaptophysin, prepared onto a slide, and had images taken at 40X.



Supplementary Figure 1. Histology (A) Tumors from each condition (Control, DOV, SNG, or combination) in the mice xenograft study were stained for (A) synaptophysin, (B) AR, or (E) H&E and images were taken at 4X and 40X. Control samples were stained for (C) synaptophysin and (D) AR as well and images were taken at 4X and 40X.



Supplementary Figure 2. Tumors from each condition (Control, DOV, SNG, or combination) in the mice xenograft study were stained for E-Cadherin, Ki67, and P63. Images were taken of each stain at (A) 4X and (B) 40X.

DISCUSSION

Androgen deprivation therapy (ADT), the current method of treatment for prostate cancer, has shown to be extremely effective with a response rate of 80%, but over half of these diagnoses develop hormone insensitive variants of the disease within 16 to 18 months. Neuroendocrine cells do not express the androgen receptor (AR), the main target of ADT, and secrete a variety of peptide hormones and growth factors, resulting in resistance to treatment and promotion of disease progression. Neuroendocrine prostate cancer occasionally occurs *de novo*, but neuroendocrine differentiation has been shown to mainly develop because of hormone therapy, with treatment related-neuroendocrine prostate cancer accounting for approximately 25% of late stage prostate cancers. Prior studies also showed that neuroendocrine differentiation increased as hormone therapy duration increased. As of now, promotion of neuroendocrine prostate cancer is a deadly problem in androgen deprivation therapy, but inhibition of LSD1 represents a possible solution to this problem.

Treatment of PCa has focused on targeting AR with effective therapies. Unfortunately, current methods have been unable to address the new problems that arise in resistant forms of the disease that no longer rely on traditional AR signaling, such as neuroendocrine differentiation. Previous studies have shown that LSD1 upregulation is capable of inducing AR transcription, independent of ligand binding. In addition, prior studies have found that DOV is able to induce NE differentiation, but the mechanism remains unknown. In our study, we have discovered that DOV-induced NE differentiation may partly be through an LSD1-dependent mechanism. In our *in vitro* study, DOV treated cells showed elevated levels of LSD1 in addition to NE markers. In contrast, cells treated with a combination of DOV and SNG showed significantly reduced levels of LSD1 and NE markers. This group was also observed to show much less NE differentiation morphologically as well.

Morphologically, the combination treated cells were seen to be much less differentiated than DOV treated cells. Similarly, when LSD1 was knocked down in 22Rv1 cells or when another LSD1 inhibitor (sp2509) was used in combination, there was no noticeable NE differentiation after 3 weeks of DOV treatment. Western blot analysis confirmed that SNG and sp2509 treated cells as well as LSD1 knockdown cells under DOV-treatment displayed significantly lower levels of NE markers compared to DOV treated cells.

Combination treatment reducing NE differentiation has been clearly shown in the first two experiments and the same trend was observed in the mice xenograft study. Western blot analysis of protein extracted from tumors showed reduced levels of NE marker expression in combo treated cells. In histology stains of these tumors, combination treated tumors displayed reduced levels of NE marker

staining when compared to DOV treated tumors. Overall, combination treatment reduced tumor growth most significantly. This could be because DOV results in elevated levels of LSD1 which then sensitizes the tumors to SNG, making SNG more effective. Although the mechanism of neuroendocrine differentiation is still not fully understood, our results suggest that LSD1 may play a central role in NE differentiation. Thus, LSD1 may represent a promising target for future therapies. SNG was found to inhibit DOV-induced NE differentiation *in vitro* and *in vivo*.

LSD1 inhibitors may be able to address the problems in the current treatment. SNG, as a dual inhibitor of AR and LSD1, can reduce the progression of CRPC in addition to differentiation into neuroendocrine prostate cancer. SNG may be an ideal solution to the shortcomings of the current mode of treatment as this drug may be effective in treatment of primary prostate cancer as well as advanced forms of the disease. Thus, ADT in conjunction with SNG treatment has the potential to address multiple variations of this disease simultaneously.

REFERENCES

1. *Neuroendocrine differentiation in prostatic carcinoma.* (n.d.). Retrieved June 19, 2020, from <https://onlinelibrary.wiley.com/doi/epdf/10.1002/%28SICI%291097-0045%2819990501%2939%3A2%3C135%3A%3AAID-PROS9%3E3.0.CO%3B2-S>
2. *Epidemiology of Prostate Cancer.* (n.d.). Retrieved June 19, 2020, from <https://www.ncbi.nlm.nih.gov/pmc/articles/PMC6497009/>
3. *Neuroendocrine-like prostate cancer cells: neuroendocrine transdifferentiation of prostate adenocarcinoma cells in: Endocrine-Related Cancer Volume 14 Issue 3 (2007).* (n.d.). Retrieved June 19, 2020, from <https://erc.bioscientifica.com/view/journals/erc/14/3/0140531.xml#ABRAHAMSSON-1999>
4. *Neuroendocrine-like prostate cancer cells: neuroendocrine transdifferentiation of prostate adenocarcinoma cells in: Endocrine-Related Cancer Volume 14 Issue 3 (2007).* (n.d.). Retrieved June 19, 2020, from <https://erc.bioscientifica.com/view/journals/erc/14/3/0140531.xml>
5. *The importance of the measurement of circulating markers in patients with neuroendocrine tumours of the pancreas and gut. in: Endocrine-Related Cancer Volume 10 Issue 4 (2003).* (n.d.). Retrieved June 19, 2020, from <https://erc.bioscientifica.com/view/journals/erc/10/4/14713258.xml>
6. Beltran, H., Tagawa, S. T., Park, K., MacDonald, T., Milowsky, M. I., Mosquera, J. M., Rubin, M. A., & Nanus, D. M. (2012). Challenges in recognizing treatment-related neuroendocrine prostate cancer. *Journal of Clinical Oncology : Official Journal of the American Society of Clinical Oncology*, 30(36), e386-9. <https://doi.org/10.1200/JCO.2011.41.5166>
7. Berruti, A., Mosca, A., Porpiglia, F., Bollito, E., Tucci, M., Vana, F., Cracco, C., Torta, M., Russo, L., Cappia, S., Saini, A., Angeli, A., Papotti, M., Scarpa, R. M., & Dogliotti, L. (2007). Chromogranin A Expression in Patients With Hormone Naïve Prostate Cancer Predicts the Development of Hormone Refractory Disease. *Journal of Urology*, 178(3), 838–843. <https://doi.org/10.1016/j.juro.2007.05.018>
8. Bonner, J. A., Sloan, J. A., Rowland, K. M., Klee, G. G., Kugler, J. W., Mailliard, J. A., Wiesenfeld, M., Krook, J. E., Maksymiuk, A. W., Shaw, E. G., Marks, R. S., & Perez, E. A. (2000). Significance of neuron-specific enolase levels before and during therapy for small cell lung cancer. *Clinical Cancer Research : An Official Journal of the American Association for Cancer Research*, 6(2), 597–601. <http://www.ncbi.nlm.nih.gov/pubmed/10690544>
9. Conteduca, V., Oromendia, C., Eng, K. W., Bareja, R., Sigouros, M., Molina, A., Faltas, B. M., Sboner, A., Mosquera, J. M., Elemento, O., Nanus, D. M., Tagawa, S. T., Ballman, K. V., & Beltran, H. (2019). Clinical features of neuroendocrine prostate cancer. *European Journal of Cancer*, 121, 7–18. <https://doi.org/10.1016/j.ejca.2019.08.011>
10. Ellis, L., & Loda, M. (2018). LSD1: A single target to combat lineage plasticity in lethal prostate cancer. In *Proceedings of the National Academy of Sciences of the United States of America* (Vol. 115, Issue 18, pp. 4530–4531). National Academy of Sciences. <https://doi.org/10.1073/pnas.1804205115>
11. Hellerstedt, B. A., & Pienta, K. J. (2002). The Current State of Hormonal Therapy for Prostate Cancer. *CA: A Cancer Journal for Clinicians*, 52(3), 154–179. <https://doi.org/10.3322/canjclin.52.3.154>
12. Hirano, D., Okada, Y., Minei, S., Takimoto, Y., & Nemoto, N. (2004). Neuroendocrine Differentiation in Hormone Refractory Prostate Cancer Following Androgen Deprivation Therapy. *European Urology*, 45(5), 586–592. <https://doi.org/10.1016/j.eururo.2003.11.032>
13. Hirano, D., Okada, Y., Minei, S., Takimoto, Y., & Nemoto, N. (2004). Neuroendocrine Differentiation in Hormone Refractory Prostate Cancer Following Androgen Deprivation Therapy. *European Urology*, 45(5), 586–592. <https://doi.org/10.1016/j.eururo.2003.11.032>
14. Hu, C. D., Choo, R., & Huang, J. (2015). Neuroendocrine differentiation in prostate cancer: A mechanism of radioresistance and treatment failure. In *Frontiers in Oncology* (Vol. 5, Issue APR, p. 90). Frontiers Media S.A. <https://doi.org/10.3389/fonc.2015.00090>
15. Kasprzak, A., Zabel, M., & Biczysko, W. (n.d.). *Selected Markers (Chromogranin A, Neuron-Specific Enolase, Synaptophysin, Protein Gene Product 9.5) in Diagnosis and Prognosis of Neuroendocrine Pulmonary Tumours.*
16. Nakano, Y., Wiechert, S., & Bá Nfi Correspondence, B. (2019). Overlapping Activities of Two Neuronal Splicing Factors Switch the GABA Effect from Excitatory to Inhibitory by Regulating REST. *CellReports*, 27, 860-871.e8. <https://doi.org/10.1016/j.celrep.2019.03.072>
17. Nobels, F. R. E., Kwekkeboom, D. J., Coopmans, W., Schoenmakers, C. H. H., Lindemans, J., De Herder, W. W., Krenning, E. P., Bouillon, R., & Lamberts, S. W. J. (1997). Chromogranin A as Serum Marker for Neuroendocrine Neoplasia: Comparison with Neuron-Specific Enolase and the α -Subunit of Glycoprotein Hormones. *The Journal of Clinical Endocrinology & Metabolism*, 82(8), 2622–2628. <https://doi.org/10.1210/jcem.82.8.4145>
18. Regufe da Mota, S., Bailey, S., Strivens, R. A., Hayden, A. L., Douglas, L. R., Duriez, P. J., Borrello, M. T., Benelkebir, H., Ganesan, A., Packham, G., & Crabb, S. J. (2018). LSD1 inhibition attenuates androgen receptor V7 splice variant activation in castration resistant prostate cancer models. *Cancer Cell International*, 18(1), 71. <https://doi.org/10.1186/s12935-018-0568-1>
19. Rickman, D. S., Beltran, H., Demichelis, F., & Rubin, M. A. (2017). Biology and evolution of poorly differentiated neuroendocrine tumors. In *Nature Medicine* (Vol. 23, Issue 6, pp. 664–673). Nature Publishing Group. <https://doi.org/10.1038/nm.4341>
20. Siegel, R. L., Miller, K. D., & Jemal, A. (2020). Cancer statistics, 2020. *CA: A Cancer Journal for Clinicians*, 70(1), 7–30. <https://doi.org/10.3322/caac.21590>
21. Sun, G., Alzayady, K., Stewart, R., Ye, P., Yang, S., Li, W., & Shi, Y. (2010). Histone Demethylase LSD1 Regulates Neural Stem Cell Proliferation. *Molecular and Cellular Biology*, 30(8), 1997–2005. <https://doi.org/10.1128/mcb.01116-09>
22. Terry, S., & Beltran, H. (2014). The many faces of neuroendocrine differentiation in prostate cancer progression. In *Frontiers in Oncology: Vol. 4 MAR* (p. 60). Frontiers Research Foundation. <https://doi.org/10.3389/fonc.2014.00060>
23. Thanasapawat, T., Natarajan, S., Rommel, A., Glogowska, A., Bergen, H., Krcek, J., Pitz, M., Beiko, J., Krawitz, S., Verma, I. M., Ghavami, S., Klonisch, T., & Hombach-Klonisch, S. (2017). Dovitinib enhances temozolomide efficacy in glioblastoma cells. *Molecular Oncology*, 11(8), 1078–1098. <https://doi.org/10.1002/1878-0261.12076>
24. Theisen, E., Bearss, J., Sorna, V., Bearss, D., & Sharma, S. (2013). Abstract 3: Targeted inhibition of LSD1 in castration-resistant prostate cancer. *Cancer Research*, 73(8 Supplement), 3.1-3. <https://doi.org/10.1158/1538-7445.am2013-1003>
25. Toffolo, E., Rusconi, F., Paganini, L., Tortorici, M., Pilotto, S., Heise, C., Verpelli, C., Tedeschi, G., Maffioli, E., Sala, C., Mattevi, A., & Battaglioli, E. (2014). Phosphorylation of neuronal Lysine-Specific Demethylase 1LSD1/KDM1A impairs transcriptional

- repression by regulating interaction with CoREST and histone deacetylases HDAC1/2. *Journal of Neurochemistry*, 128(5), 603–616. <https://doi.org/10.1111/jnc.12457>
26. Torres-Méndez, A., & Bonnal, S. (n.d.). A novel protein domain in an ancestral splicing factor drove the evolution of neural microexons. *Nature Ecology & Evolution*. <https://doi.org/10.1038/s41559-019-0813-6>
 27. Yadav, S. S., Li, J., Stockert, J. A., Herzog, B., O'Connor, J., Garzon-Manco, L., Parsons, R., Tewari, A. K., & Yadav, K. K. (2017). Induction of Neuroendocrine Differentiation in Prostate Cancer Cells by Dovitinib (TKI-258) and its Therapeutic Implications. *Translational Oncology*, 10(3), 357–366. <https://doi.org/10.1016/j.tranon.2017.01.011>
 28. Zibetti, C., Adamo, A., Binda, C., Forneris, F., Toffolo, E., Verpelli, C., Ginelli, E., Mattevi, A., Sala, C., & Battaglioli, E. (2010). Alternative splicing of the histone demethylase LSD1/KDM1 contributes to the modulation of neurite morphogenesis in the mammalian nervous system. *Journal of Neuroscience*, 30(7), 2521–2532. <https://doi.org/10.1523/JNEUROSCI.5500-09.2010>

CHAPTER 7

Sanguinarine hinders cancer stem cell derived Prostate cancer initiation through Lysine Specific Demethylase 1 inhibition

Victor Pham, Merci Mino, Erik Tran, Jack Pearce, Vinh Le, Thanh Le, and Xiaolin Zi

ABSTRACT

Tumor-initiating cancer stem cells, a cornerstone of PCa's heterogeneous cell population, may exist in many instances in which Prostate Cancer (PCa) forms castration resistant prostate cancer (CRPC). Cancer stem cells (CSCs) represent cells that are resistant to chemotherapy, with surviving populations leading to remission and may be possible for the formation of chemoresistant CRPC. It has been established that Lysine Demethylase 1A (LSD1) plays an integral role between CRPC, making it an important target in tumor-initiating cells. In our study, a previously described inhibitor of LSD1, Sanguinarine (SNG), was explored as a restrictor of CSC progression through LSD1 inhibition, ultimately resulting in the suppression of CRPC. Results indicated the ability of SNG to decrease prostaphere formation and diameter in the DU145- and 22Rv1-derived CSCs. In addition, Western blotting analysis and Real-time qPCR for LSD1 and stem cell associated genes show a significant reduction in both CSC derived PCa of 22Rv1 and DU145 cell lines. Further ex-vivo studies portrayed a significant reduction in tumor growth and progression as well as a reduction in LSD1 and Oct4 protein expression level for SNG-treated mice compared to untreated mice. Overall, the results from this study display an important targeting of the LSD1 gene pathway in CSCs to prevent PCa differentiation into its more severe form, CRPC.

BACKGROUND

Despite significant advancements in Prostate cancer (PCa) screening and treatment, PCa remains the second leading form of cancer in American men.² Statistical estimates for the year 2020 predict 191,930 new cases of PCa and 33,330 PCa-related deaths.¹ Some common treatment strategies for PCa include radiotherapy, surgery, chemotherapy, and androgen-deprived therapy (ADT).³ However, in many cases, PCa will regress and circumvent ADT, forming castration resistant prostate cancer (CRPC), a more aggressive form of PCa whose cellular origin remains largely unexplored.⁹ Therefore, the mechanisms for which PCa evades ADT present a modern day need for the understanding and targeting of such mechanisms.

One area of interest lies with cancer stem cells (CSCs), a staple in PCa's heterogeneous population of cells.⁹ CSCs may play an integral role in the lethal progression of CRPC due to integral

malignant properties such as: chemoresistance, metastasis, and unchecked cell division.^{10, 19, 20} Previous research has shown an established relationship between CRPC and LSD1 upregulation.¹³ In addition to the overexpression of LSD1 in various tumor types such as bladder cancer, LSD1 and other related metabolic pathways may prove to be important targets in tumor-initiating cells¹⁴. LSD1 is identified as a histone demethylase that acts upon mono- and di-methylated histones H3 at the K4 and K9 positions,^{11,12} which are involved in stem cell biology and cancer, among other functions.^{21, 22, 30} Our previous study showed that inhibiting LSD1 via Sanguinarine (SNG) leads to the attenuation of CRPC growth and progression.¹⁸ Hence, LSD1 may be an key target for the treatment of tumor initiating CSCs of PCa.¹⁷

To further investigate whether LSD1 is important for CSC progression we explored whether Sanguinarine (SNG), previously shown to inhibit LSD1 enzymatic activity, can hinder CSC progression through LSD1 inhibition, leading to the suppression of CRPC. SNG is a quaternary benzophenanthridine alkaloid derived from poppy and *Fumaria* species, including the root of *Sanguinaria canadensis*.^{7, 29} SNG contains a wide variety of therapeutic potential, such as antifungal, anti-inflammatory, and antibacterial properties.^{4-6, 27-28} In addition, SNG is also used as an anticancer agent through the induction of apoptosis via oxidative stress and mitochondrial transmembrane infiltration among treated populations.^{8, 26} In addition to our study, we investigated the effect of SNG against stem cell activities and LSD1 activities in CSC derived from the 22Rv1 and DU145 cell lines. In totality, our results illustrate SNG-induced inhibition targets tumor-initiating CSC populations, suggesting an important role in the prevention of PCa progression and supporting the need for further inquiry into its effects.

MATERIALS AND METHODS

PCa human cell lines 22Rv1 and DU145 were acquired from ATCC. DMEM/F12, RPMI1640, penicillin-streptomycin, supplement B27/N₂, rhFGF-b, rhEGF, accutase, and fetal bovine serum (FBS) were purchased from Fisher Scientific. Sanguinarine was received from MedChem Express. Primary antibodies for LSD1, Nanog, Oct4, Sox2, B-tubulin, H3K9me2, H3K4me1, and Histone H3 were obtained from Cell signaling. Secondary mouse and rabbit antibodies and secondary fluorescent (M/R) antibodies were acquired from Santa Cruz Biotechnology. RTPCR and qPCR primers for LSD1, Nanog, Oct4, Sox2, AR, ARV7, and UBE2C were purchased from Genscript. Trypan Blue and MTT were obtained from Fisher Scientific. Balb/c nodskid mice were received from Jackson Laboratory.

FACs Cell sorter

Heterogenous 22RV1 and DU145 PCa cell lines underwent FACs cell-sorter assay to create homogeneous Bulk and CSC subpopulations. Antibodies targeting stem-cell phenotypes and characteristics were used, specifically CD44 and CD133 cell markers. Cells marked as containing either or both of the two stem-cell phenotypes were isolated to form the CSC population, with the cells absent of the former markers comprising the Bulk population.

Prostasphere formation Assay

Cells obtained from FACs cell sorter or split via accutase were used for the prostasphere formation assay. Cells were cultured in serum-free DMEM/F12 media supplemented with 2% B27, 1% N₂, 10 ng/mL rhFGF-b, and 20 ng/mL rhEGF as previously described.¹⁵ Cells were distributed into 6-well low-attachment tissue culture plate at 1000 cells/well. Treatment with multiple SNG concentrations (250nM, 500nM, 1uM, and 2uM) and dosage were applied after 24 hours of cultivating.

Western Blotting

Proteins were extracted from cells via RIPA lysis containing protease inhibitors (PI). The cells were washed twice in 1X PBS prior to 15 minutes of incubation in RIPA+PI lysis buffer on ice. Afterwards, the lysed cells were scraped and transferred into a microcentrifuge tube with 30 seconds of vortex. The lysed cells were spun down at 13k rpm for 15 minutes at 4°C, and then the supernatants were used for WB analysis. The proteins were then quantified via Lowry assay. Equal protein samples in B-mercaptoEthanol containing loading buffers were loaded into polyacrylamide gel ranging from 6% to 12%, and gel electrophoresis was run at 100 voltage for 1.5 hours in 1X running buffer. Proteins from the polyacrylamide gel were then transferred onto a PVDF membrane via electrophoresis transfer method at 100V for 45 minutes in the transfer buffer. Afterwards, the newly transferred PVDF membrane was blocked using 5% nonfat dried milk diluted with 1X TBST buffer for 1 hour. Primary antibodies were added to the incubation with a blocking buffer overnight at 4°C. The excess antibodies were later washed out with 1X TBST three times for 5 minutes on a 300rpm rotating motor. HRP-tagged secondary antibodies in blocking buffers were applied prior to autoradiography film capturing. Untreated CSC and Bulk lysates served as controls.

RNA Extraction

RNA was extracted by incubating the cells for 5 minutes on ice with RNA-Bee solution. Lysates were carefully transferred into a 2-mL centrifuge tube, and 1:2 ratio of chloroform was added. The RNA mixture was then vigorously mixed for 30 seconds followed by 5 minutes of settling on ice. The contents

were spun down for 20 minutes at 6000 rpm and 4°C. The top clear layer was transferred to a new microcentrifuge tube containing 1:1 ratio of isopropanol. The samples were mixed and incubated overnight at 4°C to precipitate the RNA contents. The RNA samples were spun down at 20 minutes at 6000 rpm and 4°C, and the aqueous solutions were carefully removed via pipetting. Addition of absolute ethanol precipitated the RNA, and a final centrifugation of 6000 rpm at 4°C for 10 minutes occurred. RNA precipitants were then air dried to evaporate any remaining alcohol; RNA-free water was added to the RNA sample. The RNA contents were quantified using a nanodrop technique and stored at -80°C for later use.

Reverse Transcription Polymerase Chain Reaction

Reverse transcription PCR (RT-PCR) was performed to reverse transcribe RNA into complementary DNA (cDNA). Approximately 2 ug of extracted RNA samples were mixed with 500 ng/ug oligo dT and random primers, and then topped off to 10 uL using nuclease-free water. The RNA mixtures were preheated at 70°C for 5 minutes allowing the annealing of primers, and then cooled to 4°C cooling for at least 10 minutes. Afterwards, a mastermix of MgCl₂, dNTP mix, 1X reaction buffer, reverse transcriptase, and RNasin inhibitor was prepared, and then added to the RNA mixture to run in the PCR. PCR was programmed to process 42°C heating for 1 hour, 70°C for 15 minutes, and cooling at 4°C. The synthesized cDNA samples were stored at -80°C for later use.

Quantitative Polymerase Chain Reaction

Upon obtaining cDNA, real-time quantitative polymerase chain reaction (qPCR) was used to characterize and quantify its corresponding gene sequence. cDNA samples were mixed with SYBR green mastermix and with 200 nM forward and reverse primers. Subsequent cDNA mixtures were run through a qPCR machine with preset settings of 95°C for 10 seconds, 55°C for 30 seconds, 72°C for 30 seconds, and interpretation for a total of 40 cycles. Following 40 cycles, the melting curve of the samples was quantified via a gradual temperature increase of 0.5°C increments every 5 seconds, starting at 55°C and ending at 95°C.

MTT Cellular viability Assay

MTT viability assay was performed to illustrate the cellular metabolic activities of CSCs, which is quantified using colorimetric measurements. Upon reaching 30 to 40% confluence, cells were treated with indicated concentration of SNG and incubation for 72 hours at 37°C. Afterwards, a concentration of 0.5 mg/mL of MTT in 1X PBS was used to treat the cells for one hour incubation at 37°C. Cells were washed with 1X PBS, and MTT dissolving solution (4% 1N HCl in isopropanol) was added and shaken at

300 rpm on a rotating motor for 5 minutes to dissociate the MTT stained cells. The solution was transferred to a 96-well plate and colorimetric measurement of cell viability was taken by a spectrophotometer reading at a 570 nm absorbance value.

Trypan Blue assay

Trypan Blue cellular staining was pursued to measure the number of dead cells and total cells within a population by exclusively labeling cells with 1:1 ratio of 2X Trypan Blue. The sample mixture was loaded onto a hemocytometer, and then visualized and counted under the microscope. Transparent cells will indicate living cells and blue stained cells will indicate dead.

Immunofluorescence (IF) staining

To determine whether the inhibitory effect of SNG involved the specific targeting of LSD1 and downstream genes, the LSD1 and Sox2 genes were immunofluorescence stained. Cell populations were briefly exposed to SNG (0 to 2 μ M). Homogeneous Bulk and CSC populations underwent a thorough wash cycle of; 5% PBST, cold methanol, 4% PFA, cold PBS, .2% TX100 PBS, and 5% FBS/PBST prior to staining. Cell samples then went through an overnight antibody incubation with 5% FBS/PBST at 4°C. After incubation, cell samples underwent two PBS wash cycles in a dark setting. Fluorescent secondary antibody incubation in 5% FBS/PBST for 1 hour at room temperature followed, still in a lowlight setting. Two more PBS wash cycles occurred before the addition of DAPI and the mounting of glass slides onto the samples. Immunofluorescence (IF) imaging of LSD1 and Oct-4 protein expression level and location was then observed under a fluorescence microscope.

In *vivo* tumor formation and analysis

Cancer cell implantation was performed on BALB/c Nodskid mice aged 4 - 6 weeks old. A mixture of PBS and 1×10^6 22RV1 CSCs were hypodermically inserted into mice. Tumors were grown until reaching a volume of 1500 mm³, approximately 3 weeks, and *ex vivo* weighings and measurements using a caliper stated beforehand¹⁶. In *vivo* tumor measurement and weight analysis were performed every 3 days for approximately three weeks.

RESULTS

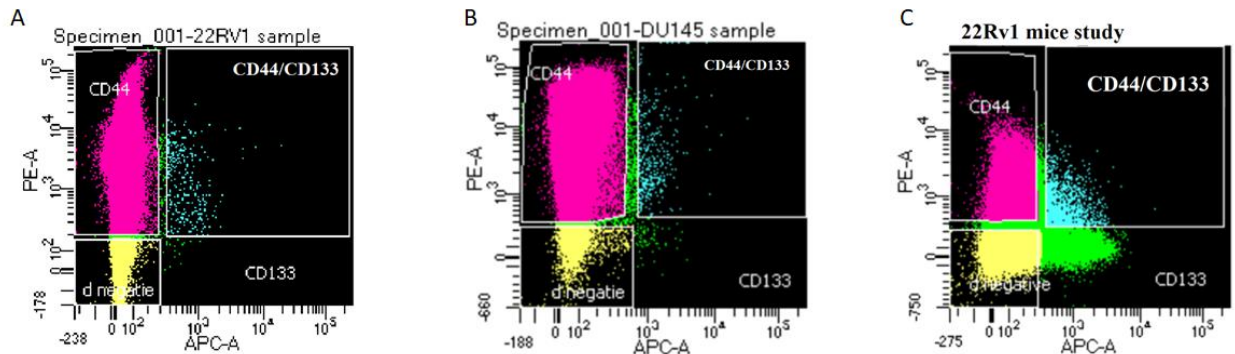


Figure 1. FACS sorting assay of homogeneous CSC and Bulk-tumor cells in 22RV1 and DU145. Heterogenous (A) 22RV1, (B) DU145, and mice study 22Rv1 cell populations were stained for stem cell-like CD44 and CD133 phenotypes and isolated via FACS Fusion cell sorter.

FACS sorting to isolate homogeneous CSC from heterogenous Bulk-tumor cells in 22RV1 and DU145.

Human PCa cells are heterogeneous populations that include CSCs, which are cancers that may differentiate and progress more vigorously and lead to poorer prognosis and greater spread than their more differentiated counterparts, i.e Bulk tumor cells.¹⁷ In addition, due to their minimal expression and easy differentiability, CSC populations located in cancerous tissue are not as pronounced. Thus, detailed means of capture and identification need to be observed for correct isolation and analysis.

To isolate CSC subpopulation from the bulk population, the cancer population was stained with antibodies that targeted established stem cell-like phenotypes, CD44 and CD133.^{24, 25} The FACS cell sorting machine facilitated the isolation of CD44+ and CD133+ expressing CSC subpopulations from the DU145 and 22Rv1 populations. Cells stained for the CD44/CD133 marker from the 22RV1 (Figure 1A) and DU145 (Figure 1B) cell lines constituted a small minority of the total population, supporting previous studies describing their limited quantity in basal populations.¹⁹ This initial assay served to establish the fundamental differences between CSC and Bulk subpopulation within the heterogeneous DU145 and 22Rv1 population.

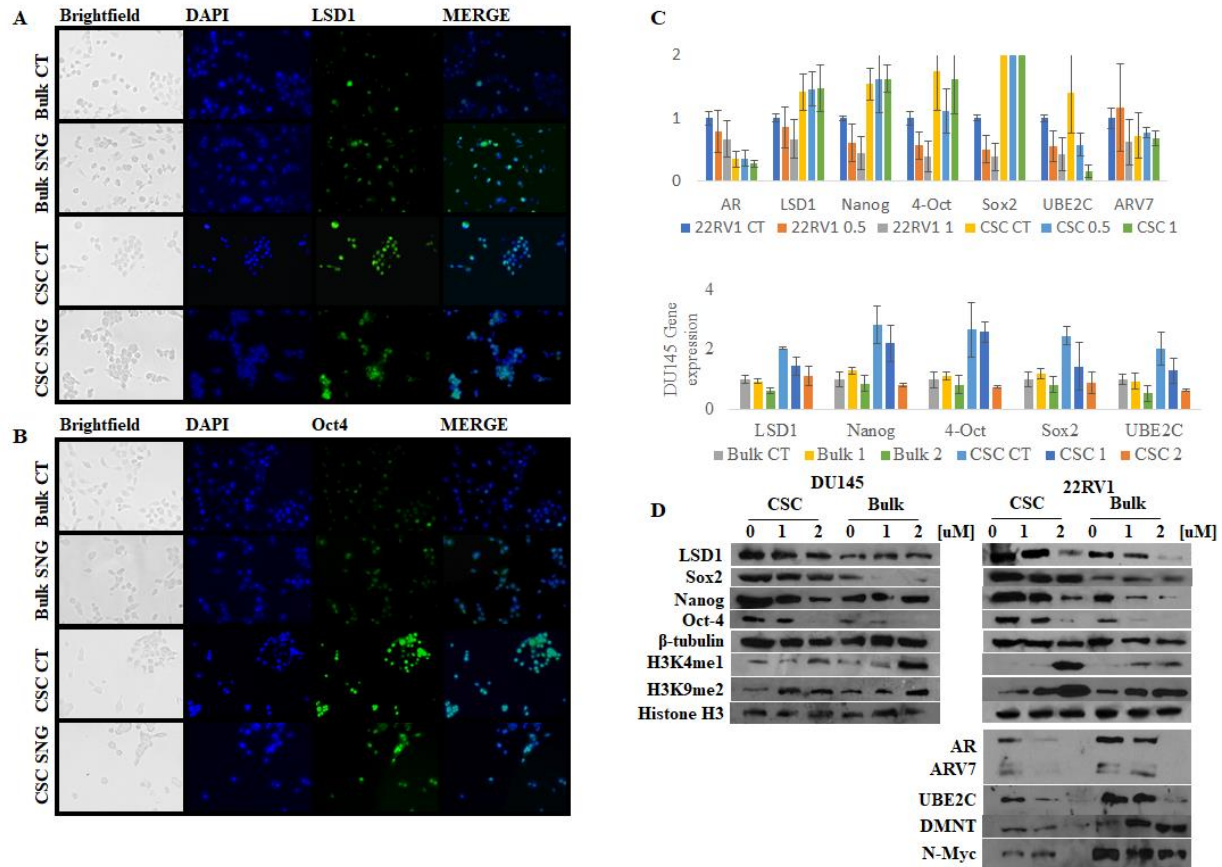


Figure 2. Sanguinarine inhibits LSD1 and AR gene expression in 22Rv1- and DU145-derived CSC. The immunofluorescence detection of LSD1 and Oct-4 proteins in (A) DU145 and (B) 22Rv1 cell lines were visualized under a fluorescence microscope at 20X magnification. (C) Real time qPCR and (D) WB analysis was performed to detect LSD1, AR, Nanog, Oct-4, and Sox2 expression and activities in DU145 and 22Rv1 cell lines under 24-hour treatment with indicated concentration of SNG. Actin and B-tubulin were used as loading controls for qPCR and WB, respectively.

Sanguinarine inhibits LSD1 and AR gene expression in 22Rv1- and DU145-derived CSC

From our previous study, SNG was shown to inhibit LSD1 in PCa, hindering their progression. Thus, we wanted to compare the protein and mRNA expression level of LSD1 among CSC and bulk cells. Immunofluorescence (IF) imaging was performed by staining CSC and bulk populations of 22Rv1 and DU145 cells with LSD1 and Oct-4 antibodies, and then their protein fluorescence level was observed under the fluorescence microscope. As a result, the CSC subpopulation showed higher fluorescence protein levels for both LSD1 (Figure 2A-B) and Oct4 (Supplementary Figure 1A-B) stained proteins when compared to the bulk population, and while under 24 hours treatment with SNG, the fluorescence level of LSD1 and Oct4 proteins decreased, suggesting a role between LSD1 and CSC progression. In addition, real-time qPCR and WB analysis were performed to determine whether CSC-derived 22Rv1 and DU145 populations may overexpress LSD1 mRNA and protein, respectively. When compared to the bulk population, the CSC subpopulation shows lower levels of AR and higher levels of stem cell markers (including Sox2, Oct4, and Nanog) and LSD1 at both the mRNA (Figure 2C) and protein sublevels

(Figure 2D). In addition, SNG was shown to downregulate LSD1 activities and stem cell markers in CSC cells, suggesting that SNG may have therapeutic implementation to attenuate CSC progression partly through LSD1 inhibition.

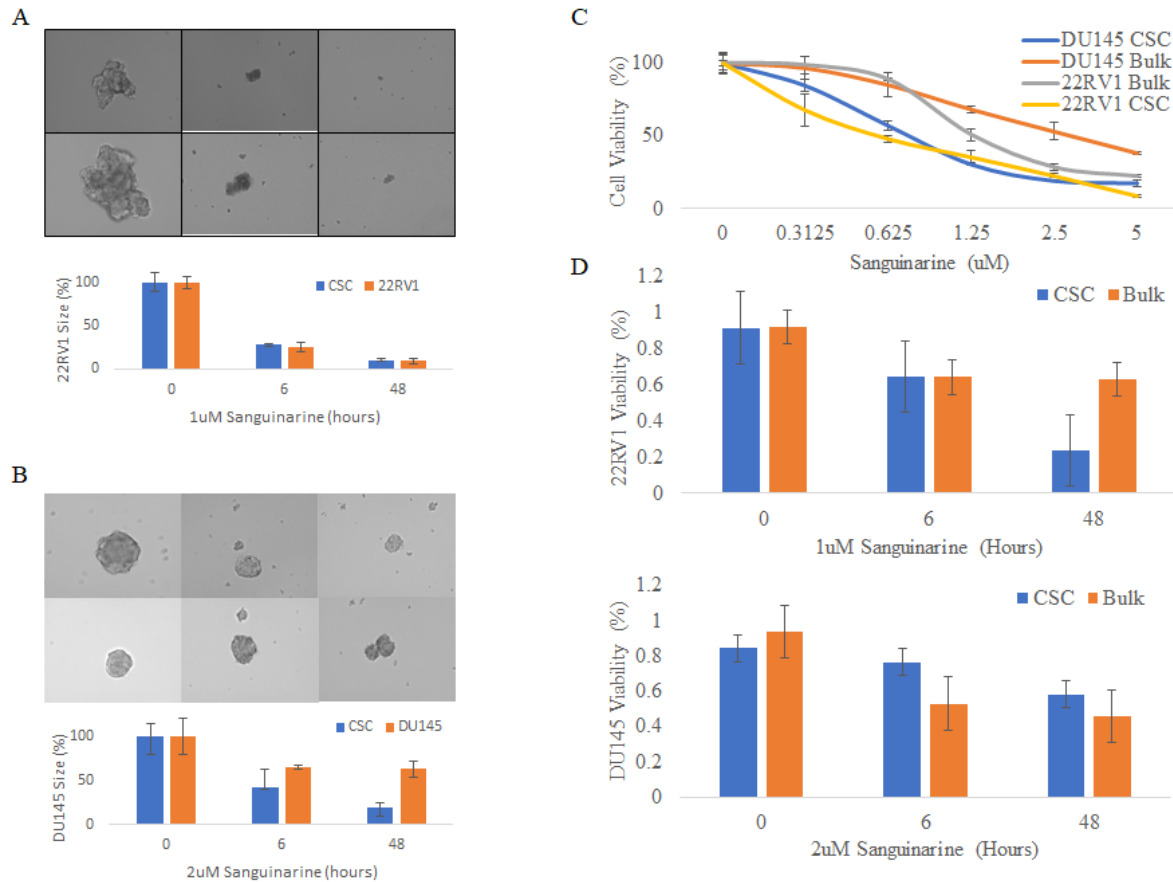


Figure 3: Sanguinarine hinders cancer stem cell prostasphere formation in a time-dependent manner. Time point treated cells were plated (1000 cells/well) in a prostasphere assay to determine lasting inhibition on (A) 22Rv1 and (B) DU145 cells to map effects of prolonged exposure to 1 uM and 2 uM SNG, respectively. (C) MTT Cell viability assay was performed on CSC-derived and Bulk 22Rv1 and DU145 populations under SNG treatment ranging from 0 to 5 uM for 72 hours. (D) Trypan blue analysis of surviving 22Rv1 and DU145 CSC and Bulk populations over 0, 6, and 48 hour timepoints under 1 uM and 2 uM SNG, respectively.

Sanguinarine hinders CSC prostasphere formation in a time-dependent manner.

Next, we explored and compared the cytotoxicity of SNG between CSC-derived PCa subpopulations and Bulk PCa populations. CSC and Bulk populations from 22Rv1 and DU145 were subjected to a two-week spheroid formation assay in the presence of 6 hours or 48 hours treatment of Sanguinarine (SNG). As a result, the growth of CSC subpopulations from 22Rv1 and DU145 were reduced by 6-hour treatment in SNG and further diminished by the 48-hour treatment in

SNG (Figure 3A-B, respectively). Consistently, the percent of viable CSC subpopulations decreased with the increasing time of SNG treatment as shown via Trypan blue viability assay (Figure

3D). These results suggest that the potency of SNG cytotoxicity may be induced in a time-dependent manner to prevent tumor prostasphere formation. We further quantified the cytotoxicity of SNG against CSC subpopulations of 22Rv1 and DU145 cells after 72 hours treatment via MTT cell viability assay. As a result, it was observed that the CSC subpopulation of both 22Rv1 and DU145 were more sensitive to SNG treatment compared to the bulk population, thus suggesting SNG may be more cytotoxic to a CSC subpopulation than the latter. (Figure 3C)

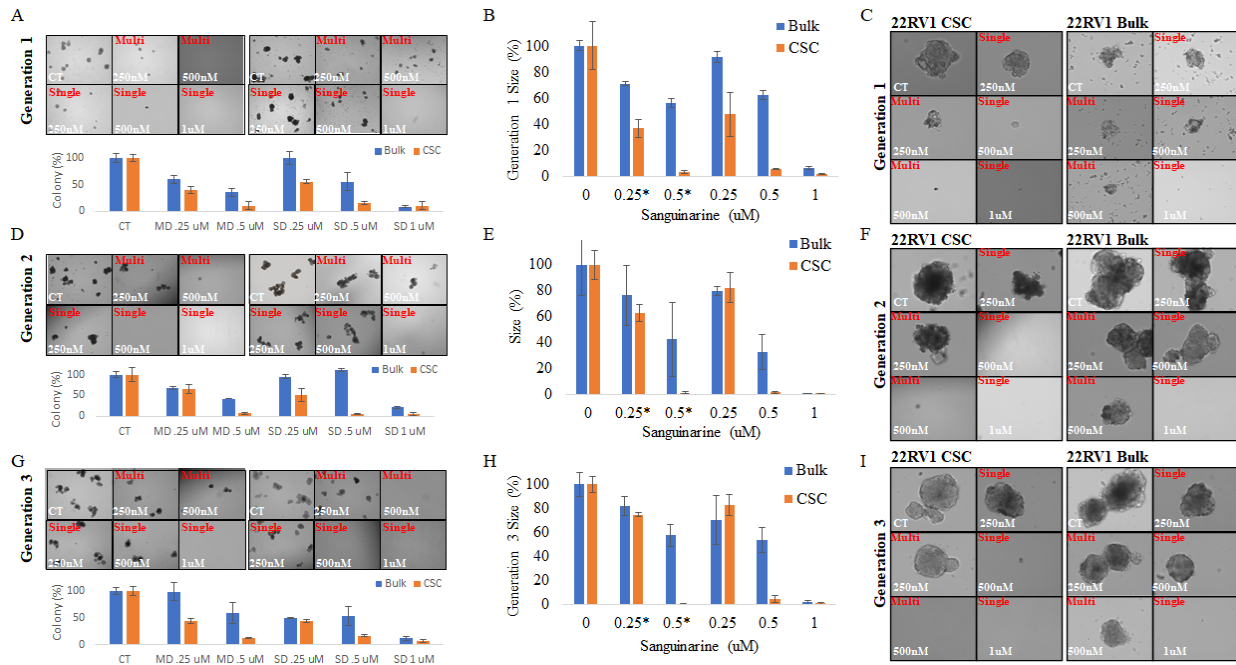


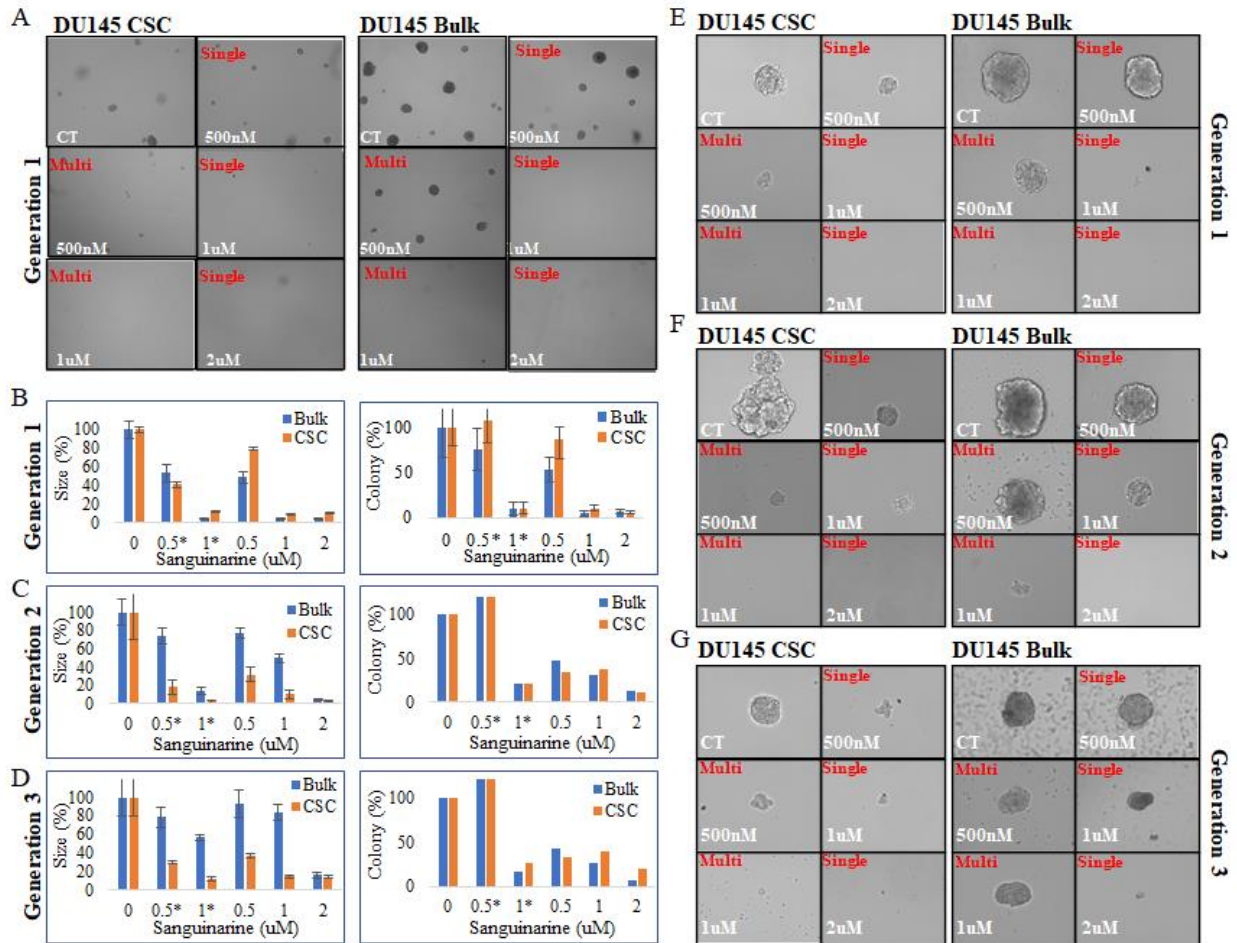
Figure 4: Sanguinarine hinders 22RV1 CSC prostasphere formation in a dose-dependent manner. Different concentrations of SNG (250nM, 500nM, and 1000nM) in single- and multi- dose regimens against CSC and Bulk prostaspheres during their (A) first, (D) second, and (G) third colony generation. Additionally, (B) first, (E) second, and (H) third generation tumor size was measured via imageJ measurement tool. First generation cells were treated either at a single exposure (once at the beginning of the spheroid formation assay) or multiple dosing program (every 4th day after induction on the 1st day) over 14 days. Subsequent generations were cultured without addition of SNG. Photomicrographs of (C) first, (F) second, and (I) third population colonies at 20x Magnification illustrate SNG effects on population number and size in the single and multi-dose regimens.

Sanguinarine hinders 22RV1 CSC prostasphere formation in a dose-dependent manner

Moreover, our study explored whether CSC development and inhibition can be further expressed through dosage frequency. Thus, over a course of two weeks culturing via protosphere formation assay, two lines of equal CSC subpopulations of 22Rv1 and DU145 cells were exposed to a one-time treatment or a multi-dose treatment with indicated concentrations of SNG for 72 hours, and the number of colonies formed and colony sizes were visualized and quantified. As a result, SNG was able to hinder the percentage of CSC subpopulation colonization and the average growth size of the CSC colonies in a dose-dependent manner (Figure 4A and 4B, respectively). In addition, the colony numbers and colony growth of the CSC subpopulation under multi-dose treatment with SNG were decreased, suggesting that SNG

may be given in multiple periods to further hinder CSC progression. To determine whether SNG renders the colonies from recovering, we extracted a small sample of 1000 cells per well from each condition and reculture them via prostasphere formation assay without treatment, indicated as Generation 2. As a result, the generation of CSC subpopulations that were previously treated with SNG had slower or hindered recovery in both colony number and size compared to the bulk population and untreated populations (Figure 4C and 4D, respectively). Similarly, the third generation of CSC subpopulation that were previously treated with SNG also had lower colony number and size recovery (Figure 4E and 4F, respectively).

A global reduction in size and colony formation among all three DU145 generations further displayed SNG's continued role in CSC recovery (Supplementary Figure 2B-D). Likewise, regeneration capabilities were also shown to be further decreased under multi dose treatment. Initial photomicrographs portraying first generation CSC colonies revealed a profound reduction as SNG dosage was increased and repeated (Supplementary Figure 2A). Furthermore, additional photomicrographs for first, second, and third generation DU145 CSCs depicted a reduction in size development among treated populations (Supplementary Figure 2E-G, respectively). These results suggest that SNG treatments may have a long-term effect on prohibiting CSC populations from a full recovery in the case of regression, thus proving possibility for therapeutic implementation.



Supplemental figure 2 Sanguinarine hinders DU145 cancer stem cell prostasphere formation in a dose-dependent manner. Renderings of different concentrations of Sanguinarine, in single and multi dose regimens on CSC (CD44+) and Bulk enriched prostasphere size and colonies in (C) first, (E) second, and (G) third generation cells. Subsequent generations were cultured SNG-free. (D) First, (F) second, and (H) third generation photomicrographs of cell size (20x) illustrate a reduction in population number and size in the single and multi SNG regimens. Photomicrographs (4x) of first generation (A) CSCs and Bulk (B) colonies map initial inhibitory effects. Cells were treated either at a single exposure (once at the beginning of the spheroid formation assay) or multiple dosing program (every 4th day after induction on the 1st day) over 14 days.

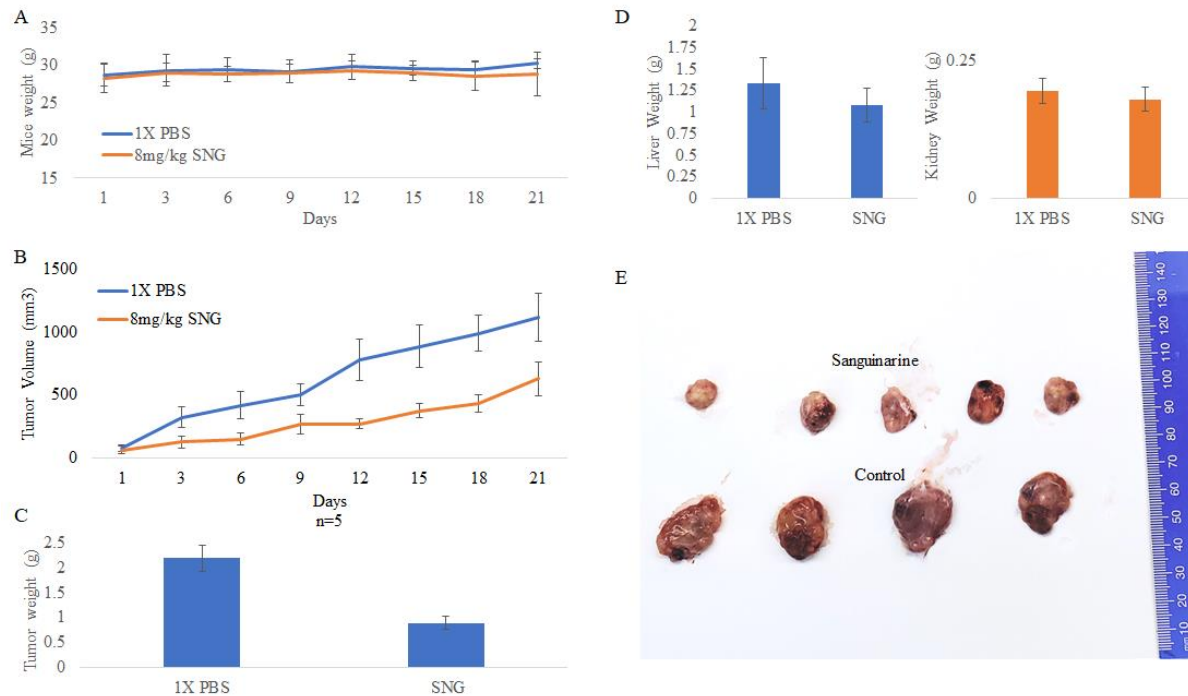


Figure 5 Sanguinarine attenuates 22RV1-derived cancer stem cell progression *in vivo*. Mice were subcutaneously injected with 50,000 CSCs with tumor (A) volume and (B) weight measurement pre and post mortem. Treated and untreated tumors were retrieved for (C) *ex vivo* measurement.

Sanguinarine attenuates 22RV1-derived cancer stem cell progression *in vivo*.

We next pursued an *in vivo* study to determine whether SNG can inhibit the tumor-initiating CSC progression. BALB/c nod skid mice were subcutaneously injected with 50,000 CSC-derived 22Rv1 cells, and the tumor progression was measured over a 3-week period as SNG was delivered daily via oral gavage. Throughout the 3-week study, we did not notice significant changes in weight of the SNG treated mice compared to control mice (Figure 5A). In addition, at the end of the study, there were no significant changes in weights of the liver (Figure 5B) and kidney (Figure 5C) of the SNG-treated mice in comparison to the control. This suggests that SNG did not have severe adverse effects against the eating habits and the overall health of the mice. Furthermore, SNG was shown to significantly reduce the CSC tumor progression volume (Figure 5C), resulting in tumor weight reduction (Figure 5D) and size reduction (Figure 5E). Overall, these results suggest SNG may inhibit CSC progression both *in vitro* and *in vivo*.

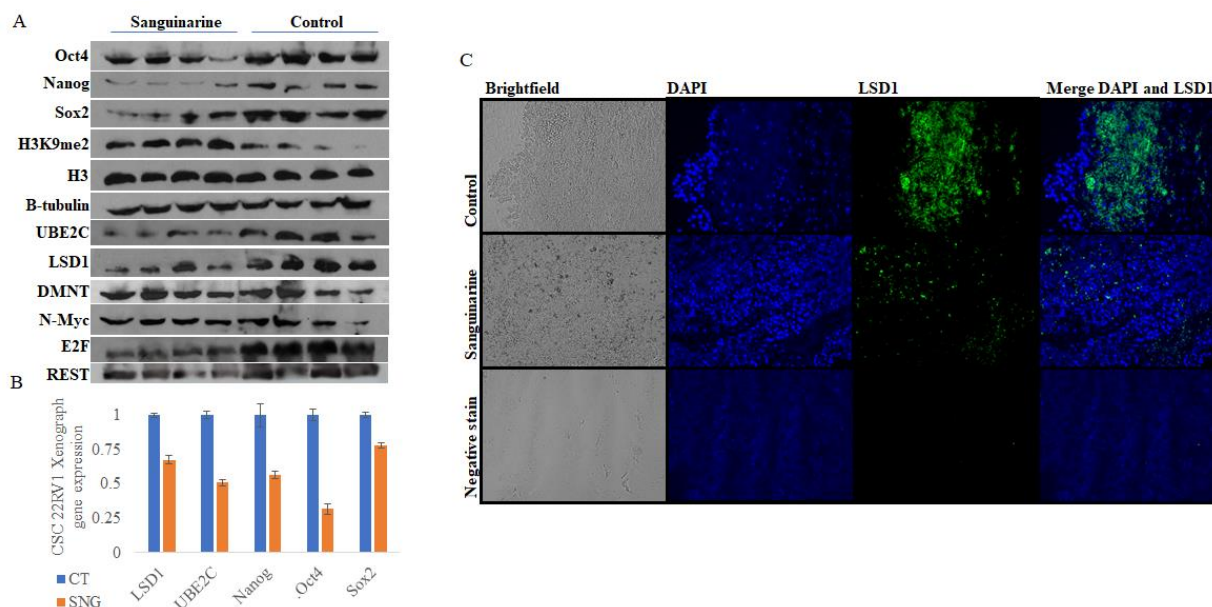
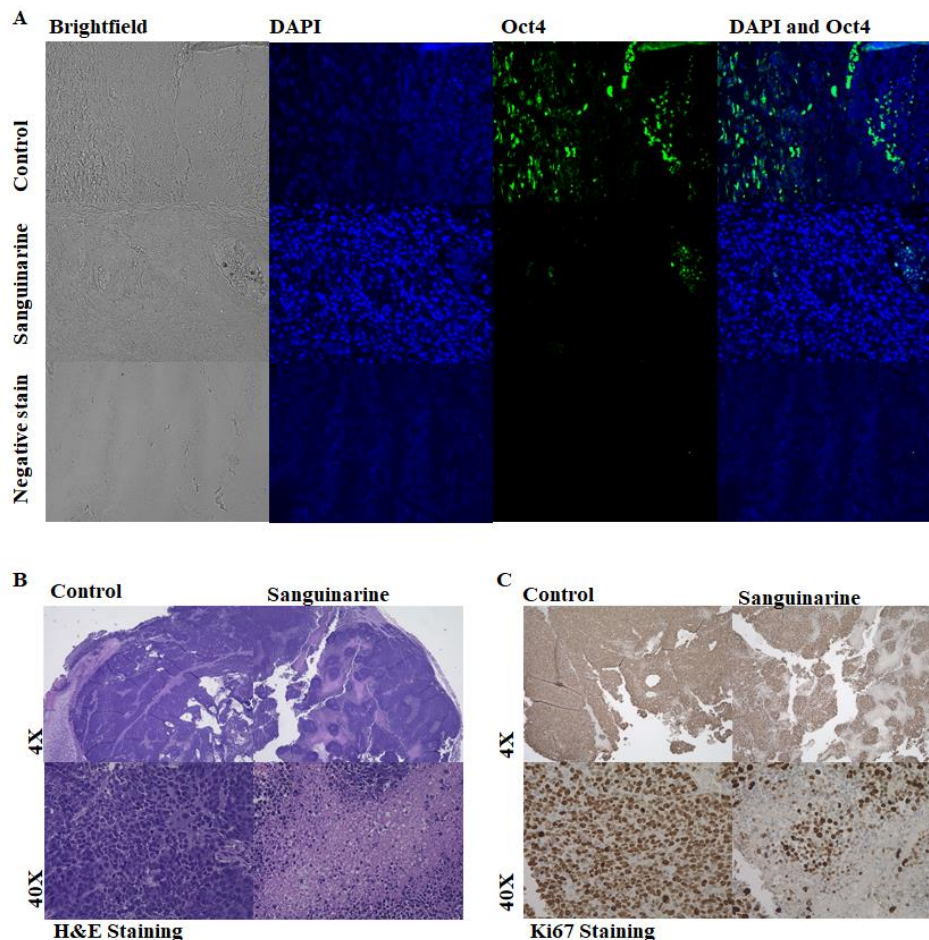


Figure 6 Sanguinarine inhibits LSD1 and AR in xenograph 22RV1-derived cancer stem cells. (A) Ex *in vivo* WB analysis for protein expression of Oct4, Nanog, Sox2, LSD1, LSD1 downstream targets, UBE2X, DMNT, N-myc, E2F, and REST from treated and untreated mice tumors. (B) Xenograft gene expression of LSD1 and stem cell associated genes for 22Rv1-derived CSCs. (C) Ex *in vivo* immunohistology fluorescence staining of LSD1 from treated and untreated mice tumors.

Sanguinarine inhibits LSD1 and AR in xenograph 22RV1-derived cancer stem cells.

We next examined the effect of SNG on the protein and mRNA level of LSD1 and stem cell markers in xenograft tumor via WB analysis and real-time qPCR, respectively. The ex *in vivo* xenograft CSC tumor treated with SNG revealed a reduction of stem cell markers and LSD1 activities at the protein level (Figure 6A) and mRNA level (Figure 6B). Immunohistology fluorescence staining of LSD1 protein expression (Figure 6D) among treated tumors depicted low fluorescence levels protein production relative to untreated samples. Finally, we assessed the effect of SNG on the expression of stem cell associated gene Oct-4 among CSC tumors, and observed that SNG significantly reduced Oct-4 fluorescence levels (Supplementary Figure 1A) among the exposed population. H&E staining revealed SNG damages to the cell nucleus and membrane staining (Supplementary Figure 1B). In addition, cell proliferation marker Ki-67 also resulted in a reduced expression among SNG-treated tumors (Supplementary Figure 1C). In all, these results indicate that SNG may reduce CSC development and progression in part through the downregulation and inhibition of LSD1, Oct-4, and Ki167 expression.



Supplementary Figure 1 Sanguinarine attenuates H&E and Ki67 tumor staining. (A) Immunofluorescence staining of Oct-4, (C) H&E staining and (D) Ki67 staining on SNG-treated and untreated 22Rv1 xenografts.

DISCUSSION

The heterogenous pool of PCa contains CSC that are more aggressive and belligerent^{9,23}; and thus can likely lead to remission and progression in patients after undergoing chemotherapy or ADT treatment. However, due to LSD1 overexpression seen in various tumor types¹⁴, it was suggested that LSD1 plays an integral role in tumor-initiating CSC progression and the progression of other forms of cancer¹³. As shown from our study, we have provided evidence that SNG could be an effective modeled inhibitor to hinder CSC progression through LSD1 inhibition and deserve future investigation and structural studies. We have shown SNG to decrease prostaphere formation and diameter in the DU145- and 22Rv1-derived CSCs. In addition, SNG treatment appears to have decreased LSD1 activities as shown from our WB analysis in the DU145- and 22Rv1-derived CSCs, providing evidence that SNG may be an effective treatment in targeting the LSD1 proliferation pathway for CSC. In addition, SNG may be

an effective means for proactive care regarding LSD1-linked CSC proliferation and differentiation as displayed by the mice tumor diameters, IF staining, and slow growth when exposed to SNG.

Because of SNG's specificity to LSD1 and AR downregulation as shown from our previous studies,¹⁸ the growth inhibition of CSC may be a result of their higher expression level of LSD1. Furthermore, this study provides a proper introduction to SNG as a clinical and possibly human oncological/chemotherapeutic drug and may also prove to be effective in reactionary measures to limit and diminish the differentiation potential and expression of CSC. Longer incubation periods of cell lines and mice under a single SNG treatment could have been conducted. In addition, improvements on FACS isolation with CSCs, cell culture methods and IF staining could be made to shorten the duration of the study and culture. However, the study's main purpose was to show SNG as a possible future oncological treatment through its ability to inhibit LSD1 expression and AR; accomplishing as such by demonstrating SNG's success in limiting bulk tumor growth and CSC proliferation profoundly as compared to untreated cell lines and mice tumors. In all, the results of this study are noteworthy and provide a key argument for further preclinical studies of this agent as an inhibitor for CSC proliferation and PCa recurrence.

REFERENCES

- National Cancer Institute. SEER Cancer Stat Facts: Prostate Cancer. Accessed at <https://seer.cancer.gov/statfacts/html/prost.html> on June 20, 2019.
- American Cancer Society. Facts & Figures 2020. American Cancer Society. Atlanta, Ga. 2020.
- Litwin MS, Tan H. The Diagnosis and Treatment of Prostate Cancer: A Review. *JAMA*. 2017;317(24):2532–2542. doi:10.1001/jama.2017.7248
- Niu, Xiaofeng, et al. “The Anti-Inflammatory Effects of Sanguinarine and Its Modulation of Inflammatory Mediators from Peritoneal Macrophages.” *European Journal of Pharmacology*, vol. 689, no. 1-3, 2012, pp. 262–269., doi:10.1016/j.ejphar.2012.05.039.
- Beuria, Tushar K., et al. “Sanguinarine Blocks Cytokinesis in Bacteria by Inhibiting FtsZ Assembly and Bundling†.” *Biochemistry*, vol. 44, no. 50, 2005, pp. 16584–16593., doi:10.1021/bi050767+.
- Zhong, Hua, et al. “Activity of Sanguinarine against *Candida Albicans* Biofilms.” *Antimicrobial Agents and Chemotherapy*, vol. 61, no. 5, 2017, doi:10.1128/aac.02259-16.
- M. Shamma, H. Guinaudeau, Anorphanoid alkaloids, *Nat. Prod.Rep.* 3 (1986) 345–35
- Chang, Mei-Chi, et al. “Induction of Necrosis and Apoptosis to KB Cancer Cells by Sanguinarine Is Associated with Reactive Oxygen Species Production and Mitochondrial Membrane Depolarization.” *Toxicology and Applied Pharmacology*, vol. 218, no. 2, 2007, pp. 143–151., doi:10.1016/j.taap.2006.10.025.
- Chen, X., et al. “Defining a Population of Stem-like Human Prostate Cancer Cells That Can Generate and Propagate Castration-Resistant Prostate Cancer.” *Clinical Cancer Research*, vol. 22, no. 17, 2016, pp. 4505–4516., doi:10.1158/1078-0432.ccr-15-2956.
- Zhang, L., Jiao, M., Li, L. et al. Tumorspheres derived from prostate cancer cells possess chemoresistant and cancer stem cell properties. *J Cancer Res Clin Oncol* 138, 675–686 (2012). <https://doi.org/10.1007/s00432-011-1146-2>
- Chen, Y., et al. “Crystal Structure of Human Histone Lysine-Specific Demethylase 1 (LSD1).” *Proceedings of the National Academy of Sciences*, vol. 103, no. 38, 2006, pp. 13956–13961., doi:10.1073/pnas.0606381103.
- Mimasu, Shinya, et al. “Crystal Structure of Histone Demethylase LSD1 and Tranylcypromine at 2.25Å.” *Biochemical and Biophysical Research Communications*, vol. 366, no. 1, 2008, pp. 15–22., doi:10.1016/j.bbrc.2007.11.066.
- Schrawat, Archana, et al. “LSD1 Activates a Lethal Prostate Cancer Gene Network Independently of Its Demethylase Function.” *Proceedings of the National Academy of Sciences*, vol. 115, no. 18, 2018, doi:10.1073/pnas.1719168115.
- Hayami, Shinya, et al. “Overexpression of LSD1 Contributes to Human Carcinogenesis through Chromatin Regulation in Various Cancers.” *International Journal of Cancer*, vol. 128, no. 3, 2010, pp. 574–586., doi:10.1002/ijc.25349.
- Tyagi, Alpna, et al. “Differential Effect of Grape Seed Extract and Its Active Constituent Procyanidin B2 3,3'-Di-O-Gallate against Prostate Cancer Stem Cells.” *Molecular Carcinogenesis*, vol. 58, no. 7, 2019, pp. 1105–1117., doi:10.1002/mc.22995.
- Liu, Chungang, et al. “LSD1 Stimulates Cancer-Associated Fibroblasts to Drive Notch3-Dependent Self-Renewal of Liver Cancer Stem-like Cells.” *Cancer Research*, vol. 78, no. 4, 2017, pp. 938–949., doi:10.1158/0008-5472.can-17-1236.
- Maitland, Norman J., and Anne T. Collins. “Prostate Cancer Stem Cells: A New Target for Therapy.” *Journal of Clinical Oncology*, vol. 26, no. 17, 2008, pp. 2862–2870., doi:10.1200/jco.2007.15.1472.
- Pham et al., 2020**
- Collins, Anne T., et al. “Prospective Identification of Tumorigenic Prostate Cancer Stem Cells.” *Cancer Research*, vol. 65, no. 23, 2005, pp. 10946–10951., doi:10.1158/0008-5472.can-05-2018.
- Yun, E.-J., et al. “Targeting Cancer Stem Cells in Castration-Resistant Prostate Cancer.” *Clinical Cancer Research*, vol. 22, no. 3, 2015, pp. 670–679., doi:10.1158/1078-0432.ccr-15-0190.
- Ellinger, Jörg, et al. “Global Levels of Histone Modifications Predict Prostate Cancer Recurrence.” *The Prostate*, vol. 70, no. 1, 2010, pp. 61–69., doi:10.1002/pros.21038.
- Chaumeil J, Okamoto I, Guggiari M, Heard E. Integrated kinetics of X chromosome inactivation in differentiating embryonic stem cells. *Cytogenet Genome Res* 2002; 99:75-84.
- Hao, J.; Madigan, M.C.; Khatri, A.; Power, C.A.; Hung, T.T.; Beretov, J.; Chang, L.; Xiao, W.; Cozzi, P.J.; Graham, P.H.; Kearsley, J.H.; Li, Y., In vitro and in vivo prostate cancer metastasis and chemoresistance can be modulated by expression of either CD44 or CD147. *PLoS One*, 2012, 7, (8), e40716.
- Collins, A.T.; Habib, F.K.; Maitland, N.J.; Neal, D.E. Identification and isolation of human prostate epithelial stem cells based on alpha(2)beta(1)-integrin expression. *J. Cell Sci.* 2001, 114, 3865-3872.
- Richardson, G.D.; Robson, C.N.; Lang, S.H.; Neal, D.E.; Maitland, N.J.; Collins, A.T. CD133, a novel marker for human prostatic epithelial stem cells. *J. Cell Sci.* 2004, 117, 3539-3545.
- Burgeiro, Ana, et al. “Rapid Human Melanoma Cell Death Induced by Sanguinarine through Oxidative Stress.” *European Journal of Pharmacology*, vol. 705, no. 1-3, 2013, pp. 109–118., doi:10.1016/j.ejphar.2013.02.035.
- Wang, Qin, et al. “Anti-Inflammatory and Neuroprotective Effects of Sanguinarine Following Cerebral Ischemia in Rats.” *Experimental and Therapeutic Medicine*, vol. 13, no. 1, 2016, pp. 263–268., doi:10.3892/etm.2016.3947.
- Rahman, Anees, et al. “Critical Role of H2O2 in Mediating Sanguinarine-Induced Apoptosis in Prostate Cancer Cells via Facilitating Ceramide Generation, ERK1/2 Phosphorylation, and Par-4 Cleavage.” *Free Radical Biology and Medicine*, vol. 134, 2019, pp. 527–544., doi:10.1016/j.freeradbiomed.2019.01.039.
- Park, Hyunjin, et al. “Sanguinarine Induces Apoptosis of Human Osteosarcoma Cells through the Extrinsic and Intrinsic Pathways.” *Biochemical and Biophysical Research Communications*, vol. 399, no. 3, 2010, pp. 446–451., doi:10.1016/j.bbrc.2010.07.114.
- Sun G, Alzayady K, Stewart R, Ye P, Yang S, Li W, Shi Y. The histone demethylase LSD1 regulates neural stem cell proliferation. *Mol Cell Biol* 2010;30: 1997–2005.

CHAPTER 8

Conclusion and Remarks

AR expression and signaling remains to be a driving force to the recurrence and progression of castration-resistant prostate cancer (CRPC) to its lethal stage even though multiple generations of AR signaling inhibitors have been used. In addition, epigenetic mechanisms, in particular LSD1 overexpression, can also coordinately enhance AR signaling and drive epithelial plasticity and trans-differentiation to neuron-like cells with loss of AR expression. Therefore, new agents that can target both AR overexpression and AR loss are urgently needed to overcome these new mechanisms of resistance to AR signaling inhibitors, such as Enzalutamide and Abiraterone.

We have discovered for the first time that Sanguinarine, a naturally occurring compound from the root of *Sanguinaria canadensis* as well as other *Fumaria* species, is a dual inhibitor of LSD1 and AR by docking into the enzymatic activation pocket and the ligand binding pocket, respectively. Additionally, *in vitro* SPR and *in vivo* CETSA assays confirmed that Sanguinarine directly binds to both LSD1 and AR with equal or very close binding affinities. Furthermore, the growth-inhibitory and anti-AR signaling effects of Sanguinarine are partially dependent on the expression levels of LSD1 as shown in LSD1 knockdown and overexpression experiments. As a natural compound that targets both AR and LSD1, Sanguinarine and its structural analogs present an ideal library to investigate. Further X-ray co-crystallography is being used to image the detailed binding positions (the interacting amino acids and distances) of SNG to LSD1 and AR. These studies would allow future chemical optimization of Sanguinarine toward a drug candidate for treatment of lethal CRPC.

Small-cell neuroendocrine prostate cancer is the most aggressive type of prostate cancer currently with no effective drug available in clinics. We have found that Dovitinib, a pan-tyrosine kinase inhibitor in prostate cancer clinical trials, can markedly induce the expression of LSD1 leading to neuroendocrine differentiation in prostate cancer cells and that Sanguinarine inhibited the Dovitinib-induced neuroendocrine trans-differentiation both *in vitro* in prostate cancer cell lines and *in vivo* in a xenograft model of prostate cancer. Sanguinarine selectively inhibits the growth of prostate cancer cell lines compared to non-malignant prostate epithelial cells and did not significantly affect body and organ weight in the mouse model, which suggests that Sanguinarine is potentially a safe compound. Similarly, SP2509, an allosteric LSD1 inhibitor, was also observed to partially prevent the Dov-induced neuroendocrine differentiation, even though with less potency compared to Sanguinarine. Furthermore, overexpression of LSD1-8a, a neuron-specific variant of LSD1, in a prostate cancer cell line induces neuron-like morphology and marked expression of neuroendocrine markers, whereas knock-down of LSD1 expression in prostate cancer cell lines hinders the Dovitinib-induced neuroendocrine differentiation.

Taken together, these results strongly support that LSD1 plays a key role in prostate cancer with neuroendocrine features and that highly-potent LSD1 inhibitor, like Sanguinarine, can be used in combination with Dovitinib to prevent neuroendocrine differentiation for enhancing the anti-tumor efficacy of Dovitinib.

Cancer stem cells or cancer initiation cells are critical for cell fate determination and the transition to heterogeneous types of cancer cells leading to tumor recurrence and drug resistant. Prostate cancer stem like cells were sorted by flow-cytometry using cancer stem cell specific biomarkers. We found that prostate cancer stem-like cells express higher levels of LSD1 than bulk heterogeneous population of prostate cancer cells. Sanguinarine is more effectively reduce the growth and regeneration of spheroids from stem cell-like prostate cancer, or tumor-initiating cells, than bulk heterogeneous population of prostate cancer cells both in vitro in cultures and in an in vivo in a prostate cancer xenograft model, which is accompanied by down-regulation of the expression of cancer stem cell markers (i.e. Nanog, Sox2, and Oct4).

In conclusion, our results demonstrate that Sanguinarine is a “first-in-class”, potent, dual inhibitor of LSD1 and AR for preventing or delaying CRPC progression through the mechanisms of down-regulating AR signaling and inhibiting neuroendocrine differentiation and cancer stem cells. LSD1 is a critical target for prostate cancer stem cells and its neuroendocrine differentiation. Sanguinarine could be further chemically and pharmacologically optimized as a drug candidate for treatment of CRPC for future clinical trials.

